The *Populus* Help System

Help texts and references for the *Populus* models are collected in a single large "portable document" file (pdf), accessible via Adobe Acrobat Reader. To minimize downloaded file sizes, we provide an English-language version as the default help system, with Spanish and Portuguese translations available as alternatives. At present, both the Spanish and Portuguese translations are incomplete, and we insert English help texts for those modules where translations are not yet available.

Populus will start Acrobat Reader in the background, and display the full system when help is requested, with a set of bookmarks corresponding to the model menus in the program for easy navigation. After looking at a help screen, we suggest that you minimize the reader rather than closing it, to speed subsequent access. The *Populus* help system is configured so that users may print pages (and we explicitly permit printing for any non-profit teaching use), but cannot extract, edit, or alter it for other applications.

Density-Independent Population Growth

Density-independent growth models offer an extremely simple perspective on changes in population size by assuming away many potential complications. For example, two sets of counteracting processes affect population size; birth and immigration increase populations while death and emigration decrease them. To simplify, assume that (a) immigration and emigration balance, leaving birth and death as the only determinants of population density. Let's also assume that (b) all individuals are identical (especially with respect to their probabilities of dying or producing offspring), (c) the population consists entirely of parthenogenetic females, so that we can ignore complications associated with mating, and (d) environmental resources are infinite, so that the only factors affecting population size are the organisms' intrinsic birth and death rates. These assumptions allow a simplistic model of population growth, and it is instructive to present the model in two formats for different kinds of life histories.

Case I. Exponential Growth with Continuous Breeding

First we will consider an organism like *Homo sapiens* or the bacteria in a culture flask, with continuous breeding and overlapping generations. All ages will be present simultaneously, and population size will change steadily in small increments with the birth and death of individuals at any time. This *continuous* population growth is best described by a differential equation, with instantaneous rates defined over infinitely small time intervals.

If: N = population size

b = instantaneous birth rate per female

d = instantaneous death rate per female

then population growth is given as:

$$\frac{\mathrm{d}N}{\mathrm{d}t} = (b - d)N$$

If we collect the *per capita* birth and death rates in a single parameter $r = b - d$ called the *intrinsic rate of increase* or *exponential growth rate*, then:

$$\frac{\mathrm{d}N}{\mathrm{d}t} = rN$$

This expression states that population growth is proportional to N and the instantaneous growth rate, r. When $r = 0$, birth and death rates balance, individuals just manage to replace themselves, and population size remains constant. When $r < 0$, the population shrinks toward extinction, and when $r > 0$, it grows.

We integrate the differential form of this continuous growth model to project future population sizes:

$$N(t) = N(0)e^{rt}$$

Although r is an instantaneous rate, its numerical value is only defined over a finite interval. If this rate remains constant, then we can predict future population size, $N(t)$ from a knowledge of the constant growth rate (r), the present population size, $N(0)$, and the time over which growth occurs (t).

Case II. Geometric Growth with Discrete Generations

Now we consider a density-independent growth model that is more appropriate for many plants, insects, mammals, and other organisms that reproduce seasonally. Individuals in such a population comprise a series of *cohorts* whose members are at the same developmental stage. Assume that an interval begins with the appearance of newborns, and that if individuals survive long enough, they produce another cohort of offspring at the beginning of the next interval. Parents may all die before the offspring are born (like annual plants), or they may survive to reproduce again so that generations are partially overlapping (like many mammals). In either case youngsters appear in nearly synchronous groups separated by intervals without recruitment. This *discrete* population growth is best described by a finite difference equation.

If: N_t = population size at time t

b = births per female per interval

p = probability of surviving the interval, then:

$$N_{t+1} = pN_t + pbN_t = \left(p + pb\right)N_t$$

Redefining the collective term with birth and death rates as a single parameter $\lambda = (p + pb)$, which gives the number of survivors plus their progeny,

$$N_t = \lambda N_{t-1} = \lambda\left(\lambda N_{t-2}\right) = \lambda^t N_0$$

λ is the *geometric growth factor*, or *per capita* change in population size over a discrete interval, t. If $\lambda = 1$, then individuals just manage to replace themselves and population size remains constant. If $\lambda < 1$, the population shrinks toward extinction, and if $\lambda > 1$, it grows larger. As long as λ remains constant, we can predict future population sizes from the growth rate (λ), the present population size (N_0), and the interval over which growth occurs (t), using the equation

$$N_t = \lambda^t N_0$$

References

Alstad, D. N. 2001. *Basic Populus Models of Ecology*. Prentice Hall. Upper Saddle River, NJ. Chapter 1.

Case, T. J. 2000. *An Illustrated Guide to Theoretical Ecology*. Oxford University Press. New York. pp. 1-13.

Cohen, J. E. 1995. *How Many People Can the Earth Support?* W. W. Norton & Co. New York.

Elton, C. 1958. The Ecology of Invasions by Animals and Plants. Methuen, London.

Roughgarden, J. 1998. *Primer of Ecological Theory.* Prentice Hall, Upper Saddle River, N. J. pp. 55-60.

von Foerster, H., P. M. Mora and L. W. Amiot. 1960. Doomsday: Friday, 13 November, A.D. 2026. Science 132:1291-5.

Density-Dependent Population Growth

This module simulates density-dependent population growth, assuming a linear negative feedback of population size on *per capita* growth. It requires specification of a starting population size $N(0)$, a maximum sustainable population size or environmental carrying capacity K, a *per capita* intrinsic growth rate r, and (optionally) a feedback lag τ. The program includes continuous, lagged continuous, and discrete simulations.

Density-dependent models assume that population size affects *per capita* growth. While the feedback of density on growth can take many forms, the logistic model imposes a negative linear feedback. Note that if K is the environmental carrying capacity (quantified in terms of individuals, N), then $K - N$ gives a measure of the unused carrying capacity, and $(K - N)/K$ gives the fraction of carrying capacity still remaining. Thus

$$\frac{\mathrm{d}N}{\mathrm{d}t} = rN\left(\frac{K-N}{K}\right)$$

If N is near zero, the carrying capacity is largely unused, and $\mathrm{d}N/N\mathrm{d}t$ is near r. If $N = K$, the environment is totally used or occupied, and $\mathrm{d}N/N\mathrm{d}t = 0$. In this continuous, differential equation model, r is an instantaneous rate, but its numerical value is defined over a finite time period.

To project a time trajectory of logistic population growth, we need to integrate the differential equation from time (0) to time (t).

$$N(t) = \frac{K}{1 + \left(\frac{K - N(0)}{N(0)}\right) e^{-(rt)}}$$

A plot of $N(t)$ with respect to time gives a sigmoid (S-shaped) trajectory, where growth is nearly exponential when N is near zero, and slows to equilibrium at $N = K$. When initial population size exceeds the carrying capacity, numbers fall in an asymptotic approach toward K

Sometimes the feedback of density on per capita growth rate is not instantaneous. For example, the effect of malnutrition on population growth might not be strongly evident before malnourished juveniles reach reproductive age. We can simulate this process by assuming that growth rates are affected by population size in some previous time period. Thus

$$\frac{\mathrm{d}N}{\mathrm{d}t} = rN(t)\left(1 - \frac{N(t-\tau)}{K}\right)$$

where τ is a time lag. There is no definite integral for this equation, so we project time trajectories by summing instantaneous changes in population size via numerical integration. Because the lag is delayed by an amount τ, a growing population may reach and overshoot the carrying capacity before the negative feedback term causes the population to stop growing or decline. The resulting oscillation may damp to a stable equilibrium or continue indefinitely as a limit cycle.

A population with discrete generations or cohorts cannot adjust instantaneously to changes in density-dependent feedback, because births occur only once in each generation or cohort interval. There is an implicit lag associated with the period of discrete population growth increments. With the lagged logistic model of the previous section, lag time, τ, could vary in length; but with a discrete logistic model it is constant, fixed by the interval of discrete time steps. As a result, *r* and *K* alone determine the dynamics. When *r* is small, the population may not grow fast enough to overshoot carrying capacity within the lag time of a single cohort interval; but as *r* increases, sustained oscillations are more likely. Several approaches have been used to formulate difference equations analogous to the continuous logistic equation, but they yield similar results. The version implemented in *Populus* is:

$$N_{t+1} = N_t e^{r\left(1-\frac{N_t}{K}\right)}$$

With a small population-growth rate, *r*, this discrete model gives a sigmoid approach to equilibrium, just like continuous and lagged logistic models. With increasing *r* values, discrete logistic dynamics show damped oscillation; then 2-point cycles of constant period and amplitude; and then cycles that include 4 points, 8 points, 16 points, etc., before repeating. Finally, very large *r* values cause population size to fluctuate in a way that is extremely sensitive to initial conditions, and never settles into a precisely repeating cycle, a regime that mathematicians term "chaotic."

References

Alstad, D. N. 2001. *Basic Populus Models of Ecology*. Prentice Hall. Upper Saddle River, NJ. Chapter 2.

Case, T. J. 2000. *An Illustrated Guide to Theoretical Ecology*. Oxford University Press. New York. pp. 103-155.

Hutchinson, G. E. 1978. *An Introduction to Population Biology*. Yale University Press, pp. 1-40.

May, R. M. 1974. Biological populations with non-overlapping generations: stable points, stable cycles, and chaos. Science 156:645-647.

May, R. M. 1976. Models for Single Populations. In: *Theoretical Ecology: Principles and Applications*, R. M. May, Ed. Sinauer Associates, Sunderland, MA.

Age-Structured Population Growth

Youngsters and oldsters give birth and die at different rates. To keep track of these differences and their effect on population growth, biologists divide an organism's life into a series of discrete intervals, each representing a cohort of individuals that are about the same age and have similar expectations of survival and fertility. By listing S_x, the number of surviving individuals in each cohort by age, x, we can specify the composition of an age-structured population. We can also tabulate age-specific changes of fertility and survival in a life table, or $l_x m_x$ schedule. The first component, l_x, is the average probability of survival from birth to age x. The second component, m_x, is the average number of female offspring that a female can expect to acquire when she reaches age x. With these life history parameters, we can then project population growth by cohort, or with a weighted average of fertility and survival rates over all ages.

This *Populus* module provides three different visual representations of a life history, allowing students to see a life-table or $l_x m_x$ schedule, a life-cycle graph of the age classes and transition probabilities, or a population state vector listing S_x, the number of survivors in each age class, with the Leslie projection matrix. Students can compare views, and provide the data to initiate a demographic projection in any of the three formats. There are output graphs showing changes in population size, population composition, the expectation of future progeny, and a tabular output illustrating the computations that project population composition, based on the $l_x m_x$ schedule, the initial S_x values, and assumptions about the timing of reproduction and population censuses.

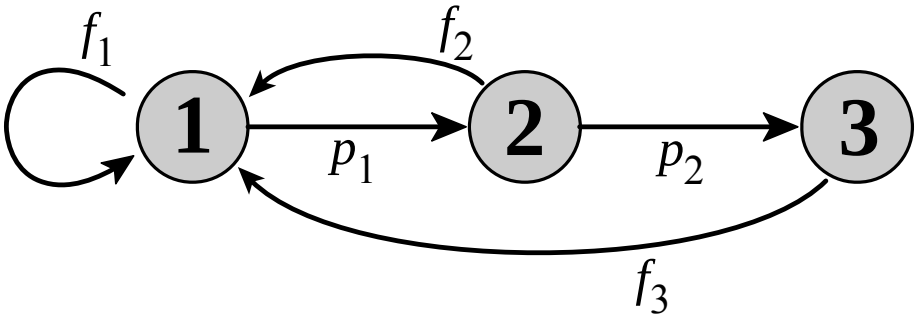

Figure 1. Hypothetical life cycle graph illustrating the process of demographic projection. Shaded circles represent three successive ages, with arrows indicating the transition probabilities. The projection interval is the same as the discrete period between reproductive seasons. Each arrow indicates the passage of a projection interval, so that progeny born to age-1 parents will themselves be 1 year of age at the next time step, when their parents will have reached age 2.

There are several ways of specifying the age-specific fertilities and probabilities of survival for a demographic projection. Fertilities can be tabulated as the average number of offspring accruing to a female when she reaches age x (this is the m_x of an $l_x m_x$ schedule), or the number of progeny of an age x female that are expected to be alive after the next projection interval (this is the f_x from the first row of a Leslie Matrix). Survival probabilities can be specified over x projection steps from age 0 to age x (this is l_x) or a single projection step from ages x-1 to x, or x to x+1 (this is the p_x just below the diagonal of a Leslie Matrix). The different styles of visual representation require *Populus* to convert and manipulate these survival and fertility parameters, and the exact details depend on assumptions about the timing of population censuses and reproduction of the

organisms in question. When reproduction occurs seasonally at discrete intervals and the population census comes immediately after reproduction, then

$$p_x = \frac{l_x}{l_{x-1}} \quad \text{and} \quad f_x = p_x m_x$$

If censuses are made immediately before reproduction, then newborn individuals must survive a full projection interval before they are tabulated in their first census, so

$$p_x = \frac{l_{x+1}}{l_x} \quad \text{and} \quad f_x = l_1 m_x$$

Finally, when reproduction is continuous rather than pulsed in discrete seasons, the length of projection time steps is arbitrary, and probabilities of survival and reproduction are averages of the values at the beginning and end of each interval.

$$p_x = \frac{l_x + l_{x+1}}{l_{x-1} + l_x} \quad \text{and} \quad f_x = \left(\frac{1 + l_1}{2}\right)\left(\frac{m_x + p_x m_{x+1}}{2}\right)$$

Projecting a Constant $l_x m_x$ Schedule

Consider a hypothetical population with discrete reproduction, comprised at an initial post-reproductive census only of S_0 newborn individuals. At the next census, $l_1 S_0$ of those newborns will still be alive; they will have just passed age 1, each producing m_1 newborn progeny of their own, so that the new population is comprised of two cohorts. If l_x and m_x values remain constant, this process can be projected indefinitely.

x	l_x	m_x	$S_x(0)$	$S_x(1)$	$S_x(2)$	$S_x(3)$	$S_x(4)$	$S_x(5)$
0	1.0	0	4	2	6	5.5	10.3	12.1
1	0.5	1	0	2	1	3	2.8	5.1
2	0.25	5	0	0	1	0.5	1.5	1.4
3	0	-	0	0	0	0	0	0
		$\Sigma S_x = N$	4	4	8	9	14.5	18.5

The first three columns in this table give x, l_x and m_x. The shaded fourth column gives a hypothetical initial population, consisting in this case of 4 newborn individuals. The projection of this population to subsequent time steps 1-5 is made for each succeeding time step by first tabulating the number of 1- and 2-step-old adults, and then adding the progeny they can expect on reaching each age x. The projection shows that if l_x and m_x remain unchanged, the ratio of successive population sizes, $\lambda = N_{t+1}/N_t$, often converges on a constant value, and the proportional representation of each age class then reaches a constant Stable Age Distribution. Thus, a population with a constant age-specific schedule of survival and reproduction may be started with any arbitrary composition, but will usually settle down to a constant growth rate, λ, and a stable age distribution.

It is also possible to project the constant growth of an age structured population with some simple weighted average rate estimates. The Net Reproductive Rate, R_0, gives the number of

female progeny expected to accrue during the entire lifetime of an individual female. It is calculated as

$$R_0 = \sum l_x m_x$$

which is the sum of offspring produced in each age interval, weighted by the mother's probability of surviving to that age. The mean generation length or cohort generation time, T_c, is estimated as

$$T_c \approx \frac{\sum x l_x m_x}{\sum l_x m_x} = \frac{\sum x l_x m_x}{R_0}$$

the weighted average of a female's ages when each of her progeny are born. From these two averages, we can approximate population growth, λ or r, as

$$\lambda \approx \frac{R_0}{T_c} \qquad \text{or} \qquad r \approx \frac{\ln R_0}{T_c}$$

This approximation is fairly accurate for semelparous life histories (where organisms only breed once, like the *Onchorhynchus* salmon of the North Pacific) or populations that are not growing significantly. For iteroparous (multiple-brooding) life histories in growing populations, we determine r with any desired precision by successive approximation using the Lotka-Euler equation,

$$\sum e^{-rx} l_x m_x = 1$$

Matrix Projection

The *Populus* program represents population composition as a vector whose elements are S_x values, the numbers of individuals in each age class. To project a subsequent composition, this vector is multiplied by a transformation matrix (the "Leslie Matrix"), which has age-specific fertility values, f_x, in its first row, and probabilities of surviving from one age to the next, p_x, below the diagonal. The product of this matrix multiplication is a new vector, specifying the S_x values of the population at the next succeeding census. Students who need to review the basics of matrix multiplication can consult the *Populus* book. The Lotka-Euler equation is the characteristic equation of this projection matrix, and λ is its dominant eigenvalue.

$$\begin{pmatrix} S_1(t+1) \\ S_2(t+1) \\ S_3(t+1) \\ \vdots \\ S_n(t+1) \end{pmatrix} = \begin{pmatrix} f_1 & f_2 & f_3 & \cdots & f_n \\ p_1 & 0 & 0 & \cdots & 0 \\ 0 & p_2 & 0 & \cdots & 0 \\ \vdots & \ddots & \ddots & \cdots & \vdots \\ 0 & 0 & 0 & p_{n-1} & 0 \end{pmatrix} \begin{pmatrix} S_1(t) \\ S_2(t) \\ S_3(t) \\ \vdots \\ S_n(t) \end{pmatrix}$$

Computational Notes

Reproductive Value, V_x, is a function of age. This is the expected number of future female progeny for a female of age x, relative to the expected future output of a newborn female, R_0.

$$V_x = \left(\frac{e^{rx}}{l_x}\right)\left(\sum_{y=x}^{\infty} e^{-ry} l_y m_y\right)$$

When students elect to initiate a demographic simulation by specifying elements of the Leslie Matrix and population state vector, it is necessary for our program to specify l_x in terms of p_x, and m_x in terms of f_x and p_x. For continuously reproducing organisms, I am not aware that these relations have been published previously. The solution worked out by *Populus* programmer Amos Anderson is that

$$l_x = \prod_{i=0}^{i=x-1} p_i - l_{x-1} \quad \text{and} \quad m_x = \frac{4 f_{x-1}}{p_0 p_{x-1}} - \frac{m_{x-1}}{p_{x-1}}$$

Any m_x can then be found recursively, working backward from the first $m_x = 0$.

References

Alstad, D. N. 2001. *Basic Populus Models of Ecology*. Prentice Hall. Upper Saddle River, NJ. Chapter 3.

Case, T. J. 2000. *An Illustrated Guide to Theoretical Ecology*. Oxford University Press. New York. pp. 45-103.

Caswell, H. 1989. *Matrix Population Models*. Sinauer Associates, Sunderland, MA. 328 pp.

Jenkins, S. H. 1988. Use and abuse of demographic models of population growth. Bulletin of the Ecological Society of America 69:201-7.

Lanciani, C. A. 1987. Teaching quantitative concepts of population ecology in general biology courses. Bulletin of the Ecological Society of America, 68:492-95.

Leslie, P. H. 1945. On the use of matrices in certain population mathematics. Biometrika 33:183-212.

May, R. M. 1976. Estimating *r*: a pedagogical note. American Naturalist 110:496-499.

Stage-Structured Populations

Matrix projection is easily adapted to population analyses using categories other than age. For example, many perennial plants pass through a series of recognizable life-history stages, beginning as seeds, germinating to form vegetative stages that may grow for several years, and finally developing reproductive structures that produce new seeds. The precise duration of each stage can vary from plant to plant, depending on environmental conditions such as access to light, water, and soil nutrients. Seeds might germinate at their first opportunity, or remain dormant in the soil for an extended period. Vegetative stages with ample resources may produce flowers and seeds from an early age. In contrast, "century plants" of the desert southwest (*Agave kaibabensis*) grow as vegetative rosettes for many years before producing a single flower stalk and dying. It can be difficult or impossible to determine the age of such plants, and much more convenient to base demographic analyses on the stages of their life history. Some plants reproduce both sexually and vegetatively, so the analysis of these life cycles can be complex.

Caswell (1982, 1989) introduced graphical techniques that make it easier to keep track of complex stage-structured life cycles. The first example in Figure 1 shows a Caswell life-cycle graph for an age-structured population, but with four stages, represented by numbered circles.

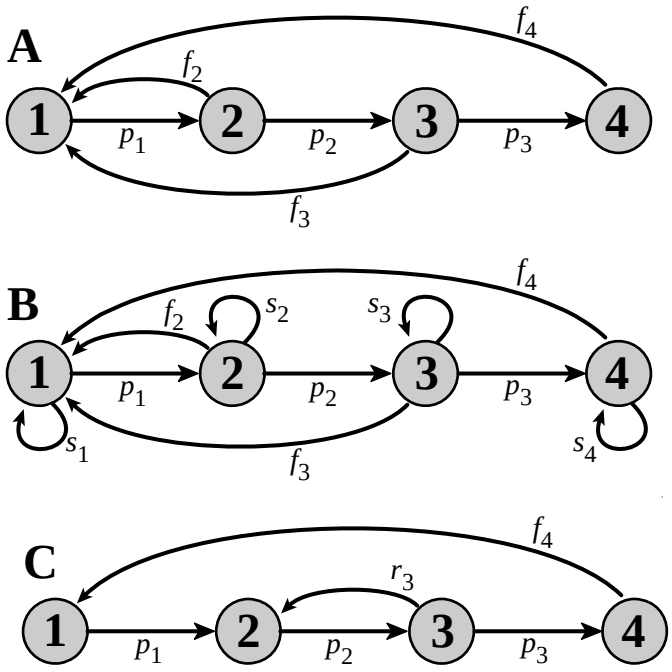

Arrows connect stage nodes *i* and *j* if individuals in stage *i* at time *t* can contribute individuals to node *j* at time *t*+1, by surviving, growing, or reproducing. Survival and fertility parameters are defined just as they were in *Populus* simulations of Age-Structured Population Growth, and the stage-projection matrix that corresponds to this life-cycle diagram is

$$\mathbf{A} = \begin{pmatrix} 0 & f_2 & f_3 & f_4 \\ p_1 & 0 & 0 & 0 \\ 0 & p_2 & 0 & 0 \\ 0 & 0 & p_3 & 0 \end{pmatrix}$$

Notice that it has the same form as the Leslie matrix of the previous section.

An important difference between stage- and age-structured populations is that the organisms may remain in one stage over several projection intervals. The second diagram in Figure 1 illustrates such cases. The coefficients "*p*" give the probabilities of moving from one stage to the next; *s* values give the probability of remaining in the same stage through the next time step; and *f* is the fertility coefficient, as before. The matrix that we use to project the changing composition of this population over time must include the probabilities of advancing to a new stage and remaining in the same stage at each time step. Probabilities of advancing, *p*, run diagonally across the age projection matrix in positions where the row (*i*) and column (*j*) addresses are $i = j+1$. Probabilities of remaining in place at the next census, *s*, go diagonally across the projection matrix in positions where $i = j$. The stage-projection matrix corresponding to life cycle B of Figure 4.8 is

$$\mathbf{B} = \begin{pmatrix} s_1 & f_2 & f_3 & f_4 \\ p_1 & s_2 & 0 & 0 \\ 0 & p_2 & s_3 & 0 \\ 0 & 0 & p_3 & s_4 \end{pmatrix}$$

Life-cycle graphs can illustrate natural histories that are even more complex. All of the projection matrices we have studied to this point confine reproductive parameters to the top row; new individuals are always in stage 1 when first counted. This is not necessarily the case in stage-structured populations. The third case in Figure 4.8 represents a life cycle where individuals produce stage-1 progeny if they reach stage 4, but also produce stage-2 progeny if they reach stage 3. These two kinds of progeny could be seeds and vegetative tillers, respectively. Now the projection matrix will have reproductive parameters below its top line.

$$\mathbf{C} = \begin{pmatrix} 0 & 0 & 0 & f_4 \\ p_1 & 0 & r_3 & 0 \\ 0 & p_2 & 0 & 0 \\ 0 & 0 & p_3 & 0 \end{pmatrix}$$

It is also possible for a plant to regress to some earlier stage. For example, a large vegetative plant that suffers heavy herbivory and loses much of its biomass may regress to a small vegetative stage.

These examples of age- and stage-structured population growth demonstrate that the tools of matrix projection are quite flexible, facilitating study of both simple and complex life cycles.

They also allow conclusions to be drawn about the dynamics of structured populations, directly from properties of the projection matrix. Advanced students who wish to explore these techniques further will find valuable guidance in Caswell (1989).

References

Alstad, D. N. 2001. *Basic Populus Models of Ecology*. Prentice Hall. Upper Saddle River, NJ. Chapter 3.

Case, T. J. 2000. *An Illustrated Guide to Theoretical Ecology*. Oxford University Press. New York. pp. 45-103.

Caswell, H. 1982. Stable population structure and reproductive value for populations with complex life cycles. Ecology 63:1223-1231.

Caswell, H. 1989. *Matrix Population Models*. Sinauer Associates, Sunderland, MA. 328 pp.

Lotka-Volterra Competition

Density-dependent growth models like the logistic equation simulate an intraspecific competitive process; resources become limiting as the population increases, and the per capita growth rate declines. In this program, an additional term is added to the logistic to represent interspecific density-dependent effects, and a pair of the resulting expressions comprise the "Lotka-Volterra competition equations," which provide a simple and historically important vehicle for thinking about competitive interactions.

In the Lotka-Volterra equations, densities of both species are subtracted from the carrying capacity to give a density-dependent feedback term, and the number of interspecific competitors is weighted by a term called the competition coefficient which varies with the species' similarity in resource requirements. Thus

$$\frac{\mathrm{d}N_1}{\mathrm{d}t} = r_1 N_1 \left(\frac{K_1 - \left(N_1 + \alpha N_2 \right)}{K_1} \right)$$

$$\frac{\mathrm{d}N_2}{\mathrm{d}t} = r_2 N_2 \left(\frac{K_2 - \left(N_2 + \beta N_1 \right)}{K_2} \right)$$

where N_1 represents the density of species 1, K_1 is the environmental carrying capacity of species 1, r_1 is its intrinsic rate of increase, and α is the competition coefficient, a proportionality constant defining the amount of K_1 used by every individual of species 2. In the second expression, β is an analogous coefficient weighting the effect of each species 1 individual on K_2.

This pair of simultaneous non-linear differential equations has no unique solution. Any combination of parameters derived from the first equation affects the dynamics of the second. This difficulty does not prevent them from offering interesting insights. Returning to the premise of the lecture: we want to predict the outcome of competition. The equations describe a dynamic interaction that goes to some equilibrium outcome (coexistence or displacement) and remains constant. At this outcome point,

$$\frac{dN_1}{dt} = 0 \quad \text{and} \quad \frac{dN_2}{dt} = 0$$

Thus we can set both Lotka-Volterra equations equal to zero, and produce expressions which define the relative numbers of sp_1 and sp_2 at equilibrium. For example,

$$\frac{dN_1}{dt} = 0 = r_1 N_1 \left[\frac{K_1 - N_1 - \alpha N_2}{K_1} \right]$$

The expression is equal to zero if $r = 0$ and/or if $N_1 = 0$, but these are trivial cases of a population with no individuals, or no growth potential. The interesting case is the one where the parenthetic feedback expression is equal to zero:

$$0 = \left[\frac{K_1 - N_1 - \alpha N_2}{K_1} \right]$$

$$0 = K_1 - N_1 - \alpha N_2$$

$$N_1 = K_1 - \alpha N_2 \quad \text{or} \quad N_2 = \frac{K_1}{\alpha} - \frac{1}{\alpha} N_1$$

Equations 5-7 give a straight line. If we plot a phase plane graph of N_2 on the y-axis and N_1 on the x-axis, the x-intercept = K_1; the y-intercept = K_1/α; and the slope is $-1/\alpha$. If we plotted N_1 on the y and N_2 on the x, the slope would be $-\alpha$.

Figure 1 shows the ratio of relative abundances of N_1 and N_2 for which $dN_1/dt = 0$. The line is called an *ISOCLINE*. The y-intercept shows that K_1/α is the number of *species*$_2$ that can hold changes in *species*$_1$ density at 0.

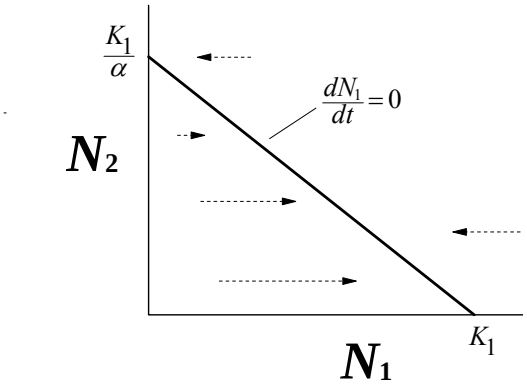

Figure 1. Isocline (zero net growth line) for Species 1.

If the number of *species*$_1$ and *species*$_2$ corresponds to a point inside the isocline, $dN_1/dt >$ zero, and N_1 will increase. If the density pairs fall outside the isocline, then $dN_1/dt < 0$ and the population size (of N_1) will fall. The *species*$_1$ isocline says nothing about *species*$_2$ dynamics.

Corresponding arguments for *species*$_2$:

$$0 = K_2 - N_2 - \beta N_1$$

$$N_2 = K_2 - \beta N_1 \quad \text{and} \quad N_1 = \frac{K_2 - N_2}{\beta}$$

The points on the isocline are combined abundances of *species*$_1$ and *species*$_2$ that can hold $dN_2/dt = 0$. K_2/β is the number of *species*$_1$ that can hold $N_2 = 0$. The slope of this isocline is $-\beta$ (if we plot N_2 vs N_1). With relative densities representing a point inside the isocline, N_2 increases, etc.

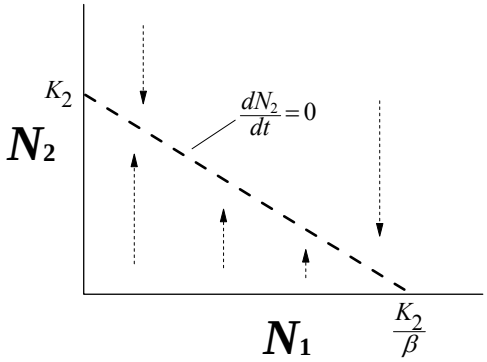

Figure 2. Isocline for Species 2. At all ratios of abundance falling on the isocline, $dN_2/dt = 0$.

Isocline Analyses of the Conditions of Coexistence and Displacement

By superimposing the isoclines of both species on the same graph, we can observe the effect of all possible N_1 and N_2 ratios on the dynamics of both species. There are 4 possible ways in which the isoclines could fall together:

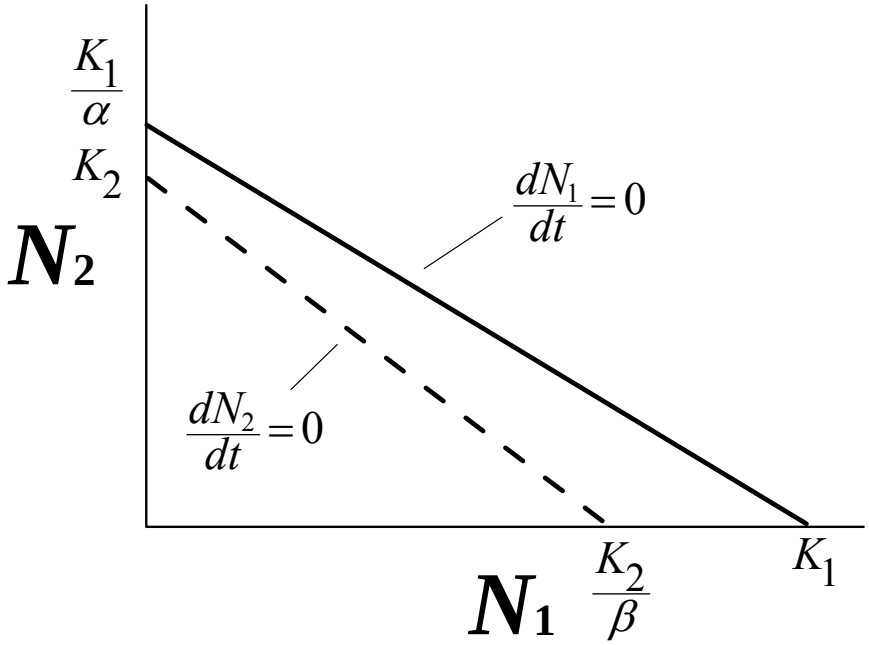

Case I:

In this case, $K_1 > K_2/\beta$. This implies that the N_1 which holds $dN_2/dt = 0$ is smaller than the N_1 which holds $dN_1/dt = 0$. Therefore, *species*$_1$ is inhibiting *species*$_2$ more strongly than it inhibits itself. In this case, the outcome is always competitive displacement. Note also that $K_2 < K_1/\alpha$, so N_2 is inhibiting itself more strongly than it inhibits N_1.

Case II:
This case is just the opposite of Case I. Here $K_2 > K_1/\alpha$, thus *species*$_2$ displaces *species*$_1$.

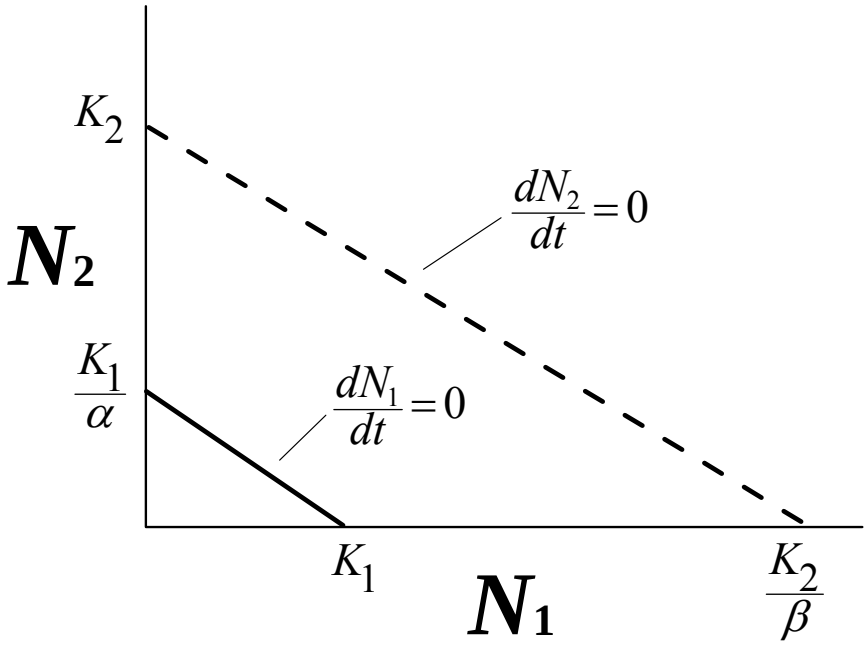

Case III:

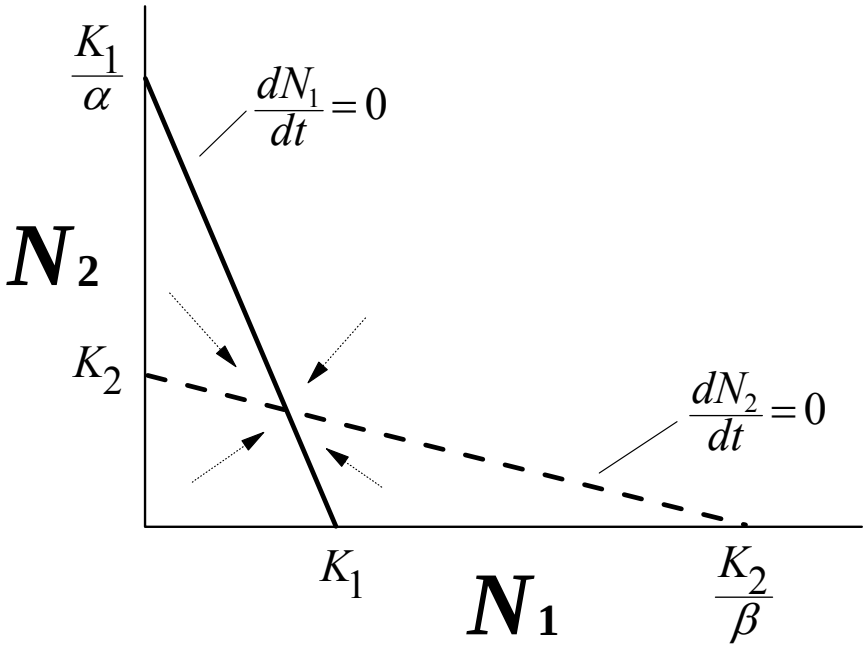

In Case III, the isoclines cross, producing an equilibrium poin, where $dN_1/dt = 0 = dN_2/dt$. Here $K_2/\beta > K_1$, and $K_1/\alpha > K_2$. Thus each species inhibits itself more than it inhibits the other. These are the conditions required for the stable coexistence of competitors.

Case IV:

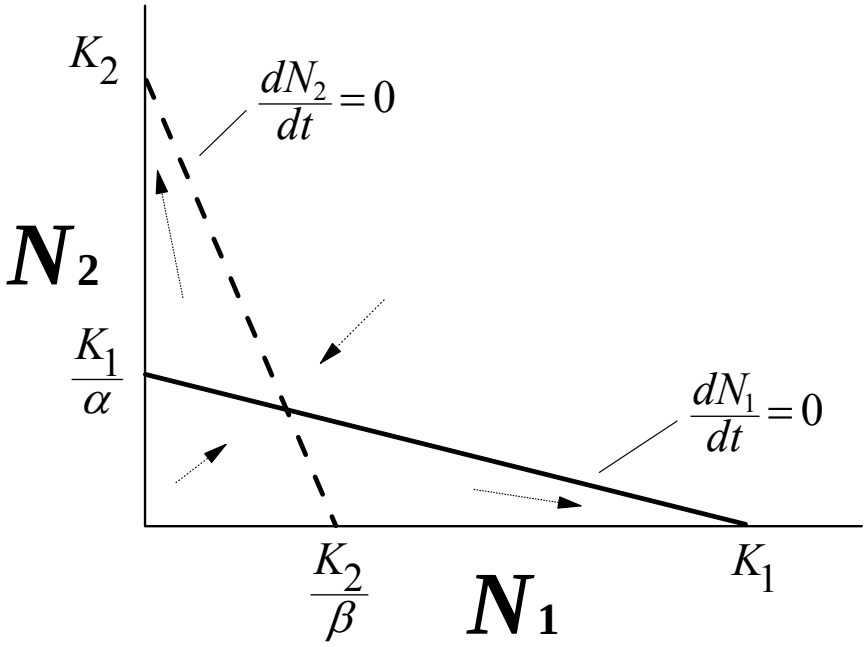

Here each species inhibits the other more than it inhibits itself, because $K_1/\alpha < K_2$, and $K_2/\beta < K_1$. The outcome of this case is always competitive displacement; either species may win,

depending on the initial starting ratios. Note the equilibrium point. Plot vectors to demonstrate that the equilibrium is unstable.

The Lotka-Volterra Competition Model has largely been replaced in the thinking of ecologists by models that offer much more mechanistic insight, like the Resource Competition Models of Stewart & Levin, and Tilman. It is most often used in ecological pedagogy to introduce the technique of isocline analysis, which is widely use to investigate the behavior of models near their equilibria.

References

Alstad, D. N. 2001. *Basic Populus Models of Ecology*. Prentice Hall, Upper Saddle River, NJ. Chapter 4.

MacArthur, R. H. 1972. *Geographical Ecology*. Harper & Row. New York. pp. 21-58.

Hutchinson, G. E. 1978. *An Introduction to Population Ecology*. Yale University Press. New Haven. pp. 117-151.

Keddy, P. A. 1989. *Competition*. Chapman & Hall, New York. pp. 48-79.

Infectious Microparasitic Diseases

Parasites ranging from viruses and bacteria to fungi, helminths and arthropods can cause infectious diseases that have a strong influence on the dynamics of their hosts. Roughly a third of the inhabitants of Europe succumbed to plague during the Black Death pandemic of 1348 and 1349. Parasites can also serve our management objectives, offering a biological means for controlling agricultural pests. In 1950-1952 a *Myxoma* pox virus of the tropical forest rabbit, *Sylvilagus brasiliensis*, was introduced into Australia and Europe to control European rabbits, *Oryctolagus cuniculus*. The resulting myxomatosis produced case-mortality rates of 99.8%, rabbit populations fell by more than 95%, and survivors were subsequently restricted to marginal, non-agricultural habitats.

These host-parasite interactions differ from those of predators and prey because the diseases do not necessarily kill the host, and because recovered hosts often develop a long-term immunity to reinfection. To simplify the analysis of disease dynamics, it is useful to distinguish between micro- and macroparasites. Microparasites (like the *Variola* viruses that caused smallpox) reproduce quickly, reaching tremendous population densities within a host. The duration of infections is often limited by host defenses and short relative to host life span, and recovered victims may develop lifetime immunity. As a result, microparasite dynamics are driven largely by transmission between hosts, and their essentials can be captured by models that classify host individuals as susceptible, infected, or recovered and subsequently immune, without accounting for within-host abundance of the parasite. In contrast, macroparasites (like intestinal flatworms) typically cause chronic and persistent infections. Disease severity depends on the number of parasites present, and a small fraction of the host population may harbor most of the parasites. Satisfactory models of macroparasite dynamics must account for this host-to-host variation in parasite abundance.

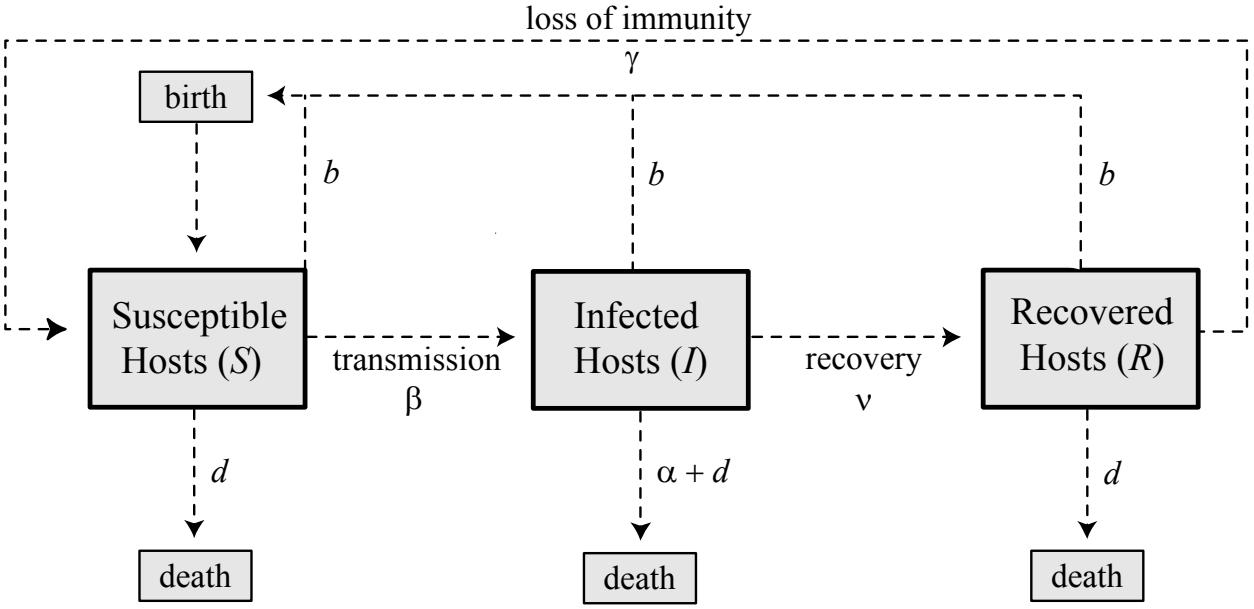

Figure 1. Schematic of a host-microparasite model, with the host population divided into susceptible, infected, and immune classes, after Anderson and May, 1992.

The *Populus* microparasite simulation presents a model developed by Anderson and May (1979, 1982) from classic approaches of Ross (1916, 1917) and Kermack & McKendrick (1927), and includes an alternative transmission process detailed by Getz & Pickering (1983). The model describes a host population of size N, containing susceptible individuals (***S***) who are not infected, infected individuals (***I***) who can pass the parasite to others, and immune individuals (***R***) who have encountered the disease and recovered (Figure 1). Susceptible individuals arise through birth or the loss of immunity at *per capita* rates b and γ, respectively. Individuals leave the susceptible class through natural mortality (rate d), or by acquiring the parasite (*per capita* rate β) after encountering an infected host. They leave the infected category through natural mortality (rate d), disease-induced mortality (rate α), or through recovery (rate ν) of hosts that become immune.

The model assumes that (1) individuals are uninfected at birth, (2) newly infected hosts can transmit the disease immediately, (3) there is no age structure among hosts, (4) the disease does not affect host fecundity, and (5) host populations are large enough so that chance can be ignored. The basic Anderson & May model assumes further that (6) that there is no density-dependent feedback among hosts other than parasite-induced mortality, and (7) infections occur in direct proportion to the number of encounters between susceptible and infected individuals, set by the product of their respective population densities (SI). We call this mass-action infection process *density-dependent transmission*.

To summarize, the model parameters are:

N = total host population density
S = susceptible host density
I = infected host density
R = immune host density
b = the host birth rate
d = host natural mortality rate
α = disease-induced mortality rate
β = between-host transmission rate
ν = recovery rate of infected hosts
γ = rate of immunity loss

Based on these assumptions, we can specify a differential equation for the dynamics of each host class as follows:

$$\frac{\mathrm{d}S}{\mathrm{d}t} = b\left(S + I + R\right) - dS - \beta SI + \gamma R \tag{1}$$

$$\frac{\mathrm{d}I}{\mathrm{d}t} = \beta SI - \left(\alpha + d + \nu\right) I \tag{2}$$

$$\frac{\mathrm{d}R}{\mathrm{d}t} = \nu I - \left(d + \gamma\right) R \tag{3}$$

The terms represent transition arrows in Figure 1. For example, the two positive terms in equation 1 represent increments to the susceptible S class resulting from birth and the loss of immunity. The two negative terms represent losses due to natural mortality and disease transmission.

We can add these three expressions to specify change in the total host population size,

$$\frac{dN}{dt} = (b - d)N - \alpha I \tag{4}$$

Theoretical ecologists often assume that population size is large, so that a deterministic model (like the one embodied in these equations) gives the expectation of an analogous stochastic version. With a nonlinear transmission term (βSI) in equations 1 and 2, any covariance between S and I will cause this assumption to be violated. S and I will covary whenever the population is not homogeneously mixed. Since it is unlikely that one individual will have an equal probability of encountering every other population member, we should bear this assumption in mind as we consider implications of the basic microparasite model.

Dynamics

Although microparasites often reproduce rapidly within a susceptible host, transmission between hosts is the critical feature of their dynamics. We define the *net reproductive rate* of a disease as the number of newly infected individuals produced by a single infected host introduced into a population of susceptibles. From equation 2, the *per capita* increase of infected individuals is

$$\frac{dI}{I dt} = \beta S - (\alpha + d + \nu) \tag{5}$$

This implies that the infected class is incremented by a product of transmission rate (β) and the number of susceptibles (S), and decremented by a sum of three rates, due to diseased-induced mortality (α), natural mortality (d), and host recovery (ν). The reciprocal of $(\alpha + d + \nu)$ is the average interval during which an infected individual can transmit the disease, and the number of new cases that it will cause during this period is βS. So the net reproductive rate, R_0, is

$$R_0 = \frac{\beta S}{\alpha + d + \nu} \tag{6}$$

Intuitively, it might seem reasonable to derive this net reproductive rate by integrating equation 5 over the average lifetime of a diseased host, but such an estimate would include cases caused by secondary transmission.

R_0 must equal or exceed 1.0 for the disease to persist, so we can set $R_0 = 1$ and rearrange equation 6 to specify the susceptible host density (S) necessary to sustain the parasite (assuming that the various rates remain constant and the population is homogeneously mixed).

$$S = \frac{\alpha + d + \nu}{\beta} \tag{7}$$

This minimum S is often called N_T, the disease's threshold host-population density; it is a minimum number of susceptible hosts (a resource concentration) required by the parasite, which will decline to extinction unless $S > N_T$.

Following the analyses often applied to predator-prey systems, it is interesting to ask whether microparasitic diseases might regulate host populations. If we define the *intrinsic growth rate* of

uninfected hosts as $r = b - d$ and the *prevalence* of the disease (the infected fraction of the host population) as $y = I/N$, then equation 4 can be rearranged to give

$$\frac{\mathrm{d}N}{\mathrm{d}t} = (r - \alpha y) N \tag{8}$$

This shows that if the induced mortality (α) is sufficiently large it will compensate intrinsic growth (r), and the disease can regulate host density at a stable value, N^*. The prevalence of the disease at this equilibrium is found by setting $\mathrm{d}N/\mathrm{d}t = 0$ in equation 8, giving

$$y^* = \frac{r}{\alpha} \tag{9}$$

and because at equilibrium the overall death rate ($\alpha+d$) will equal the birth rate (b), the proportion of host deaths attributable to the disease will be

$$\frac{b-d}{b} \tag{10}$$

Frequency-Dependent Transmission

The homogeneous mixing assumed in equations 1-3 (particularly in the density-dependent transmission term βSI) is often inappropriate. For example, in many species, individuals have a limited number of sexual partners. A sexually transmitted disease will be transmitted in proportion to its frequency among mates, and the number of diseased individuals in the population as a whole is only relevant to the degree that it sets disease frequency in the subset of partners. Getz and Pickering (1983) add frequency-dependent transmission to the basic system of equations 1-3:

$$\frac{\mathrm{d}S}{\mathrm{d}t} = b(S + I + R) - dS - \frac{\beta SI}{N} + \gamma R \tag{11}$$

$$\frac{\mathrm{d}I}{\mathrm{d}t} = \frac{\beta SI}{N} - (\alpha + d + \nu) I \tag{12}$$

$$\frac{\mathrm{d}R}{\mathrm{d}t} = \nu I - (d + \gamma) R \tag{13}$$

These three expressions can be summed to produce a differential equation for total population growth identical to equation 4.

The dynamics of this system are fundamentally different from those of the density-dependent transmission model. If we examine threshold conditions as we did in arriving at equation 7, we find that

$$\frac{S}{N} = \frac{\alpha + d + \nu}{\beta} \tag{14}$$

The host population may grow exponentially, or parasites may drive the host to extinction. In either case, because $S/N \le 1$, there is no threshold, the infection can spread at very low

susceptible densities, and parasites are no longer able to regulate host density at a stable equilibrium. This is the basis of May's observation that "Sexually transmitted parasites, which produce long-lasting infections and do not induce acquired immunity in recovered hosts, can be admirably adapted to persist in low-density populations of promiscuous hosts" (May 1983, p38).

References

Alstad, D. N. 2001. *Basic Populus models of Ecology*. Prentice Hall, Upper Saddle River, NJ. Chapter 6.

Anderson, R. M. 1982. Transmission dynamics and control of infectious disease agents. IN: Anderson, R. M., and R. M. May (eds), *Population Biology of Infectious Diseases* (Dahlem Conference Report). Springer-Verlag, 315 pp.

Anderson, R. M., and R. M. May. 1979. Population biology of infectious diseases: Part I. Nature 280:361-7.

Anderson, R. M., and R. M. May. 1982. Directly transmitted infectious diseases: control by vaccination. Science 215:1053-60.

Anderson, R. M., and R. M. May. 1991. *Infectious disease in humans*. Oxford University Press. ISBN 019 854 5991.

Getz, W. M. and J. Pickering. 1983. Epidemic models: thresholds and population regulation. American Naturalist 121:892-8.

May, R. M. 1983. Parasitic infections as regulators of animal populations. American Scientist 71:36-45.

Macroparasitic Infections

Helminthes like intestinal tapeworms and nematodes tend to produce chronic infections in which both morbidity and parasite reproduction depend on the worm burden of individual hosts. Parasites are often over-dispersed, so that a few hosts harbor many worms, and host-to-host variance in parasite loads may be extreme. As a result, it is not sufficient to divide a host population into susceptible, infected and resistant classes; successful macroparasite models must track the worm burden of individual hosts, either explicitly, or by assuming some probability distribution of parasite loads. This module implements a basic model by Roy Anderson and Robert May (*cf*. A & M 1978; M & A 1978, 1979) that characterizes between-host variation in worm burdens with a negative binomial distribution. We also incorporate a modified version of the model by Andy Dobson and Peter Hudson (1992) that introduces a "hypobiotic" stage of arrested parasite development which occurs following infection, but before maturation into adult worms that affect host vitality. Dobson & Hudson instituted this modification to portray the biology of *Trichostrongylus tenuis*, a nematode parasite of red grouse in England and Scotland.

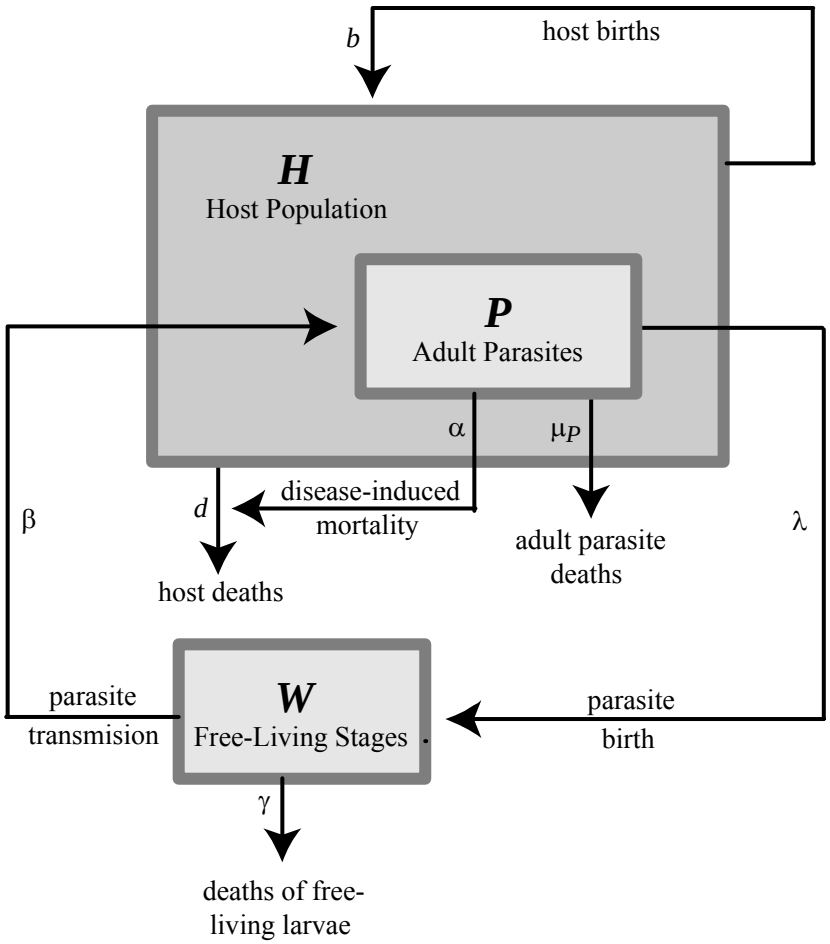

Figure 1. Schematic of a basic Anderson-May macroparasite model with direct transmission. Eggs or parasite larvae are shed from the host into the environment, and infect new victims without passage through a secondary host. Redrawn after Hudson (http://www.abo.fi/fak/mnf/biol/nni/prc1_phuds.html).

Parameters for the basic Anderson & May macroparasite model are:

H = total host population size (numbers)
P = total parasite population size (total numbers of adult worms)
W = population of free-living infective stage (eggs & larvae)
b = the host birth rate (/time)
d = the host natural mortality rate (/time)
α = disease-induced mortality rate (/worm/time)
β = transmission rate per host contact (/host/time)
λ = birth rate of parasite eggs or larvae (/time)
k = negative binomial aggregation parameter (a dimensionless constant inversely proportional to assumed parasite aggregation among hosts)
μ_P = natural mortality rate of adult parasites (/time)
γ = infective stage mortality rate (/time)

Based on these assumptions, we can specify a differential equation for the dynamics of hosts and parasites in each shaded box of the schematic as follows:

$$\frac{dH}{dt} = (b-d)H - \alpha P \tag{1}$$

$$\frac{dP}{dt} = \beta WH - (\mu_P + d + \alpha)P - \alpha \frac{P^2}{H}\left(\frac{k+1}{k}\right) \tag{2}$$

$$\frac{dW}{dt} = \lambda P - \gamma W - \beta WH \tag{3}$$

The final term in equation (2), $\alpha \frac{P^2}{H}\left(\frac{k+1}{k}\right)$, scales the negative effect of parasite-induced host mortality on parasite dynamics with parasite abundance and aggregation.

Anderson and May also proposed a simplified version of this model by assuming that the infective stages (W) are short lived, and hence likely to be at their equilibrium based on current values of H and P. If $dW/dt = 0$, then equation (3) can be solved for W as a function of H and P, $W = \frac{\beta H \lambda P}{\gamma + \beta H}$. Substituting this value into equation (2) rephrases the model in two equations, allowing a two-dimensional isocline analysis:

$$\frac{dH}{dt} = rH - \alpha P \tag{4}$$

$$\frac{dP}{dt} = \frac{\lambda HP}{H_0 + H} - (\mu_P + d + \alpha)P - \alpha \frac{P^2}{H}\left(\frac{k+1}{k}\right) \tag{5}$$

Here $r = b - d$ and $H_0 = \gamma/\beta$, which varies inversely with the transmission efficiency of the parasite.

The dynamics of this model depend on the parasite birth rate, λ, the host and parasite death rates, *d* and μ_P, respectively, and the disease-induced host mortality rate α. If

$$\lambda - (\mu_P + d + \alpha) > (b - d)\left(\frac{k+1}{k}\right) \tag{6}$$

then the parasite is capable of regulating host at an equilibrium where P*/H* = (b-d)/ α. If inequality (6) is not met, but

$$\lambda - (\mu_P + d + \alpha) > 0 \tag{7}$$

then hosts grow exponentially at a rate lower than the disease-free rate. Finally, if inequality (7) is not met, then the parasite cannot be maintained (May & Anderson 1979).

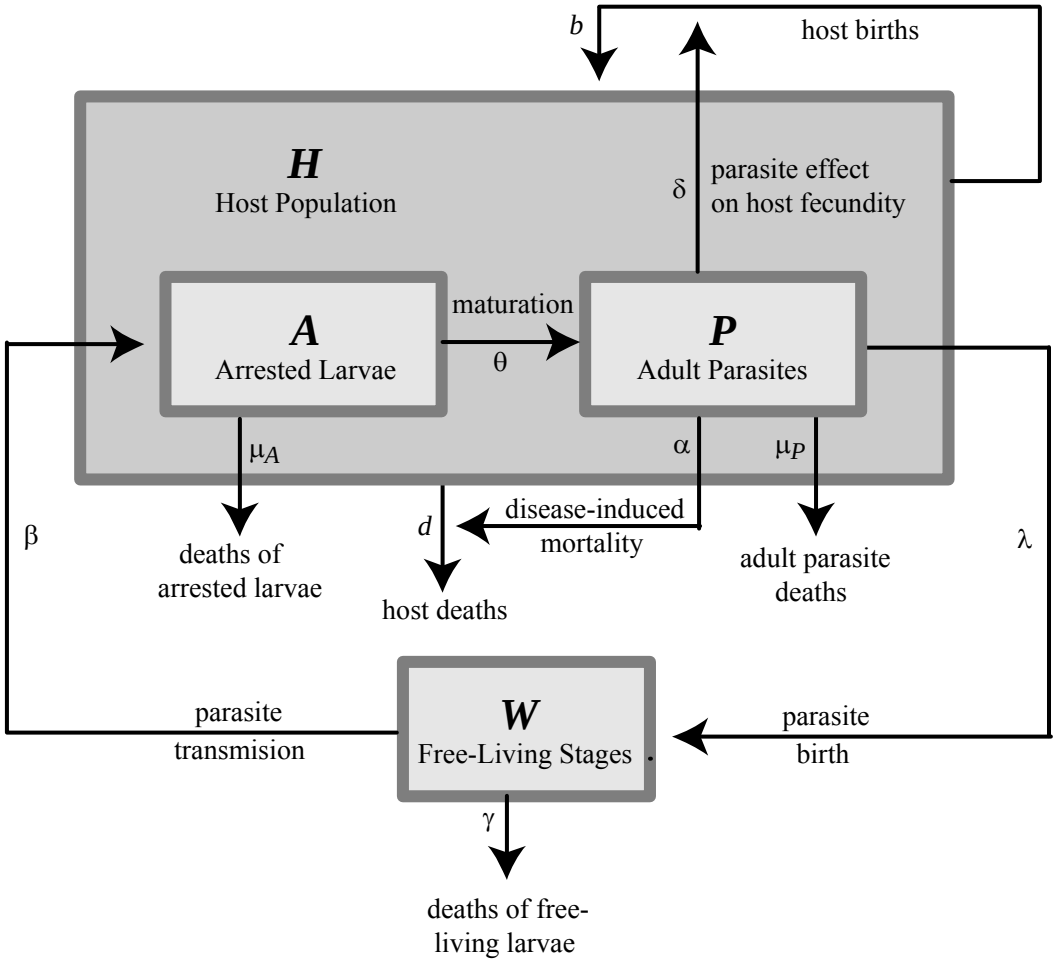

Figure 2. Schematic of the Dobson & Hudson red grouse model, with an arrested "hypobiotic" stage after host infection. Redrawn after Dobson & Hudson 1992.

For the Dobson & Hudson Red Grouse model incorporating "hypobiosis," a quiescent stage of arrested development by the parasite after entering a host bird, there are three additional parameters:

μ_A = natural mortality rate of arrested parasites (/time)
δ = the effect of parasites on grouse fecundity (/worm/time)
θ = the rate at which arrested larvae develop into adult worms (/time)

The Dobson & Hudson model is decoupled, like the two-equation simplified version of Anderson & May; it assumes that the infective stages outside the host are short-lived relative to the arrested and adult stages in the host, with densities near the equilibrium determined by host (H) and parasite (P) densities. As a result, there are three equations representing hosts (H), and the arrested (A) and adult parasite (P) stages.

$$\frac{dH}{dt} = (b-d)H - (\alpha - \delta)P \tag{8}$$

$$\frac{dA}{dt} = \frac{\lambda HP}{(H_0 + H)} - (\mu_A + d + \theta)A - \alpha\frac{PA}{H} \tag{9}$$

$$\frac{dP}{dt} = \theta A - (\mu_P + d + \alpha)P - \alpha\frac{P^2}{H}\left(\frac{k+1}{k}\right) \tag{10}$$

The dynamics of the Dobson & Hudson model show that parasite effects on host fecundity introduce oscillations in host and parasite abundance when $\alpha/\delta > k$. While the presence of an arrested host stage affects the period of cycles caused by this fecundity effect, the arrested stage does not cause oscillations on its own.

References

R. M. Anderson and R. M. May. 1978. Regulation and stability of host-parasite population interactions: I. Regulatory Processes. Journal of Animal Ecology 47:219-47.

R. M. May and R. M. Anderson. 1978. Regulation and stability of host-parasite population interactions: II. Destabilizing Processes. Journal of Animal Ecology 47:249-67.

R. M. May and R. M Anderson. 1979. Population biology of infectious diseases: Part II. Nature 280:455-61.

Dobson, A. P. and P. J. Hudson. 1992. Regulation and stability of a free-living host-parasite system: *Trichostrongylus tenuis* in red grouse. II. Population Models. Journal of Animal Ecology 61:487-498.

Hudson, P. J., D. Newborn and A. P. Dobson. 1992. Regulation and stability of a free-living host-parasite system: *Trichostrongylus tenuis* in red grouse. I. Monitoring and parasite reduction experiments. Journal of Animal Ecology 61:477-486.

Evolution of Disease Virulence

Why are some parasites highly virulent, while others are much less harmful to their hosts? Selection should favor a level of virulence that maximizes the rate of increase of the pathogen. Theoretically, this optimum virulence depends on the functional relationship between a pathogen's transmissibility, and its effect on host mortality.

How can genotypes with reduced virulence become established in a host population, if these genotypes suffer a reproductive disadvantage relative to their more virulent progenitors? Most disease models shown that the R_o of a pathogen strain depends directly on the density of susceptible hosts in the population. When this density is high, a parasite may benefit from an increased rate of transmission, even if this results in killing the present host more quickly. But if susceptible hosts are rare, then a more temperate parasite may be favored, since this pathogen strain will be maintained within a host longer despite its lower infectivity.

This *Populus* module demonstrates a model by Richard Lenski and Robert May; it assumes that any evolutionary change in the virulence of a parasite will affect the density of susceptible hosts, and this change in the density of susceptible hosts will generate new selective pressures on the pathogen. Thus, the model synthesizes ecological dynamics and evolutionary genetics. The framework is almost identical to an Anderson & May micro-parasitic disease model with only infected and susceptible hosts (there is no immune class). We define parameters for the model as follows:

H = density of susceptible hosts — e = disease induced death rate (virulence)

I = density of infected hosts — b = transmission rate per contact

d = death rate not due to infection — a = birth rate of susceptible hosts

p = fraction of birth rate "a" for infected hosts

(actually, $a = a_0 - a_1(H - I)$, whereby a_0 is the density-independent component of the birth rate, and a_1 is the density-dependent component). With these parameters, the dynamics of the susceptible and infected host classes are

$$\frac{dH}{dt} = aH + apI - dH - bHI \qquad (1)$$

$$\frac{dI}{dt} = bHI - dI - eI \qquad (2)$$

We can imagine several routes by which transmission and virulence could be coupled. If we assume that virulence is a strictly increasing function of the transmission rate, then there are three possibilities: (a) an ever increasing, nonlinear relationship, by which a small increase in the transmission rate b is associated with a large increase in virulence, (b) a linear relationship between b and e, or (c) a saturating relationship between virulence and transmission rate, such that a small increasing in e confers a large increase in b.

It is probably easiest to understand this model via alternating analyses of infected and susceptible host dynamics. Assume that *e*, the disease-induced mortality rate, is a strictly increasing function of the pathogen's transmission rate, *b*. The relationship can be described as:

$$e(b) = c_1 + c_2 b + c_3 b^2 \tag{3}$$

where c_1, c_2, and c_3 are constants. If $c_3 = 0$, this relationship is linear; if $c_3 = c_2 = 0$, then virulence is constant and independent of the transmission rate.

Substituting this function for $e(b)$ into equation 2, we find that:

$$\frac{\mathrm{d}I}{I\mathrm{d}t} = b\left(H - c_2\right) - c_3 b^2 - \left(d + c_1\right) \tag{4}$$

To find the value of *b* that optimizes the *per capita* rate of increase of the disease, we can differentiate this expression with respect to *b*, set it equal to 0, and solve for *b*.

$$b_{\mathrm{opt}} = \frac{\left(H - c_2\right)}{\left(2c_3\right)} \tag{5}$$

Thus, if $b < b_{\mathrm{opt}}$, an increase in the rate of transmission will be favored at the expense of higher virulence, and if $b > b_{\mathrm{opt}}$, selection will favor decreased virulence. Note that b_{opt} depends directly on the density of susceptible hosts.

At a particular ecological equilibrium, the disease will reduce *H* down to *H**. However, any strain of parasite that is associated with a lower threshold density of susceptible hosts (less than *H**) will be able to invade this system at its ecological equilibrium, and then further reduce the density of susceptible hosts to a new value of *H**. A mutant parasite with a transmission rate *b*' and a virulence level *e*' can invade if:

$$\frac{\mathrm{d}I'}{I'\mathrm{d}t} = b'H^* - d - e' > 0 \quad \text{and thus} \quad \frac{b'}{b} > \frac{\left(d + e'\right)}{\left(d + e\right)} \tag{6}$$

If these conditions are satisfied, then the new mutant will invade and reduce the density of susceptible hosts to an even lower level, thus driving the previously existing strain of pathogens extinct. Assuming a nonlinearly increasing relationship between *b* and *e*, this strain will have a new value of $b' < b$, and $e' < e$. Successive iterations of this feedback between ecological and evolutionary dynamics leads to progressive reductions in *H**, *b*, and *e*. (Note however, that selection cannot favor a totally non-transmissible and absolutely avirulent parasite because such a strain would always have a negative rate of increase in a population of susceptible hosts.)

For any given parasite strain, *H** will be given by:

$$H^* = \frac{\left(d + c_1\right)}{\left(b + c_2 + c_3 b\right)} \tag{7}$$

To find the minimum density of susceptible hosts given the above constraints, we differentiate *H** with respect to *b* and set this equal to 0:

$$\frac{dH^*}{db} = c_3 - \frac{(d + c_1)}{b^2} = 0 \qquad (8)$$

Solving for b, we find that $b^* = \left(\frac{(d + c_1)}{c_3} \right)^{\frac{1}{2}}$. Plugging this value back into the expression for H^* yields the minimum possible density of susceptible hosts. Note that the value of b^* above is NOT the optimal transmission rate for ALL strains of the disease, but only applies to the culmination of successive evolutionary and ecological iterations. A parasite with a transmission rate b^* is, at its ecological equilibrium, not invasible by any other strain of parasite with any other values for b and e.

In the treatment above, we solve for an ecological equilibrium density of hosts, obtain the optimal transmission rate that corresponds to this density, and then solve for a new ecological equilibrium ... and so on, until we reach the minimum density of susceptible hosts that we can sustain give our constraints of c_1, c_2, and c_3. This decoupling of the ecological and evolutionary processes is one extreme approach that is valid if we assume that ecological time scales are always faster than evolutionary time scales (which may or may not be true). An alternative approach is to integrate the dynamics numerically so that the evolutionary optimum is tracked instantaneously as the ecological dynamics unfold. To do this, we use equations 1 & 2 and set $b = b_{opt}$, and $e = e(b_{opt})$. Thus, as H decreases due to the spread of the disease, b_{opt} and $e(b_{opt})$ also decrease. The same trend towards reduced virulence is observed as previously described, and we obtain the same final equilibrium values. In addition, we can observe plots of how the densities of H and I change over time, and how the values of b_{opt} and $e(b_{opt})$ also change.

According to resource-based competition theory, two consumers that share a single limiting resource cannot stably coexist in a homogeneous habitat. Moreover, the consumers can be ranked by competitive ability according to the equilibrial density of resource that would remain in the presence of that consumer alone (R^*). Thus, any consumer that holds the resource at a lower concentration than another consumer can invade and competitively displace the first. With respect to this model, the competing consumers are the different parasite genotypes, and the limiting resource is the density of uninfected hosts.

References

Anderson, R. M., and R. M. May. 1979. Population biology of infectious diseases: Part I. Nature 280:361-7.

Anderson, R. M., and R. M. May. 1982. Directly transmitted infectious diseases: control by vaccination. Science 215:1053-60.

Anderson, R. M., and R. M. May. 1991. *Infectious Disease in Humans*. Oxford University Press. ISBN 019 854 5991.

Lenski, R.E. and May, R.M. 1994. The evolution of virulence in parasites and pathogens: reconciliation between two competing hypotheses. Journal of Theoretical Biology, 169:253-265.

May, R. M. and R. M. Anderson. 1983. Host-Parasite Coevolution. In: *Coevolution*, D. J. Futuyma and M. Slatkin, eds. Sinauer Associates.

Population Biology of Bacterial Plasmids

Many bacteria carry extra-chromosomal genetic elements that can confer important adaptations. For example, bacterial antibiotics that inhibit the growth of competitors are often the product of 'bacteriocinogenic plasmids' that code both a toxic agent and a mechanism that makes the host cell resistant to its effect. These extra-chromosomal elements are replicated and transmitted vertically in the course of bacterial cell division, and may have infectious horizontal transmission between cells via either a protein-encapsulated viral particle, or cell-to-cell contact in bacterial conjugation. Horizontal transmission may occur within- and between bacterial species, and even between different genera. It is the mechanism by which multiple drug resistances have been acquired by important human pathogens.

This *Populus* module simulates the population dynamics of a conjugationally transmitted plasmid, based on a model by Frank Stewart and Bruce Levin (1977). It describes the growth of bacteria with and without plasmids, in liquid culture with two distinct modes of resource supply. The first, which Stewart and Levin call the 'equable mode,' is a chemostat. Fresh sterile medium (with resource concentration c μg/ml) drips in at a constant rate, W ml per hr. With culture volume V, the flow rate through the habitat is $\rho = W/V$ turnovers per hr. The second, 'seasonal' mode of resource supply involves serial transfer. In this case, bacteria are introduced into a culture containing R_0 μg/ml of resource, and grow until its concentration is lowered to the point where their population is static. Then an aliquot of the static culture is withdrawn and used to inoculate the succeeding culture vessel, resulting in a boom and bust cycle of resource availabilities contrasting with the steady-state chemostat. For both regimes of resource supply, bacteria with and without plasmids grow at rates that are assumed by be saturating functions of resource concentration.

The parameters of the Stewart-Levin Plasmid model are as follows:

- V = volume of the culture habitat.
- n, n_+, n_* = densities of plasmid-free cells, plasmid-carrying cells that acquired the extra-chromosomal element vertically or were part of the initial inoculum, and plasmid-carrying transconjugant cells that acquired the element via horizontal infection.
- r = concentration of limiting resource in the culture habitat.
- $\psi(r)$, $\psi_+(r)$ = growth rate of plasmid-free and plasmid-bearing bacterial cells, which are functions of resource concentration.
- e, e_+ = quantities of resource required for one cell division.
- $\varphi(r)$, $\varphi_+(r)$ = rates of resource uptake for plasmid-free and plasmid-bearing cells, which are functions of resource concentration.
- τ = vegetative segregation rate (rate of plasmid loss per bacterial cell division). Simulation options allow this parameter to be set constant or to vary proportionally with ψ.
- γ = conjugational transfer parameter. Simulation options allow this parameter to be set constant or to vary proportionally with ψ.
- c = concentration of resource in the inflowing stock medium.
- W = rate at which nutrient solution enters; also the washout rate of medium and bacteria
- $\rho = W/V$, the culture turnover rate.
- R_0 = initial concentration of limiting resources in 'seasonal' serial culture.
- d = fraction of stationary-phase cells transferred to fresh habitat in serial inoculation.

$N = n + n_+ + n_*$, the total concentration of bacteria.
$\alpha = \alpha(r) = 1 - \psi_+/\psi$ = the selective-growth-rate advantage of plasmid-free cells over plasmid-carrying cells, a function of resource concentration.
$\beta = \beta(r) = 1 - \varphi_+/\varphi$ = the selective resource-uptake-rate advantage of plasmid-free cells over plasmid-carrying cells, a function of resource concentration.
F, $F_+ = n/N$ and $(n_+ + n_*)/N$, the frequencies of plasmid-free and plasmid-bearing cells.
P, P_+, Q, Q_+ = parameters allowing growth rate to be specified as a hyperbolic function of resource concentration.

To simulate the equable or chemostat mode of resource supply, we integrate differential equations characterizing the dynamics of n, n_+, n_*, and r (equations 1-4). The original Stewart and Levin paper tracked n, n_+, and r, but at Bruce's suggestion we have subdivided the plasmid-carrying bacteria into vertically and horizontally infected classes so that students can observe the quantitative effect of transconjugation.

$$\frac{dn}{dt} = n\psi(r) - \gamma n(n_+ + n_*) + \tau(n_+ + n_*) - \rho n \tag{1}$$

$$\frac{dn_+}{dt} = (n_* + n_+)\psi_+(r) - \tau n_+ - \rho n_+ \tag{2}$$

$$\frac{dn_*}{dt} = \gamma n(n_+ + n_*) - \tau n_* - \rho n_* \tag{3}$$

$$\frac{dr}{dt} = \rho(c - r) - e_+\psi_+(r)(n_+ + n_*) - e\psi(r)n \tag{4}$$

Equation (1) for non-plasmid-carrying bacteria has four terms. The first, $+n\psi(r)$, models their population growth, which is a saturating function of resource concentration, r. The second term, $-\gamma n(n_+ + n_*)$, models transconjugation, which is proportional to the contract rate between plasmid-carrying and non-carrying cells. The third term, $+\tau(n_+ + n_*)$, implements the segregational loss of the extra-chromosomal element during bacterial cell division, and the last term, $-\rho n$, models washout, as new medium drips into the chemostat. Terms in equations (2-4) are analogous. We assume that rate constants for the two classes of plasmid-bearing bacteria are the same.

For the seasonal mode of resource supply modeling a serial transfer experiment, we have a corresponding set of differential equations describing the dynamics between transfers. In each case, the equation is the same as its equable analog, without the ρ term modeling chemostat throughput.

$$\frac{dn}{dt} = n\psi(r) - \gamma n(n_+ + n_*) + \tau(n_+ + n_*) \tag{5}$$

$$\frac{dn_+}{dt} = (n_* + n_+)\psi_+(r) - \tau n_+ \tag{6}$$

$$\frac{dn_*}{dt} = \gamma n(n_+ + n_*) - \tau n_* \tag{7}$$

$$\frac{\mathrm{d}r}{\mathrm{d}t} = -e_{+}\psi_{+}(r)(n_{+} + n_{*}) - e\psi(r)n \tag{8}$$

Numerical integration of these equations runs for a finite time interval (the time between serial transfers), and is then interrupted while resource concentration is restored to R_0, and bacterial cell densities are diluted before beginning a new growth interval.

The dynamics of this model are most interesting when there are differences in the resource-dependent-growth and -uptake rates of bacteria with and without plasmids, so that natural selection operates on their relative frequencies. Stewart and Levin define several new parameters so that these differences can be easily specified. First, so that the bacterial growth rates can be saturating, hyperbolic (Monod) functions of resource availability, they define P and Q, such that

$$\psi(r) = \frac{Pr}{Q + r} \qquad \text{and} \qquad \psi_{+}(r) = \frac{P_{+}r}{Q_{+} + r}$$

Then, to implement differences in population growth and resource uptake with and without the plasmid,

$$\alpha(r) = 1 - \frac{\psi_{+}(r)}{\psi(r)} \qquad \text{and} \qquad \beta(r) = 1 - \frac{e_{+}\psi_{+}(r)}{e\psi(r)}$$

For most of the comparative simulations in their paper, Stewart & Levin use standard values of $P = 0.738$ per hr, $Q = 4/0$ μg/ml, and $e = 6.25 \times 10^{-7}$ μg/cell derived from Bruce's empirical research.

Plasmid bearing cells must synthesize more DNA than non-bearing cells; they are likely to require more resource uptake per cell cycle, to grow more slowly, and hence to be at a selective disadvantage relative to non-plasmid-bearing cells unless they confer some important adaptation. One consequence of these differences is that a plasmid can only be maintained (or invade and become established) in continuous chemostatic culture if the cell density and transconjugation rate are sufficient to offset segregational loss and the selective disadvantage associated with the plasmid,

$$\gamma N > \alpha\rho + \tau$$

It should seem intuitively reasonable that it will be easier to maintain a plasmid in cultures with a sluggish turnover rate (small ρ) and/or a higher input resource concentration, c, which will raise resource-dependent uptake and growth rates. Stewart and Levin arrive analytically at a concise summary of these effects, pointing out that if $c\gamma/e\tau < 1$, then plasmid-bearing cells are incapable of establishment and maintenance in the culture. If $c\gamma/e\tau > 1$, then there is a limiting value of ρ below which the plasmid can become established and persist. By implication,

> "There is a broad range of conditions where conjugative plasmids can become established and where plasmid-bearing bacteria will maintain high frequencies, even when these factors considerably reduce the fitness of their host cells.

> The implications of this conclusion frighten us. It suggests that the more prudent use of antibiotics need not result in a decrease in the frequency of bacteria carrying R Factors. It also suggests that if the containment procedures fail and the chimeric plasmids being produced by recombinant DNA techniques become incorporated on a conjugative plasmid, they too could become established and maintained in natural populations of bacteria, even if their carriage reduces the fitness of their host cell." (Stewart & Levin, p. 223)

When plasmid-bearing cells have a selective growth-rate advantage (α is negative, presumably because the plasmid confers some important adaptation), then plasmid-free cells are only maintained in the culture by segregational loss of the cytoplasmic element. Then the equilibrial frequency of plasmid-free cells is determined by the relative rates of conjugational transfer and segregational loss as

$$F = \frac{\tau}{\gamma N - \alpha\psi}$$

In the seasonal model of resource supply with constant transconjugation and segregation parameters, differences in the growth rates of plasmid-bearing and plasmid-free cells are much less important in determining whether the plasmid can invade and reach high frequency, so long as the serial transfer interval is long relative to the time required for bacteria to exhaust the resources in each serial transfer. This occurs because the constant γ remains high even as growth rate slows. If $\gamma \propto \psi$, then the values of γ, τ and α all play a role in determining the equilibrial frequency of the plasmid.

Reference

Stewart, F. M. and B. R. Levin. 1977. The population biology of bacterial plasmids: *a priori* conditions for the existence of conjugationally transmitted factors. Genetics 87:209-228.

Temperate Phage

This *Populus* module simulates a model by Frank Stewart and Bruce Levin (1984) depicting the population biology of virulent and temperate bacteriophage interacting with sensitive, lysogenic, and resistant bacterial hosts. Virulent bacteriophage adsorb to specific receptor sites on a sensitive host and inject their genetic material, initiating a latent period of phage reproduction. The host cell then lyses, releasing infective phage particles. "Temperate" phage reproduce by this same lytic process; however their genetic material may also be stabilized as a "prophage" that persists through many host replication cycles in descendents of the infected cell. The bacteria that carry a prophage, called "lysogens," are immune to further infection by phage of the same type, but many be induced to enter a lytic cycle. "Resistant" hosts are bacteria to which neither virulent nor temperate phage adsorb.

Stewart and Levin use this model to explore classic ecological questions of predator-prey or host-parasite interaction, "(i) What stabilizes the association between these populations? (ii) What is the role of phage in regulating the densities of bacterial populations? And (iii) What are the directions and effects of selection in these populations? Superimposed on these questions is that of the nature of the selective pressures leading to the evolution and maintenance of these two distinct mechanisms of phage replication." (S & L, p. 94)

Parameters of the model are as follows:

T, V = population densities of Temperate and Virulent phage, respectively, in particles per ml.

S, L, R = population densities of Sensitive, Lysogenic, and Resistant host bacteria, in cells per ml.

r = concentration of a unique limiting resource in the culture vessel, μg/ml.

$\Psi_L(r)$, $\Psi_S(r)$, $\Psi_R(r)$ = host bacterial growth rates, which are assumed to be monotonically increasing functions of resource concentration.

e = conversion efficiency, a constant defining the rate of resource uptake, which increases proportionally with the bacterial growth rate.

δ_V, δ_T = constants defining the rate of phage adsorption in proportion to the joint densities of sensitive hosts and phage particles.

β_V, β_T = the number of free viral particles produced per infection of virulent and temperate type.

λ = the proportion of temperate phage adsorptions onto sensitive hosts that produce lysogens. The remaining adsorptions (1- λ) lyse.

ξ = lysogen induction rate, per cell per hr.

τ = rate of prophage loss through vegetative segregation, per cell, per hr.

C = the concentration of limiting resources in the input stock solution, μg/ml.

ρ = the flow/dilution rate of the culture chemostat, per hour.

P = is the maximum bacterial growth rate on unlimited resources.

Q = half-saturation constant, the concentration of resources at which the bacteria grow at half their maximal rate.

α = a selection coefficient defining the proportional difference in growth rates between the different host-cell types.

Stewart and Levin assume that these populations grow without lags in a chemostat, with inputs of fresh stock medium determining both the rate of resource supply, and the washout/mortality rate of the bacteria and free virus particles. Bacterial growth is assumed to be a hyperbolic function of resource concentration, so for example,

$$\psi_L(r) = \frac{P_L r}{Q_L + r} \tag{1}$$

In their paper, they consider 5 increasingly complex cases with different numbers of participants.

Case I. Lysogens and free phage. In this simplest case it is assumed that $\tau = 0$, so that there is no segregational loss producing sensitive hosts. Then it is only necessary to model resource concentration and the densities of lysogens and free temperate phage particles, with three equations:

$$\frac{\mathrm{d}r}{\mathrm{d}t} = \rho(C - r) - e\psi_L(r)L \tag{2}$$

$$\frac{\mathrm{d}L}{\mathrm{d}t} = \psi_L(r)L - \xi L - \rho L \tag{3}$$

$$\frac{\mathrm{d}T}{\mathrm{d}t} = \xi\beta_T L - \delta_L LT - \rho T \tag{4}$$

This simple interaction will persist as long as the growth of lysogens exceeds their loss due to induction and washout, $\psi_L(r) > \xi + \rho$. As soon as $\tau > 0$, then segregational loss of the viral genome will produce sensitive hosts, as follows:

Case II. Temperate phage, lysogens and sensitive cells. Here to simplify the equations with multiple host types, selection coefficients, α are used to set the proportional differences in host growth rates. Then the model takes the form

$$\frac{\mathrm{d}r}{\mathrm{d}t} = \rho(C - r) - e\psi_L(r)\left[L + \{1 - \alpha_S\}S\right] \tag{5}$$

$$\frac{\mathrm{d}L}{\mathrm{d}t} = \psi_L(r)L + \lambda\delta_T ST - (\xi + \rho + \tau)L \tag{6}$$

$$\frac{\mathrm{d}S}{\mathrm{d}t} = (1 - \alpha_S)\psi_L(r)S - \delta_T ST + \tau L - \rho S \tag{7}$$

$$\frac{\mathrm{d}T}{\mathrm{d}t} = \xi\beta_T L + \beta_T(1 - \lambda)\delta_T ST - \delta_T LT - \rho T \tag{8}$$

If lysogens are maintained as in the previous case and there is a non-zero rate of segregational loss, then sensitive cells will be present at a frequency depending on the rates of segregation and growth, and the infection rates. With a positive segregation rate, temperate phage cannot persist without sensitive hosts; but if sensitive cells have a growth advantage and phage cannot be maintained in sensitive-only culture, then sensitive bacteria may eliminate lysogens and free

temperate phage. The Stewart and Levin stability analysis of this case is complex, and interested students should consult their paper.

Case III. Temperate phage, lysogens, sensitive, and resistant hosts. In this case, the model includes five equations:

$$\frac{\mathrm{d}r}{\mathrm{d}t} = \rho\left(C - r\right) - e\psi_L\left(r\right)\left[L + \left\{1-\alpha_S\right\}S + \left\{1-\alpha_R\right\}R\right] \tag{9}$$

$$\frac{\mathrm{d}L}{\mathrm{d}t} = \psi_L\left(r\right)L + \lambda\delta_T ST - \left(\xi + \rho + \tau\right)L \tag{10}$$

$$\frac{\mathrm{d}S}{\mathrm{d}t} = \left(1-\alpha_S\right)\psi_L\left(r\right)S - \delta_T ST + \tau L - \rho S \tag{11}$$

$$\frac{\mathrm{d}R}{\mathrm{d}t} = \left(1-\alpha_R\right)\psi_L\left(r\right)R - \rho R \tag{12}$$

$$\frac{\mathrm{d}T}{\mathrm{d}t} = \xi\beta_T L + \beta_T\left(1-\lambda\right)\delta_T ST - \delta_T LT - \rho T \tag{13}$$

In some cases, resistant hosts will be unable to invade this system, and the equilibria will be the same as those of the previous case. Alternatively, if resistant cells have a higher growth rate than both sensitive cells and lysogens, then $\alpha_R < \alpha_S$, and $\alpha_R < \dfrac{\xi+\tau}{\rho+\xi+\tau}$, and they will ultimately eliminate sensitive cells, lysogens, and phage from the culture. The final possibility with this system occurs when $\alpha_S < \alpha_R < 1 - \dfrac{\rho}{\hat{\psi}}$. Then there is an equilibrium with all three cell types present.

Case IV. Lysogens and sensitive bacteria with virulent and temperate phage.

$$\frac{\mathrm{d}r}{\mathrm{d}t} = \rho\left(C - r\right) - e\left[\psi_L\left(r\right)L + \psi_S\left(r\right)S\right] \tag{14}$$

$$\frac{\mathrm{d}L}{\mathrm{d}t} = \psi_L\left(r\right)L + \lambda\delta_T ST - \delta_V LV - \left(\xi + \rho + \tau\right)L \tag{15}$$

$$\frac{\mathrm{d}S}{\mathrm{d}t} = \psi_S\left(r\right)S - \delta_T ST - \delta_V SV + \tau L - \rho S \tag{16}$$

$$\frac{\mathrm{d}T}{\mathrm{d}t} = \xi\beta_T L + \beta_T\left(1-\lambda\right)\delta_T ST - \delta_T LT - \rho T \tag{17}$$

$$\frac{\mathrm{d}V}{\mathrm{d}t} = \beta_V\delta_V\left(S + L\right)V - \rho V \tag{18}$$

For this version of the model, if $\delta_V\beta_V < \dfrac{\rho}{\hat{S}+\hat{L}}$, temperate phage eliminate the virulent phage. If $\delta_V\beta_V > \left(1-\lambda\right)\beta_T\delta_T$ and $\alpha_S < \dfrac{\tau+\xi}{\tilde{\psi}}$ where $\tilde{\psi} = \dfrac{\rho}{1-\alpha_R}$, then virulent phage will eliminate the

temperate phage. Finally, if $\delta_V \beta_V > \dfrac{\rho}{\hat{S}+\hat{L}}$ and either $\delta_V \beta_V < (1-\lambda)\beta_T \delta_T$ or $\alpha_S > \dfrac{\tau+\xi}{\tilde{\psi}}$, then both host types and both phage types can coexist.

Case V. Sensitive, lysogenic, and resistant bacteria with temperate and virulent phage.

$$\frac{\mathrm{d}r}{\mathrm{d}t} = \rho(C-r) - e\left[\psi_L(r)L + \psi_S(r)S + \psi_R(r)R\right] \tag{19}$$

$$\frac{\mathrm{d}L}{\mathrm{d}t} = \psi_L(r)L + \lambda\delta_T ST - \delta_V LV - (\xi+\rho+\tau)L \tag{20}$$

$$\frac{\mathrm{d}S}{\mathrm{d}t} = \psi_S(r)S - \delta_T ST - \delta_V SV + \tau L - \rho S \tag{21}$$

$$\frac{\mathrm{d}R}{\mathrm{d}t} = \psi_R(r)R - \rho R \tag{22}$$

$$\frac{\mathrm{d}T}{\mathrm{d}t} = \xi\beta_T L + \beta_T(1-\lambda)\delta_T ST - \delta_T LT - \rho T \tag{23}$$

$$\frac{\mathrm{d}V}{\mathrm{d}t} = \beta_V \delta_V (S+L)V - \rho V \tag{24}$$

For this case, if $\alpha_R < \alpha_S$ and/or $\alpha_R > 0$, then resistant bacterial will eliminate sensitive and lysogenic bacteria. Alternatively, if $\alpha_R > \alpha_S$ and/or $\alpha_R < 0$, then the presence of resistant hosts will have little qualitative effect on the equilibria summarized for Case IV.

Reference

Stewart, F. M. and B. R. Levin. 1984. The population biology of bacterial viruses: why be temperate? Theoretical Population Biology 26:93-117.

Haploid Hosts and Parasites

This model simulates allelic frequency trajectories in a simple host-parasite interaction. Both host and parasite are assumed to be haploid, with a single di- or tri-allelic autosomal locus. Allelic frequencies are h_1, h_2, and h_3 (optionally) in the host, and p_1, p_2 and p_3 in the parasite. Parasite 1 is most successful on host 1, and suffers a fitness penalty when it encounters host 2 (or 3). Host 1 suffers a fitness penalty when it is attacked by parasite 1, but not from encountering parasite 2 (or 3). Encounters are assumed to occur in proportion to the genotypic frequencies.

To run the model, specify initial allelic frequencies for the host and parasite, the fitness penalty for parasitized hosts and rebuffed parasites, a mutation or migration rate for the parasites, the number of host generations to be simulated, and the number of parasite generations per host generation.

This model incorporates variations in parasite specificity and host resistance. Because type 1 parasites prosper on type 1 but not on type 2 hosts, the success of type 1 parasites will depend on the relative frequencies of type 1 and type 2 hosts. Similarly, the success of type 1 hosts will vary with the relative frequency of the parasite types. This frequency-dependent coevolutionary interaction implies that rare types will realize a fitness advantage relative to the more common ones, giving the model an inherent tendency toward oscillation. Depending on the fitness coefficients and mutation-migration rates, these oscillations can damp to equilibrium or form stable limit cycles.

The recursion equations that are iterated for each new generation of the diallelic version are as follows:

$$h_1' = \frac{h_1\left(1 - sp_1\right)}{sh_1 + 1 + sp_1 - s - 2sp_1h_1}$$

$$p_1' = \frac{p_1\left[h_1 + \left(1-t\right)h_2\right]}{p_1\left[h_1 + \left(1-t\right)h_2\right] + \left[h_2 + \left(1-t\right)h_1\right]}$$

where s is the penalty to the host of being parasitized, and t is the penalty to the parasite of being rebuffed.

Marginal and mean fitnesses in recursions for the tri-allelic version incorporate additional terms:

$$h_1' = \frac{h_1\left(1-s\right)p_1 + h_1p_2 + h_1p_3}{h_1\left[\left(1-s\right)p_1 + p_2 + p_3\right] + h_2\left[\left(1-s\right)p_2 + p_1 + p_3\right] + h_3\left[\left(1-s\right)p_3 + p_1 + p_2\right]}$$

$$p_1' = \frac{p_1\left[h_1 + \left(1-t\right)h_2 + \left(1-t\right)h_3\right]}{p_1\left[h_1 + \left(1-t\right)h_2 + \left(1-t\right)h_3\right] + p_2\left[h_2 + \left(1-t\right)h_1 + \left(1-t\right)h_3\right] + p_3\left[h_3 + \left(1-t\right)h_1 + \left(1-t\right)h_2\right]}$$

Reference

Seger, J., and W. D. Hamilton. 1988. Parasites and Sex. pp 176-193 in *The Evolution of Sex*, R. E. Michod and B. R. Levin, eds. Sinauer Associates, Inc. Sunderland, MA. Figures 1 & 2 and related text.

HIV Dynamics, Pathogenesis and Treatment

This section of the *Populus* package presents a trio of models by Martin Nowak and collaborators, illustrating viral dynamics within an individual host, the development of immunodeficiency and AIDS, and strategies for treatment. The first and third models are summarized in a review paper (Wodarz, D. and M. A. Nowak. 2002. Mathematical Models of HIV Pathogenesis and Treatment. BioEssays 24:1178-1187), which is available in pdf format on the Nowak website. The second model is a fairly complex portrayal of viral evolution within a single infected host, compiled from half a dozen papers dating from the early 1990's, listed in the references.

Model I: Basic Viral Dynamics

Virus particles attack individual host cells and harness host-cell machinery to produce virus. A basic model of this process tracks the dynamics of uninfected host cells, x, infected host cells, y, and free virus particles in the host's blood, v. Assume that uninfected cells are produced at rate λ and die at rate dx, that free virus particles infect uninfected cells in proportion to the product of their abundances, βxy, that infected cells produce virus at rate ky, that infected cells die at rate ay, and free virus particles are removed from the blood at rate uv. This means that the average lifespan of an infected host cell is $1/a$, the average lifespan of a free virus particle is $1/u$, and the burst size, or total viral load produced by one infected host cell is k/a. The basic dynamics are as follows:

$$\frac{\mathrm{d}x}{\mathrm{d}t} = \lambda - dx - \beta xv \tag{1a}$$

$$\frac{\mathrm{d}y}{\mathrm{d}t} = \beta xv - ay \tag{1b}$$

$$\frac{\mathrm{d}v}{\mathrm{d}t} = ky - uv \tag{1c}$$

In an uninfected host ($y_0 = 0$), host cell dynamics converge on $x = \lambda/d$. One infected cell gives rise to new infections at the rate $\frac{\beta kx}{u}$, and if host cells are initially at the uninfected equilibrium, then the net reproductive rate of virus is $R_0 = \frac{\beta\lambda k}{adu}$. If this net reproductive rate is greater than $R_0 = 1$, then there will be a chain reaction of infection, and explosive viral replication. This cannot continue indefinitely however, because the supply of uninfected host cells becomes depleted. At equilibrium after the infection runs its course, $x^* = \frac{x_0}{R_0}$, $y^* = \frac{(R_0 - 1)du}{\beta k}$, and $v^* = \frac{(R_0 - 1)d}{\beta}$.

Two classes of anti-viral therapy currently available for retroviruses like HIV are reverse transcriptase inhibitors that prevent infection of new cells, and protease inhibitors that prevent infected cells from producing infectious viral particles. We could model reverse transcriptase inhibition, assuming 100% effectiveness, by setting $\beta = 0$ with the infection at equilibrium. This gives an exponential decline of virus in the blood, but there is a lag caused by the persistence of

infected cells that have a longer half life than free virus. The dynamics of infection following treatment with protease inhibitors are similar. Both therapies show the half life of infected CD4+ cells to be on the order of 1-3 days, while that of free virus is only a few hours.

A problem with these therapies is that while most virus production is from infected CD4+ cells, some of it comes from macrophages and dendritic cells with a much longer half life. For this reason, and because of the toxicity and side effects of reverse transcriptase and protease inhibitors, it is not possible to continue therapy long enough to clear the infection completely. This opens the door for evolutionary changes in the virus leading to AIDS.

Model II: The AIDS Threshold

The interaction between human immunodeficiency virus (HIV) and the immune system has a complex and protracted development. In a typical progression, the virus replicates rapidly during the first weeks or months following infection. Then an immune response produces antibodies ("seroconversion") that reduce viral abundance, and free virus may be undetectable during a variably long asymptomatic interval before the development of AIDS (Acquired Immunodeficiency Syndrome). Viral abundance and growth rates during this interval are low, and there is a constant or slowly decreasing concentration of CD4+ T-lymphocytes, helper cells that bind HIV at the CD4 receptor and contribute soluble components of the immune defense. Finally, CD4+ cell densities collapse, viral replication increases, and the victim succumbs to opportunistic infections or malignancies.

HIV is an RNA retrovirus; its replication in infected cells is mediated by reverse transcription to a corresponding DNA provirus. Because the mutation rate during reverse transcription is quite high, 10^{-4} or more per base, and because the entire genome comprises about 10^4 bases, every virus particle is likely to be unique. Viral isolates from a single patient comprise an assemblage of related genotypes, called a quasispecies. These mutants may have important differences in replication rate, virulence, cell tropism, and surface antigens. For example, there are five hypervariable regions (V1-V5) in gp120, the viral envelope protein. The change of a single amino acid among 30 in the V3 loop can inhibit binding of host antibodies. These "escape mutants" then increase in abundance until they are countered by a new immune response. Thus HIV is extraordinarily variable, and this variability allows it to continually sidestep the host's immune system. As the asymptomatic period continues, this frequency-dependent selection gradually increases viral antigenic diversity.

Three mechanistic classes of hypotheses have been advanced to integrate these observations. (1) Immunological theories suggest that HIV gradually weakens the immune system by killing CD4+ cells, or that homologies between the gp120 protein and molecules produced by the major histocompatibility complex may induce autoimmune disorders. (2) Cofactor theories derive from the observation that HIV replicates in activated CD4+ cells, hence other infectious agents that result in CD4+ activation may enhance the growth of HIV. This implies that opportunistic infections are a cause rather than a consequence of AIDS. (3) Virological theories focus on evolutionary changes in the viral quasispecies to explain the long asymptomatic period and eventual development of AIDS. This *Populus* simulation reproduces a virological model presented by Nowak, et al. (1991).

Parameters of the Threshold Model:

v_i = the abundance of the ith among n different antigenic strains of HIV within an infected individual.

y = the total abundance in the blood of CD4+ host cells, T-lymphocytes (helper cells that bind HIV at the CD4 receptor and contribute soluble components of the immune defense).

x_i = the abundance of strain-specific CD4+ cells promoting immune responses to viral strain i.

z = the abundance of cross-reactive CD4+ cells promoting immune responses across all viral strains.

r_i = the growth rate of viral strain i, defined to include a rate of replication ($r_i y$) from infected CD4+ cells (y) and a background rate of replication (r_i') from other host cell types like macrophage, monocytes, etc.

$s_i z v_i$ = the death rate of strain i due to cross-reactive CD4+ cells.

$p_i x_i v_i$ = gives the death rate of viral strain i due to strain-i-specific CD4+ cells.

K is the rate at which CD4+ cells recruit from the thymus

d is the per capita death rate of CD4+ cells.

uvy is the rate at which CD4+ cells are killed by the total quasispecies of n HIV strains.

Q sets the viral mutation rate, and thus the probability that new escape mutants are generated.

The threshold model makes three basic assumptions. (1) Replication errors alter viral antigenic properties with sufficient frequency that the viral population can persist, despite the continued induction of neutralizing antibodies. (2) There are both general and specific components of the CD4+ T-lymphocyte defense against HIV. Some CD4+ cells direct immunological attack on only a single viral strain or subset of the quasispecies, while others are cross-reactive against all strains, presumably by addressing a more conservative aspect of the viral phenotype. (3) HIV can infect and kill any CD4+ cells, without regard to the unique genotype of the virus, or the binding specificities of the CD4+ cells and their products.

These assumptions imply a fundamental asymmetry in the interaction between HIV and the immune system. Effects of the virus are generalized across all CD4+ cell types, while effects of the immune system may be either specialized on a single viral strain, or cross-reactive. The resulting dynamics can be explored by analyzing the behavior of a system of differential equations that specifies changes in the abundances of HIV strains (v_i), total CD4+ cells (y), strain-specific CD4+ cells (x_i), and cross-reactive CD4+ cells (z) with respect to time. Taking these singly, the dynamics of the ith among n different viral strains are given as

$$\frac{dv_i}{dt} = f_i(v_i, y) - v_i(s_i z + p_i x_i), \; i = 1, 2, \ldots, n \qquad (2)$$

where the term $f_i(v_i,y)$ is the reproductive rate of strain i, defined as $(r_i y + r_i')v_i$ to include a *per capita* rate of replication ($r_i y$) from infected CD4+ cells (y), and a background rate of replication (r_i') from macrophage, monocytes, etc. The term $s_i z v_i$ sets a death rate of strain i due to cross-reactive CD4+ cells, and the term $p_i x_i v_i$ gives the death rate to strain-i-specific CD4+ cells. Changes in the total abundance of CD4+ cells (y) are given as

$$\frac{dy}{dt} = K - dy - u\,v\,y \qquad (3)$$

Here K is the rate at which CD4+ cells recruit from the thymus, d is their *per capita* death rate, and uvy is the rate at which they are killed by the total quasispecies of n HIV strains. The dynamics of strain-i-specific CD4+ cells are

$$\frac{dx_i}{dt} = k\, v_i\, y - u\, v\, x_i\,,\ i = 1,\ 2,\ldots, n \tag{4}$$

The recruitment term in this equation, kv_iy, includes an activation rate, as cells from the total CD4+ pool (y) turn on a specific response in proportion to the abundance (v_i) of strain i. Strain-specific T-cells are killed by the virus at a rate uvx_i. Changes in the abundance of cross-reactive CD4+ cells are specified analogously, as

$$\frac{dz}{dt} = k'v\, y - u\, v\, z \tag{5}$$

The total number of equations in this system varies with n, the number of antigenically different viral strains, which is a function of the viral replication rates and the probability that the new mutant will evade recognition by extant strain-specific antibodies. The creation of these new escape mutants is a stochastic process, modeled by drawing a random number r between 0 and 1. The random r is compared with $Qv\Delta t$, the product of a mutation rate term, Q, the total abundance of all combined viral strains $v = \Sigma v_i$, and Δt, the time step over which mutations occur. If $r < Qv\Delta t$ then we create a new viral strain with an initial density of v_{i0}, and a new strain-specific CD4+ cell type with an initial density of 0 (i.e., $x_i(0) = 0$). The growth rate of the new strain is drawn from an exponential distribution whose mean is a model parameter.

Numerical simulations and analytical studies of this model reveal three parameter regions with qualitatively different dynamics. (1) In a parameter range where viral replication rates ($f_i[v_i,y]$) and/or cytopathic effects (uvx_i and uvz) are large relative to the immune response ($s_iz + p_ix_i$), the virus outruns the combined effects of both general and specific host defenses and the victim suffers acute viremia. There is strong selection for the fastest-growing viral strain, and little viral diversity develops. (2) When viral replication and cytopathic effects are small with respect to the cross-reactive immune response alone (s_iz), the immune system can hold viral densities at a low, chronic level indefinitely. Escape mutants may increase diversity slowly, but in this parameter range there is no critical threshold beyond which viral dynamics explode.

A far more interesting set of dynamics ensues in parameter range (3) where viral reproduction is able to outrun the cross-reactive immune response, but not the combined effects of the strain-specific and cross-reactive defenses. This implies that

$$px > r - s\, z > 0 \tag{6}$$

Under these conditions, only the generation of new escape mutants allows the virus to persist. The number of different antigenic strains increases over time, and there is a threshold diversity beyond which the immune system can no longer constrain viral growth. Nowak et al. (1991) illustrate this effect analytically with a simplified version of the model. Assume that all viral strains have the same replication rate, r, independent of CD4+ cell abundance, and that s and p in equations 1 and 4 are constant across all strains. Under these conditions, specific and cross-

reactive CD4+ cell abundances approach x and z, respectively, and equation 1 (specifying the viral dynamics) simplifies to

$$\frac{dv_i}{dt} = v_i (r - s z - p x_i) \tag{7}$$

The immune system will control strain i if $r - sz - px_i < 0$, and it will control the entire viral quasispecies if this inequality holds over all n strains. This implies an upper limit, n_c, to the number of strains that can be controlled, such that

$$n < n_c = \frac{p x}{r - s z} \tag{8}$$

The analogous threshold for the full model (equations 1-4) with r_i, s_i, u_i, p_i, and k_i all varying from strain to strain is

$$n_c = \frac{\frac{p k}{u}}{\frac{r' d}{K} - \frac{s k'}{u} + 1} \tag{9}$$

$$\text{where } r' = \frac{r_{i'}}{r_i}, \; p = \frac{p_i}{r_i}, \; s = \frac{s_i}{r_i}.$$

In simulations with the threshold model, the diversity of antigenic strains (as measured by Simpson's index, which incorporates both the number of strains and the equitability of their abundances) is low during the acute phase that follows initial infection. This is partly because the simulations begin with a single strain and new mutants accrue gradually; but even if the initial infection includes numerous antigenic types, strain-specific differences in the viral replication rate will cause one or a few fast-growing strains to dominate in the interval before an immune response develops.

After the initial viremia is suppressed, antigenic diversity increases with a series of smaller viral peaks as new strains arise and are controlled by the induction of specific responses. The peaks are lower because cross-reactive immunity increases as new antibodies are induced. The immune system may also select for slower growing mutants, because slow strains spend a larger portion of their generation inside host cells where they are protected from immune attack. When the threshold diversity is finally exceeded, the viral population escapes not from an immune system which has gradually been weakened, but from one which is fully activated and functioning at maximum capacity. During the final, acute viremia of AIDS, antigenic diversity falls again, as a result of selection for the most rapidly growing viral strains.

Stochastic processes affect the accrual of new antigenic strains, their replication rates, and the effectiveness of immune responses. As a result, progress of the disease varies among runs with the same parameter values, especially with respect to the length of the asymptomatic interval. The chance appearance of a viral strain with an unusually high replication rate can produce many escape mutants and accelerate the onset of AIDS. It also suggests that the weaker immune system of infants and the aged (smaller x or z) may lower the threshold and speed the disease, consistent with empirical observation.

Model III: Theraputic Manipulation of CTL-Mediated Control

The last model in this series focuses on dynamic interactions between virus and the host immune response. One component of that response that effectively suppresses HIV involves cytotoxic T lymphocyte (CTL) cells. When large numbers of CTL are activated, becoming CTLe "effectors," they are able to clear virus from the host's peripheral circulation; but with declining viral concentration, these effectors also decline, allowing the viremia to rebound. Long-term CTL-mediated control of HIV depends on a persistent immunological memory, in the form of CTLp "precursor" cells. CTLp concentration depends on CD4+ T helper cells, which bind and present viral antigen, inducing production of CTLp. The result is continued immune pressure on the low-density virus population, ultimately driving it to extinction. CD4+ T helper cells are infected and killed by HIV, with the indirect consequence that a substantial viremia impairs immunological memory and the long-term CTL response, allowing virus to persist and evolve as depicted by the threshold model.

Wodarz and Nowak (1999, 2000, 2002) capture these dynamics with a series of five differential equations representing healthy CD4+ T helper cells (x), infected CD4+ T helper cells (y), free virus concentration in the blood (v), CTLp "precursor" cells (w), and CTLe "effectors" (z). As in the basic viral dynamics model of Equation (1), we assume that uninfected CD4+ cells are produced at rate λ and die at rate dx, that free virus particles infect uninfected cells in proportion to the product of their abundances, βxy, that infected cells produce virus at rate ky, that infected cells die at rate ay, and free virus particles are removed from the blood at rate uv. In addition, CTLp cells are produced at rate $cxyw$ and die at rate bw. CTLe cells are activated from CTLp at rate $cqyw$ and die at rate hz. Thus

$$\frac{\mathrm{d}x}{\mathrm{d}t} = \lambda - dx - \beta xv \tag{10a}$$

$$\frac{\mathrm{d}y}{\mathrm{d}t} = \beta xv - ay \tag{10b}$$

$$\frac{\mathrm{d}v}{\mathrm{d}t} = ky - uv \tag{10c}$$

$$\frac{\mathrm{d}w}{\mathrm{d}t} = cxyw - cqyw - bw \tag{10d}$$

$$\frac{\mathrm{d}z}{\mathrm{d}t} = cqyw - hz \tag{10e}$$

Note that the concentration of CTLp increases ($cxyw$) in proportion to antigenic stimulation (y) and the concentration of uninfected CD4+ cells (x). By depressing uninfected CD4+ concentration, acute viremia can thus cause CTL activation to exceed CTLp production, reducing immunological memory and ultimately impairing the immune response. The dynamics of this system depend on the rate of viral replication. With a sufficiently low replication rate, CTL memory becomes established, and the immune system can clear the infection. When replication rates are high, CD4+ are destroyed, CTL memory is depleted and the patient is overwhelmed. In an intermediate range of replication rates, judicious use of anti-retroviral therapies may allow a sufficient viral titer for antigenic stimulation, while preserving enough CD4+ abundance to develop CTLp memory and secure long-term control of the infection.

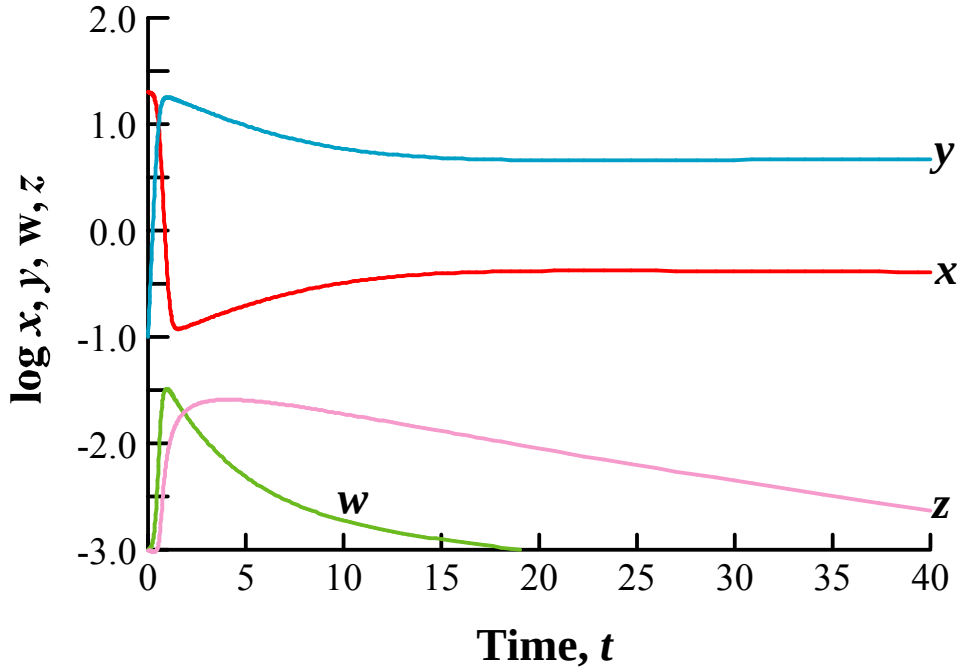

Figure 1. The pulsed-therapy model (Equations 10) with free-virus trajectory (v) omitted. For this run, $\lambda = 1$, $d = c = h = 0.1$, $\beta = 0.5$, $b = 0.01$, $a = 0.2$, $q = 0.5$, $s = 0.005$, $p = 1$, and the model was run without anti-retroviral drug treatment.

The dynamics of this model and the effects of pulsed therapy with intermediate viral replication rates are illustrated by a pair of *Populus* simulations in Figures 1 & 2. Without therapy, the parameter values employed in Figure 1 allow the infection to spread rapidly, depleting susceptible CD4+ cells (x). CTL precursor cells (w) proliferate in response to antigenic stimulation (from infected CD4+ cells, y) but this proliferation is curtailed by the depletion of uninfected CD4+ helpers (x). CTL effectors (z) differentiate from precursors (w) in proportion to infected CD4+ cell density (y), but decline with the supply of precursors. The increasing density of infected CD4+ cells (y) is initially limited by the combined effect of susceptible CD4+ cell (x) depletion and CTLe (z) phagocytes. Finally, as CTLe (z) cells disappear, infected and uninfected CD4+ cells come to equilibrium.

Figure 2 shows a corresponding simulation, with a pulse of anti-retroviral drug therapy forcing $\beta = 0$ from Time $t = 5$ to $t = 15$. All other parameter values remain as they were in Figure 1. Drug therapy allows susceptible CD4+ density (x) to recover, and the continued presence of CD4+ (x) help facilitates CTLp (w) proliferation in the presence of antigenic stimulation (y). When therapy is discontinued at $t = 15$, infected CD4+ (y) density increases, but not sufficiently to outrun the CTL response. The system then converges on an equilibrium with low levels of infection providing continued antigenic stimulation, and a sustained CTL memory. If therapy had continued indefinitely rather than stopping, infected CD4+ cell density would ultimately have fallen below the level required to maintain antigenic stimulation and CTLp memory. With different parameter values, several therapy pulses may be required to establish a sufficient CTL memory and permanent suppression of the infection, and resulting equilibria may be quite sensitive to the timing and duration of treatment pulses.

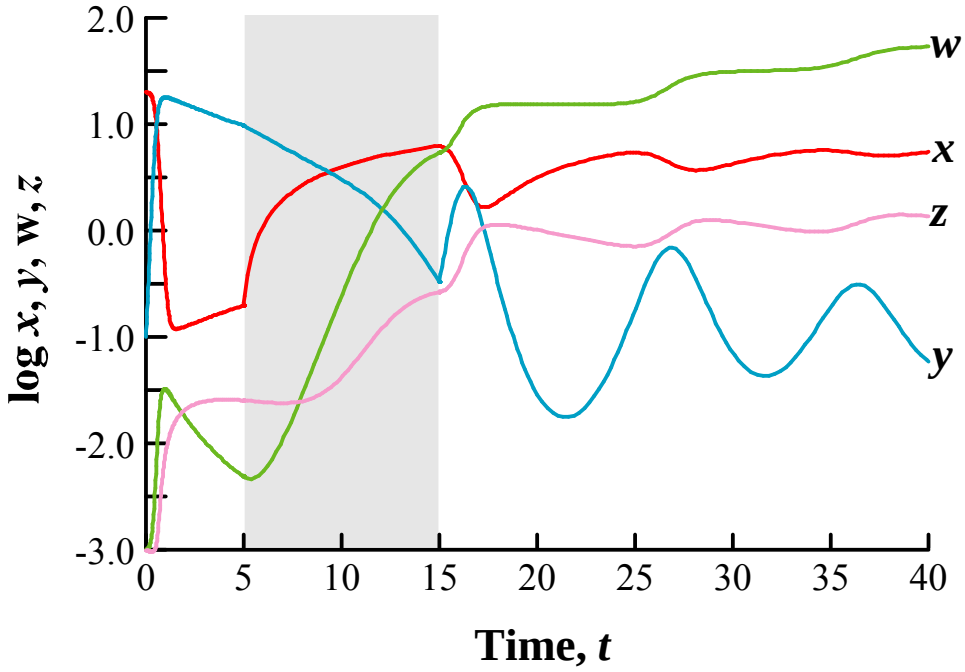

Figure 2. The pulsed-therapy model (Equations 10) with free-virus trajectory (v) omitted. All parameter values for this run were identical to those in Figure 1 ($\lambda = 1$, $d = c = h = 0.1$, $\beta = 0.5$, $b = 0.01$, $a = 0.2$, $q = 0.5$, $s = 0.005$, $p = 1$), but a pulse of anti-retroviral drug treatment from t = 5 to t = 15 forces $\beta = 0.5$ during that gray-shaded interval.

Acknowledgements

The content of this help narrative is drawn directly and entirely from the references by Nowak and collaborators, listed below. I thank Martin for helping us to implement the threshold model, more than ten years ago. I also thank Anne Bantle, who first called my attention to the more recent model of pulsed therapy and CTL memory, and Adrienne Keen, who worked through the dynamics with me, and suggested improvements in this narrative.

References

Nowak, M. A. 1992. Variability of HIV infections. J. theor. Biol. 155:1-20.

Nowak, M. A., R. M. Anderson, A. R. McLean, T. F. W. Wolfs, J. Goudsmit, and R. M. May. 1991. Antigenic diversity thresholds and the development of AIDS. Science 254:963-9.

Nowak, M. and R. M. May. 1991. Mathematical biology of HIV infections: antigenic variation and diversity threshold. Mathematical Biosciences 106:1-21.

Nowak, M. and R. M. May. 1992. Coexistence and competition in HIV infections. J. theor. Biol. 159:329-342.

Nowak, M. and R. M. May. 1993. AIDS pathogenesis: mathematical models of HIV and SIV infections. AIDS 7(suppl):S3-S18.

Nowak, M. A., R. M. May, and R. M. Anderson. 1990. The evolutionary dynamics of HIV-1 quasispecies and the development of immunodeficiency disease. AIDS 4:1095-1103.

Wodarz, D., R. M. May and M. A. Nowak. 1999. Specific therapy regimes could lead to long-term immunological control of HIV. PNAS 96:14464-9.

Wodarz, D., R. M. May and M. A. Nowak. 2000. The role of antigen-independent persistence of memory cytotoxic T lymphocytes. International Immunology 12:467-477.

Wodarz, D. and M. A. Nowak. 2002. Mathematical Models of HIV Pathogenesis and Treatment. BioEssays 24:1178-1187

Resource Competition

The traditional Lotka-Volterra model of competition is phenomenological (May 1975); its inter- and intraspecific feedbacks are related to population density by simple proportionality constants, without specifying the mechanisms of interaction between competitors. The models in this set introduce a mechanistic basis for competition. They define a "resource" as something that is consumed, with positive effect on the *per capita* growth rate of consumers. Consumers draw down resources, leading to potential equilibria where the consumption and renewal of resources on one hand, and the *per capita* birth and mortality of consumers on the other, both balance. When two species compete for the same resource, the consumer with the lowest break-even resource requirement can competitively exclude the less efficient species. Because all organisms consume resources and most risk being consumed as resources by others, mechanistic models of resource competition have made an important contribution to community ecology.

The Stewart & Levin Model

The resource competition model introduced by Frank Stewart and Bruce Levin (1973) was conceived to illustrate the interaction of bacteria in lab culture. There are two versions of the model representing different culture conditions. One version, called the "equable" mode, models a chemostat; fresh, sterile growth medium flows at constant rate into the mixed culture vessel, where the resources that it contains are taken up by bacterial consumers. The constant input is matched by a constant output or overflow, containing bacteria, waste products, and unconsumed resources. The ratio of flow to volume of the culture vessel determines a turnover, or washout rate, at which a constant fraction of the consumer population is eliminated and replaced. The model assumes that consumer-population growth is an increasing function of ambient resource concentration, and consumption is proportional to consumer-population density. With consumers initially at low density, resource concentration in the culture will be near its concentration in the inflow medium, but as consumers increase, ambient resource concentration declines, consumer growth slows, and the system may come to equilibrium.

The second version of this model, called the "seasonal" mode, is analogous to a serial dilution culture. In this case, a series of culture vessels is filled with fresh, sterile medium. One vessel is inoculated with bacterial consumers whose populations grow, drawing down resource concentrations until those resources are exhausted. Then a fraction of this culture is withdrawn and transferred to the next vessel, where the process is repeated. The dynamics of serial dilution contrast sharply with the steady-state conditions of a chemostat; they illustrate a pattern of seasonal cycles in which resources are alternately abundant and scarce.

A key component of both versions is the uptake function that specifies how consumers' resource use increases with resource concentration. Stewart & Levin use a hyperbolic function, $\varphi_i\left(r_j\right)$, which causes uptake to saturate as resources become more abundant.

$$\varphi_i\left(r_j\right) = \frac{a_i r_j}{r_j + b_i}$$

Here $\varphi_i\left(r_j\right)$ is the resource uptake rate of consumer species i with respect to r_j, the concentration of resource j at time t, a_i is the maximum growth rate of consumers on unlimited resources (a

constant), and b_i is the resource concentration at which consumers realize half their maximum growth rate (the "half-saturation constant"). The denominator becomes dominated by r_j as r_j becomes large, causing the uptake rate, $\varphi_i\left(r_j\right)$, to saturate at a_i. Values for a_i and b_i then determine the rates of uptake and consumer population growth with respect to resource concentration. In the graph at right, consumer species 1 ($a_1 = 10$, $b_1 = 5$) grows rapidly with abundant resources, while species 2 ($a_2 = 1$, $b_2 = 0.05$) has a higher growth rate when resources are scarce, but saturates at a lower maximum rate. Using the metaphor of the authors, Species 1 is an "exploiter," while Species 2 is a "gleaner."

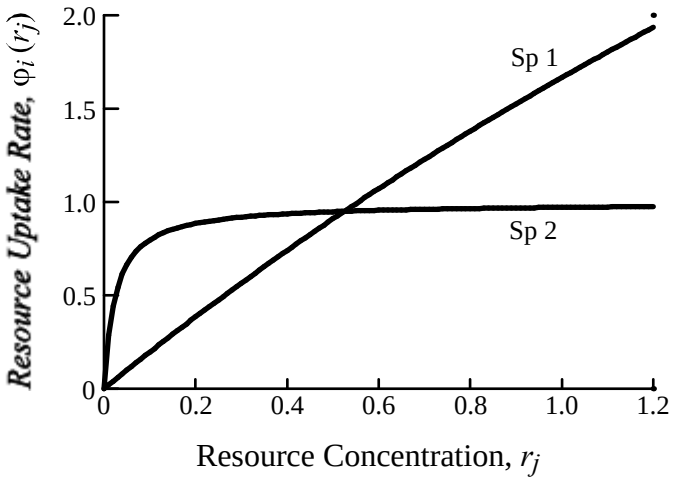

Stewart & Levin Parameter Definitions:

V = culture vessel volume
w = flow rate of culture medium through the vessel
$\rho = w/V$ = turnover/washout rate of the equable-mode chemostat
d = dilution fraction, the fraction of organisms in culture transferred to new culture volume in serial dilution (seasonal mode)
c_j = the concentration of resource j in the inflow culture medium
e_{ij} = the amount of resource j required to make a single new individual of consumer species i
$r_j(t)$ = concentration of the j^{th} resource at time t
$n_i(t)$ = concentration of the i^{th} consumer species at time t
$\varphi_{ij}(r_j)$ = uptake rate for an individual of the i^{th} species for the j^{th} resource, which is a hyperbolic function of resource concentration such that $\varphi_i\left(r_j\right) = \dfrac{a_i r_j}{r_j + b_i}$
a_i = maximal growth rate of consumers on unlimited resources, for the above uptake function
b_i = half saturation constant of consumers for the above uptake function.

The basic equations for the equable form of the model are

$$\frac{\mathrm{d}r_j}{\mathrm{d}t} = \rho\left(c_j - r_j\right) - \sum_i n_i \varphi_{ij}\left(r_j\right) \tag{1}$$

$$\frac{\mathrm{d}n_i}{\mathrm{d}t} = n_i\left[\sum_j \frac{\varphi_{ij}\left(r_j\right)}{e_{ij}} - \rho\right] \tag{2}$$

Resources (1) increase with flow in proportion to the difference between ambient concentration and concentration in the fresh medium, and decrease in proportion to uptake and the abundance of consumers. Consumer population growth (2) is proportional to consumer population size; and this proportionality is set by the difference between resource uptake (permitting the "birth" of new consumers) and "death" due to washout. By indexing the parameters, it is possible to run

the model with one consumer species on one resource ($i = j = 1$), two consumer species on one resource ($i = 2, j = 1$), and two consumer species on two resources ($i = j = 2$). For the seasonal model, the corresponding equations are

$$\frac{\mathrm{d}r_j}{\mathrm{d}t} = -\sum_i n_i \varphi_{ij}\left(r_j\right) \tag{3}$$

$$\frac{\mathrm{d}n_i}{\mathrm{d}t} = n_i\left[\sum_j \frac{\varphi_{ij}\left(r_j\right)}{e_{ij}}\right] \tag{4}$$

Because the culture is no longer a continuous-flow system, the seasonal-mode resource equation (3) lacks an inflow term, and the consumer equation (4) lacks a washout term.

Running this model in the equable mode with a single consumer species, there is a stable equilibrium when $\rho\left(c_j - r_j\right) - n\varphi_j\left(r_j\right) = 0$, so that the supply and uptake of resources balance, and $\sum_j \frac{\varphi_j\left(r_j\right)}{e_{ij}} = \rho$, so that the growth of new consumers matches their washout rate. If flow through the chemostat increases to the point where consumers can no longer replace themselves within the average residence time of the vessel, then they are gradually eliminated. In the seasonal mode, the consumer population size when resources are exhausted at the end of a season is $n_t = n_{t-1}d + \sum_j \frac{r_j}{e_{ij}}$. At equilibrium, $n_t = n_{t-1}$, and $\hat{n} = \frac{1}{1-d}\sum_j \frac{r_j}{e_{ij}}$, implying that resources just suffice to replace consumers that are left behind when transferring an inoculum from one serial culture to the next. Both the equable and seasonal models demonstrate similar equilibria when two consumer species compete for two resources. The stability criteria are a little more complex, so interested readers are referred to the original Stewart and Levin paper. Summarizing for the cases with one consumer on a single resource or two consumer species on two resources, both versions illustrate the "competitive exclusion principle."

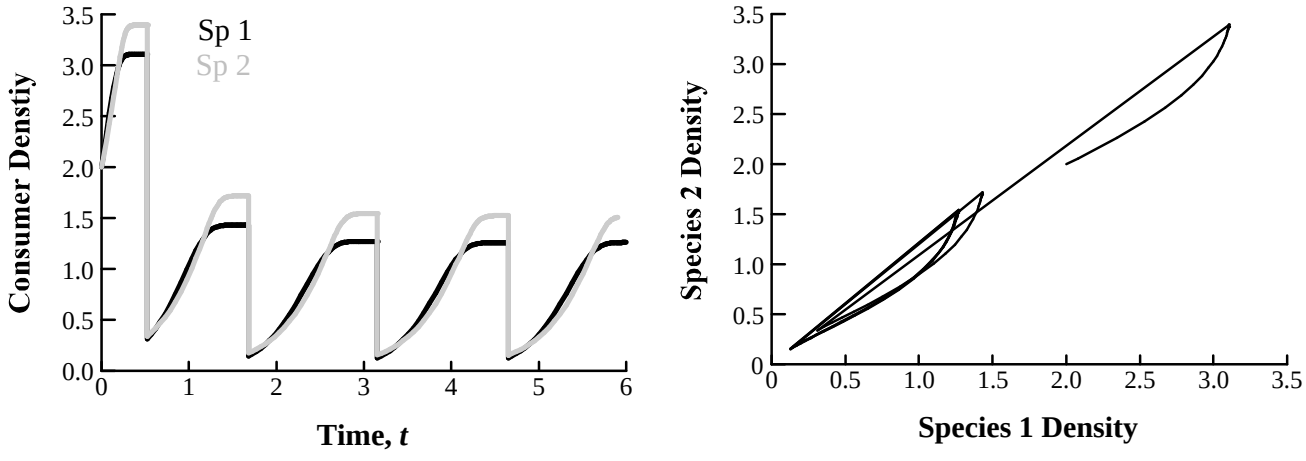

Populus simulation for the Stewart & Levin Resource Competition Model with two consumer species competing for a single resource in seasonal mode. Coexistence is possible because one species is the superior competitor at low resource concentration, while the other is superior at high concentration.

When two consumer species compete for a single resource in the equable mode, competitive exclusion is once again the rule; there are no conditions allowing stable coexistence. The seasonal mode, however, is considerably more interesting. Here the boom and bust cycles of high and low resource availability can sustain two different harvesting strategies. Graphs at the bottom of the previous page show the time trajectory and phase plane graph for the default case. The successive oscillations of the time trajectory on the left show up as loops in the phase diagram on the right, with the successive peaks connected by a straight downward line for each serial dilution. Each growth loop in the phase diagram starts out to the right, because species 1 grows more rapidly at high initial resource concentration, then it turns upward because species 2 grows better when resources are nearly depleted. In essence, coexistence is possible because one species is the superior competitor at low resource concentration, the other is superior at high concentration, and the continuous cycle of availability in the serial dilution culture prevents either consumer from extirpating its competitor.

The Tilman Model

A more complex model studied by Minnesota colleague Dave Tilman and his students extends the mathematical analysis of Stewart and Levin, and adds graphical perspectives to explore competition for multiple resources available in varying ratios. This work has guided long-term experiments in prairie, old-field, and oak-savanna systems at our Cedar Creek research station in Minnesota, but Dave's early resource competition experiments pitted algal consumers against each other in chemostatic culture; that is probably the easiest venue for thinking about the underlying ideas. The basic mathematical structure of the Tilman model is similar to that of Stewart and Levin, with some changes of nomenclature that we will duplicate for comparison with the original papers.

Tilman Parameter Definitions:

- N_i = the population density (expressed either as number of individuals per unit area or biomass per unit area) of consumer species i
- R_j = the concentration or availability of limiting resource j
- r_i = the maximal *per capita* growth rate of consumer species i
- k_{ij} = the concentration of resource j at which consumer species i attains half of its maximal growth rate, the "half-saturation constant"
- m_i = the mortality or washout rate (*per capita*) of consumer species i
- S_j = the "supply" point or maximum concentration of resource j in the habitat,
- a_j = a constant determining the rate at which the resource is converted from unavailable to available form,
- c_{ij} = a function (or constant) setting the consumption rate of resource j by consumer species i.

The *Populus* version of this model can incorporate up to three species of consumers and three resources, by subscripting the parameters. The simplest instance portrays a single consumer species using a single resource, so the indexing subscripts for consumers and resources are $i = j = 1$. Then changes in ambient resource concentration and consumer population density are given as

$$\frac{\mathrm{d}R_j}{\mathrm{d}t} = a_j\left(S_j - R_j\right) - \sum_i\left[N_i c_{ij}\left(\frac{\mathrm{d}N_i}{N_i \mathrm{d}t} + m_i\right)\right] \tag{5}$$

$$\frac{\mathrm{d}N_i}{\mathrm{d}t} = N_i\left[\frac{r_i R_j}{R_j + k_{ij}} - m_i\right] \tag{6}$$

These expressions have the same structure as those of Stewart & Levin, except that resource uptake is incorporated into the consumers' *per capita* growth rate, which saturates via the same hyperbolic Monod function, $\frac{\mathrm{d}N_i}{N_i \mathrm{d}t} = \frac{r_i R_j}{R_j + k_{ij}}$. One further difference is that the a_j and m_j terms decouple resource supply from the washout mortality rate, extending the model beyond its chemostat origin, where flow links resource supply with mortality.

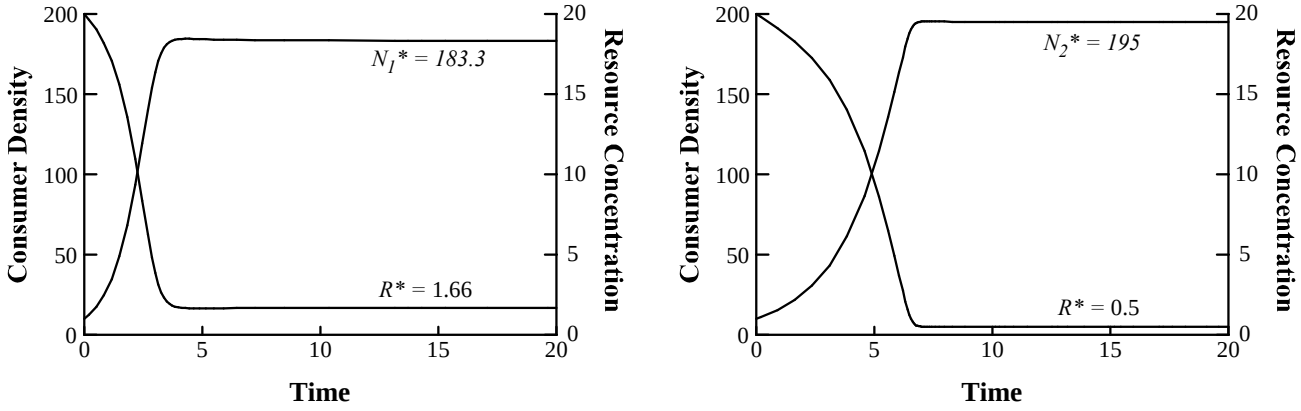

The two figures above show *Populus* simulations of equations (5) & (6) for two different consumer species. For consumer #1 on the left, $r_1 = 2$ and $k_1 = 5$. For consumer #2 on the right, $r_1 = 1$ and $k_2 = 0.5$. For both species, $c_i = 0.1$, $a_j = m_j = 0.5$, and $S_1 = R_1 = 20$. Comparing the two, species #1 grows more rapidly, but has a higher half-saturation constant, k. Species #2 grows more slowly, but its low k allows it to continue growing at resource concentrations below the equilibrial requirement of species #1, (the R^* at which $\frac{\mathrm{d}N_1}{N\mathrm{d}t} = 0$).

When two or more consumer species compete for a single resource, the species with the lowest R^* wins. The simulation at right combines the same two species, above, in competition for a single resource. The rapid growth of species #1 carries it to high initial density, but resources are quickly drawn below its break-even requirement ($R_1^* = 1.66$). Species #2 then displaces species #1 from the culture, lowering resource

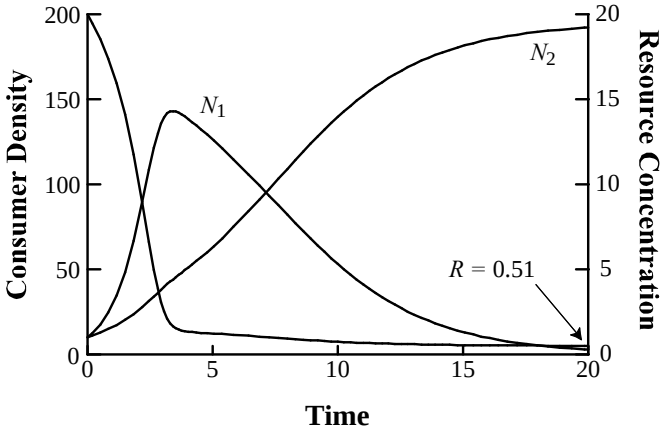

concentration to its own R_2^* = 0.5. At equilibrium (where $\frac{dN_i}{N_i dt} = 0 = \frac{dR}{dt}$), population growth equals population loss and resource supply equals resource consumption. Setting equations (5) and (6) equal to zero and solving, we have

$$R_j^* = \frac{k_{ij} m_i}{r_i - m_i} \tag{7}$$

$$N_i^* = \frac{a_i \left(S_j - R_j \right)}{c_{ij} m_i} \tag{8}$$

It is instructive to vary *k*, *m*, and *r* for several species consuming a single resource, to determine whether each species does indeed reduce the resource down to its R^* when growing in monoculture, and then to let all three consumer species compete for the same resource, to see whether the species with the lower R^* is the superior competitor at equilibrium.

Competition for Two Essential Resources

When two different resources are both essential, like the mineral nutrients and light required by plants, a consumer's growth rate is determined by the resource whose available supply is lowest relative to need. The resource competition model of equations (5) and (6) is easily generalized to *j* = 2 essential resources:

$$\frac{dR_j}{dt} = a_j \left(S_j - R_j \right) - \sum_{i=1}^{n} N_i c_{ij} \left(\frac{dN_i}{N_i dt} + m_i \right) \tag{8}$$

$$\frac{dN_i}{N_i dt} = \underset{j=1}{\overset{j=2}{\text{MIN}}} \left(\frac{r_i R_j}{R_j + k_{ij}} - m_i \right) \tag{9}$$

Here the MIN notation stipulates that the growth rate of consumer species *i* is determined either by resource *j* = 1, or by *j* = 2, whichever resource leads to the lower growth rate.

To understand the dynamics of competition for two or more essential resources, it is helpful to think about the consumers' allocation of foraging effort. On a phase-plane graph with axes representing the concentrations of R_1 and R_2, a consumer's minimum requirements form an L-shaped zero-net-growth isocline. All points on the "L" represent levels of R_1 and R_2 availability for which $\frac{dN}{dt} = 0$. They divide the plot space into a shaded region above and to the right, where there are sufficient resources available for the consumer population to grow, and a region below and to the left where $\frac{dN}{dt} < 0$, because

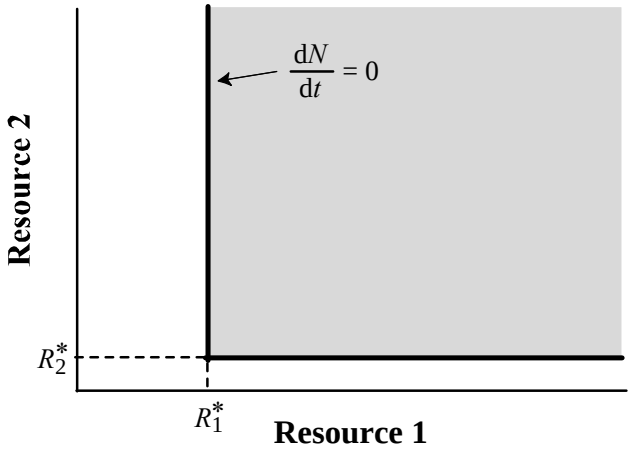

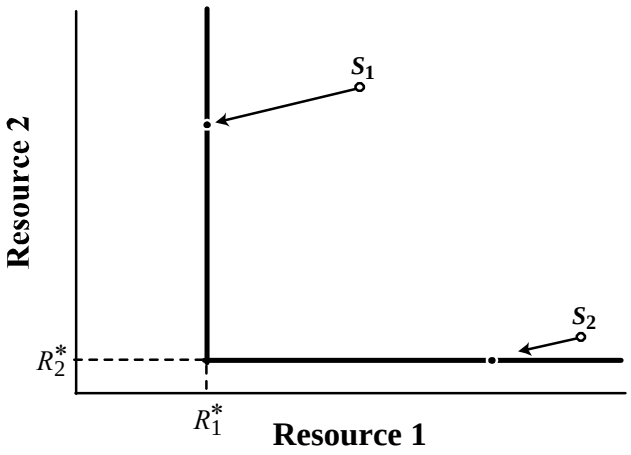

individuals do not have enough resources to replace themselves. At points along the lower limb, consumers are limited by R_2^*, it's minimum requirement for Resource 2, and at points along the upper limb, consumers are limited by R_1^*, it's minimum requirement for Resource 1. At the corner, consumer growth is simultaneously limited by both R_1 and R_2. A consumer that is foraging optimally for essential resources harvests them in this simultaneously limiting $\frac{R_2^*}{R_1^*}$ ratio. When resource concentrations lie above and to the right of the isocline so that the consumer population grows, this $\frac{R_2^*}{R_1^*}$ ratio determines the slope of an optimal foraging vector; the growing consumer population will draw resource concentrations down and to the left along this vector slope until they reach the isocline. The consumer illustrated above is an efficient user of R_2 (because R_2^* is low), but requires much more R_1, so the leftward component of its foraging vector is larger than the downward component. If the environment supplies resources in the $\frac{R_2^*}{R_1^*}$ ratio set by supply point S_1, then consumers will come to equilibrium at a point on the vertical leg of the isocline, limited by R_1. In contrast, from supply point S_2 where there is much more R_1 than R_2 available, consumers will come to equilibrium at a point on the horizontal leg of the isocline, limited by R_2.

When two or more species consume two essential resources, the relative position of their isoclines illustrates interspecific differences in resource-use efficiency. The phase diagram below reproduces the same isocline displayed above as that of consumer #1, and adds a second consumer with different resource requirements. The R_{ij}^* values are now double subscripted to denote the minimum requirement of species i for resource j, and the isoclines indicate a tradeoff in foraging efficiency. Species #1 is an efficient harvester of Resource 2, but requires a high concentration of Resource 1. In contrast, Species #2 is an efficient harvester of Resource 1, but requires a high concentration of Resource 2. This means that the optimal foraging slope of Species #1, given by the $\frac{R_{12}^*}{R_{11}^*}$ ratio, will have a larger horizontal than vertical component, while the optimal foraging slope of Species #2, given by the $\frac{R_{22}^*}{R_{21}^*}$ ratio will be more vertical than horizontal. The net effect of foraging by both consumer species is found by adding the two vectors, giving an

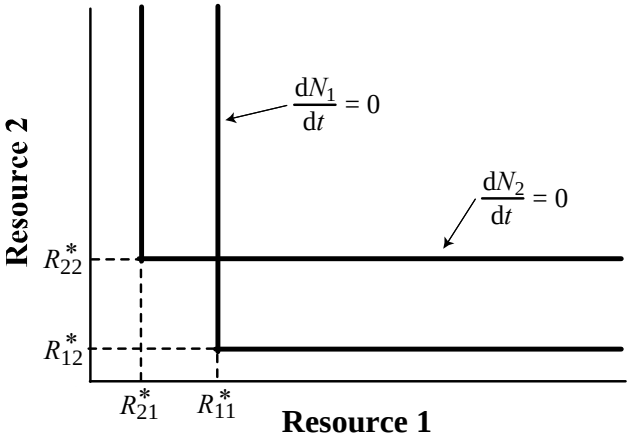

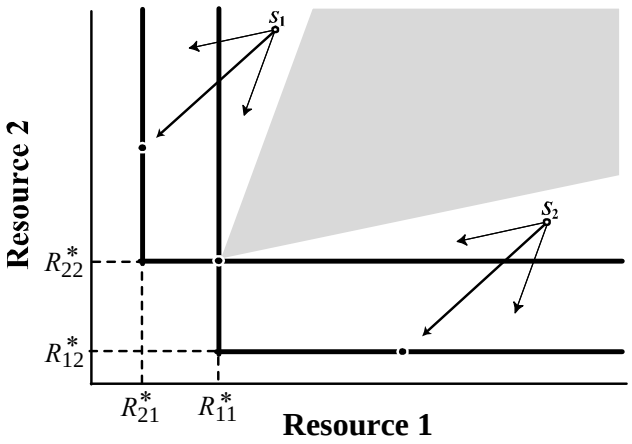

intermediate slope. When resource availabilities are above and to the right of both isoclines, then both consumer species can grow, and their combined usage draws resources down along this summation vector. From supply point S_1 at right, Resource 2 is more available than Resource 1. The foraging vectors draw resource concentration into the region where $\frac{dN_1}{dt} < 0$, ultimately ending with Species 2 alone at an equilibrium determined by R_{21}^*. From supply point S_2, Resource 1 is more available than Resource 2. The foraging vectors draw resource concentration into the region where $\frac{dN_2}{dt} < 0$, ultimately ending with Species 1 alone at an equilibrium determined by R_{12}^*. From supply points within the shaded zone projecting up and to the right from the joint equilibrium where the isoclines cross, the combined foraging of the two consumer species draws resources down to the joint equilibrium point, and the two species coexist.

The graph below shows *Populus* simulations of two species competing in environments that provide Resource 1 and Resource 2 in three different supply ratios. As before, Species 1 is an efficient consumer of Resource 2 but requires a high concentration of Resource 1, while Species 2 is an efficient consumer of resource 1 but requires a high concentration of Resource 2. The parameter values that position these isoclines are $r_1 = 1$, $m_1 = 0.5$, $k_{11} = 6$, $k_{12} = 4$, $c_{11} = 0.24$, $c_{12} = 0.12$, and $r_2 = 1.8$, $m_2 = 0.5$, $k_{21} = 5$, $k_{22} = 24$, $c_{21} = 0.1$, $c_{22} = 0.2$. From the supply point with low $R_1(0) = 14$ and high $R_2(0) = 30$, the dynamics lead to competitive exclusion of Species

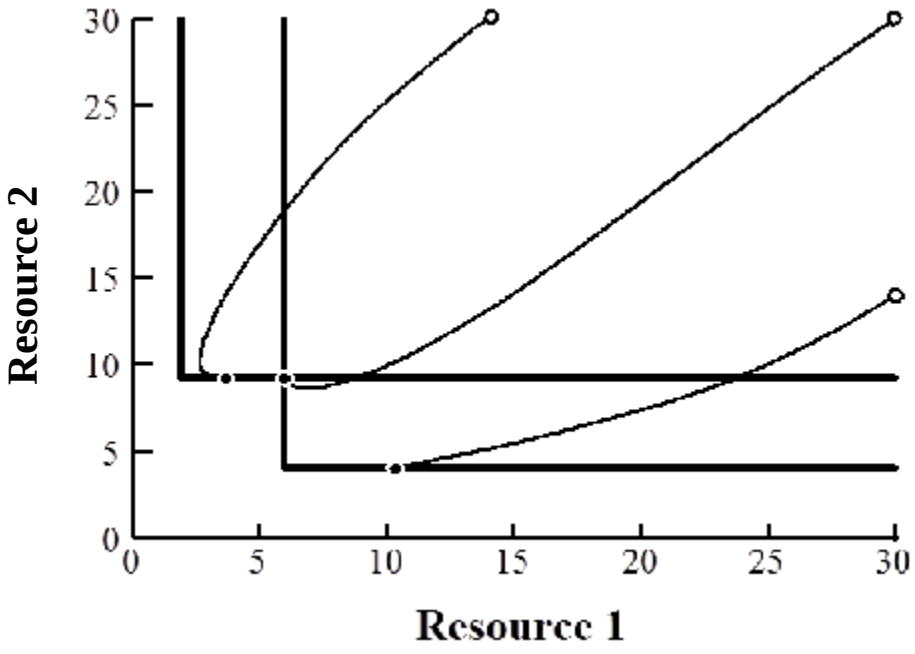

1, and an equilibrium point on the Species 2 isocline. From the supply point with high $R_1(0) = 30$ and high $R_2(0) = 30$, the dynamics lead to coexistence at the joint equilibrium where the two isoclines cross. From the supply point with high $R_1(0) = 30$ and low $R_2(0) = 14$, the dynamics lead to competitive exclusion of Species 2, and an equilibrium point on the Species 1 isocline. Thus the outcome of competition for two resources depends on the relative availability of the resources. This is determined by resource supply rates and species-specific loss rates in a given habitat. Two species can coexist stably when consuming two essential resources if each is limited by a different resource, and if each, relative to the other species, consumes more of the resource that limits it

Competition for Two Switching Resources

Although most plant resources are nutritionally essential, animal resources are often nutritionally substitutable. There are many ways in which two nutritionally substitutable resources can affect the consumer growth rate. An animal could be a generalist, foraging for all resources. Alternatively, a small animal living in a patchy environment could specialize and consume only one resource. This strategy might be favored when there are costs to foraging for both resources simultaneously, such as the cost of traveling from one patch to the next, the risk of predation during such travel, etc. If an animal specializes on one particular resource at any given instant, but may change back and forth to another resource, it is said to be "switching." In the idealized extreme, an animal might consume only the resource that leads to the higher growth rate at any given instant. Animals that foraged in such a switching manner could have their growth modeled as follows:

$$\frac{\mathrm{d}N_i}{N_i \mathrm{d}t} = \underset{j=1}{\overset{j=2}{\mathrm{MAX}}}\left(\frac{r_i R_j}{R_j + k_{ij}} - m_i \right) \tag{10}$$

$$\frac{\mathrm{d}R_j}{\mathrm{d}t} = a_j \left(S_j - R_j \right) - \sum_{i=1}^{n} N_i c_{ij} \left(\frac{\mathrm{d}N_i}{N_i \mathrm{d}t} + m_i \right) \tag{11}$$

Here the MAX notation stipulates that the growth rate of consumer species i is determined either by resource $j = 1$, or by $j = 2$, whichever resource leads to the higher growth rate. In the resource equation (11), c_{ij} is a positive constant if j is the resource that yields the higher growth rate for consumer species i, or $c_{ij} = 0$ if j is the resource that yields the lower growth rate for consumer species i. At any given instant, each consumer species will consume only that single resource that leads to the higher growth rate.

When two or more consumers switch between nutritionally substitutable resources, their isoclines have the form of an inverted and reversed "L." As was the case with essential resources, there is only a single joint equilibrium where the two isoclines cross, and together they divide the phase space into 6 regions. For the two-species, two-resource example at right,

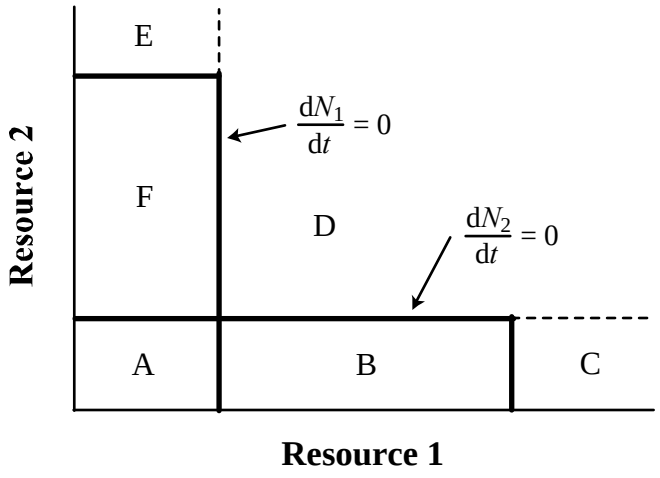

neither species can persist in zone A. In zone B, Species 1 dominates; Species 2 cannot persist even if 1 is absent. In zone C, Species 1 competitively displaces Species 2. In zone D, both species coexist. In zone E, Species 2 competitively displaces Species 1, and in zone F, Species 2 dominates; Species 1 cannot persist even if 2 is absent (Tilman 1982).

Acknowledgement

I thank Adrienne Keen, Clarence Lehman, and Lars Roe for consultation and comment on this narrative.

References

May, R. M. 1975. *Stability and Complexity in Model Ecosystems*. Princeton University Press, Princeton, New Jersey. 235 pages.

Murdoch, W. W. 1969. Switching in general predators: Experiments on predator specificity and stability of prey populations. Ecological Monographs 39:335-354.

Stewart, F. M. and B. R. Levin. 1973. Partitioning of resources and the outcome of interspecific competition: a model and some general considerations. American Naturalist 107:171-198.

Tilman, D. 1980. Resources: A graphical-mechanistic approach to competition and predation. American Naturalist 116: 362-393.

Tilman, D. 1982. *Resource Competition and Community Structure*. Princeton University Press, Princeton, New Jersey. 296 pages.h

Discrete Predator-Prey Models

This section of the *Populus* package contains a set of simulations taken from Mike Hassell's *Dynamics of Arthropod Predator-Prey Systems* and related primary literature. The models illustrate different components of predator-prey interaction, and permit analyses of their dynamic consequences. Conforming to the discrete seasonality of most arthropods, the simulations are phrased as finite recursion equations of the basic form

$$N_{t+1} = \lambda N_t \ \mathrm{f}\left(N_t, P_t\right)$$
$$P_{t+1} = cN_t\left[1 - \mathrm{f}\left(N_t, P_t\right)\right]$$

where N_t, N_{t+1}, P_t, P_{t+1} give the prey and predator population densities in successive generations, respectively, λ is the geometric growth factor for the prey (which can remain constant or change as a function of prey density), and c is the number of predators produced for each prey individual attacked (the "numerical response" of the predator). The function $\mathrm{f}(N_t, P_t)$, gives prey survival with respect to predator and prey densities, and can be varied to reflect various predator-foraging behaviors.

The biology of arthropod predators spans a wide range of complexity. Among the simplest are hymenopteran and dipteran parasitoids that seek hosts and lay one or more eggs whose subsequent development kills and consumes the victim. In contrast to predators, where immatures and both adult sexes must locate and consume prey, only the adult female parasitoid searches; moreover, the number of progeny that she produces is likely to be a simple function of the number of hosts attacked. The models in this group are framed without the complications of age structure, consistent with the simple biology of parasitoids and their hosts.

Reference

Hassell, M. P. 1978. *The Dynamics of Arthropod Predator-Prey Systems*. Monographs in Population Biology, Princeton University Press. Princeton, NJ.

The Nicholson-Bailey Model

The predator-prey model formulated by Nicholson (1933) and Nicholson and Bailey (1935) offers a basic starting point for comparison with more complex and realistic models. It is based on two simplifying assumptions: (1) the number of encounters, N_e, between P_t parasitoids or predators with host or prey is proportional to host density, N_t, and (2) these encounters are randomly distributed among hosts. This means that some hosts will be encountered more than once, and some will not be encountered at all. The number of hosts not parasitized is given by the zero term of the Poisson distribution,

$$p_0 = \exp\left(\frac{-N_e}{N_t}\right)$$

and the number of hosts actually parasitized is

$$N_a = N_t\left[1 - \exp\left(\frac{-N_e}{N_t}\right)\right]$$

The number of encounters between P_t parasitoids and their hosts N_t, can be restated as

$$N_e = aN_tP_t$$

where a is a proportionality constant called the parasitoid's area of discovery. It is a measure of searching efficiency, and can be thought of as the proportion of all hosts that will be encountered by an individual parasitoid during its lifetime. It follows that $N_e/N_t = aP_t$, and the number of parasitized hosts can be rewritten as

$$N_a = N_t\left[1 - \exp\left(-aP_t\right)\right]$$

This expression implies that parasitism will rise as a saturating function of aP_t, because parasites encounter fewer and fewer unparasitized hosts as their numbers and searching efficiency increase. Nicholson called this relationship a competition curve.

If the host survival function (the number of hosts remaining unattacked) is

$$\mathrm{f}\left(N_t, P_t\right) = \exp\left(-aP_t\right)$$

then the discrete recursion equations defining host and parasatoid dynamics are

$$N_{t+1} = \lambda N_t \exp\left(-aP_t\right)$$
$$P_{t+1} = N_t\left[1 - \exp\left(-aP_t\right)\right]$$

where λ is the intrinsic geometric growth factor of the hosts.

This model is directly analogous to the Lotka-Volterra predator-prey model, save for its formulation as a pair of finite difference equations. While the continuous Lotka-Volterra version is neutrally stable, the Nicholson-Bailey dynamics give an unstable, increasing oscillation. May (1973, 1975) showed that this difference in the models' dynamics is attributable to the built-in time lag associated with the discrete Nicholson-Bailey difference equations.

The introduction of density-dependent host growth has a stabilizing influence on Nicholson-Bailey dynamics. If you choose the density-dependent option, *Populus* substitutes a host recursion suggested by Beddington, Free and Lawton (1975) as follows:

$$N_{t+1} = \lambda N_t \exp\left\{ r\left(1 - \frac{N}{K}\right) - aP_t \right\}$$

The parasitoid recursion remains as above. The stability of this density-dependent version is determined by the host reproductive rate (given here as $r = \ln \lambda$) and by a, the parasitoids' searching efficiency or area of discovery. If the parasitoid is extremely efficient (large a) it is able to hold hosts below their carrying capacity and dynamics are affected most strongly by the unstable host-parasitoid interaction. If the parasitoid is inefficient (small a), host dynamics are stabilized by the density-dependent feedback.

References

Beddington, J. R., C. A. Free, and J. H. Lawton. 1975. Dynamic complexity in predator-prey models framed in difference equations. Nature 225:58-60.

Hassell, M. P. 1978. *The Dynamics of Arthropod Predator-Prey Systems*. Monographs in Population Biology, Princeton University Press. Princeton, NJ.

May, R. M. 1973. On relationships among various types of population models. American Naturalist 107:46-57.

May, R. M. 1975. Biological populations obeying difference equations: stable points, stable cycles, and chaos. J. Theor. Biol. 49:511-524.

Nicholson, A. J. 1933. The balance of animal populations. J. Anim. Ecol. 2:132-178.

Nicholson, A. J. and V. A. Bailey, 1935. The balance of animal populations. Part I. Proc. Zool. Soc. Lond. 1935, 551-598.

Nicholson-Bailey with Spatial Structure

This simulation comes not from Hassell's book, but from a paper by Hassell, Comins & May (1991). It assumes that the environment is subdivided into an array of rectangular patches. In each generation, two processes affect the dynamics. First, the host and parasitoid populations in each rectangular patch interact according to the Nicolson-Bailey recursions,

$$N_{t+1} = \lambda N_t e^{-aP_t}$$

$$P_{t+1} = N_t \left[1 - e^{-aP_t} \right]$$

Second, there is a dispersal phase in which a fixed fraction of the hosts (μ_N) and parasitoids (μ_P) in each patch are distributed equally among the eight adjoining patches.

While the simple Nicholson-Bailey recursions give an increasing oscillation which ultimately extinguishes host or parasitoids, this spatially structured arrangement allows more possibilities. In general, dispersal may cause the global persistence of the locally unstable Nicholson-Bailey interaction. The probability of global persistence increases with the size and complexity of the spatial array and decreases as hosts become more vagile. When the interaction persists, several different spatial patterns are possible, including spiral waves of changing host and parasitoid density, fixed "crystal lattices," and purely chaotic variation, depending on the parameter values used. For a more detailed discussion, students should consult the primary reference.

The simulation produces four different output screens. Three present the spatial array of patches, color-coding the local abundance of interacting parties. One screen gives the ratio of prey to parasitoids (N/P), one gives prey density (N), and the third gives parasitoid density (P). On all three screens, colors are coded in spectral order, with long wavelengths representing high densities or ratios, and short wavelengths representing low ones. A legend below the spatial array gives the specific values (which change from generation to generation) represented by each color. The final output is a graph of average prey and parasitoid densities per patch, across the entire array, as it changes with time.

References

Hassell, M. P., H. N. Comins and R. M. May. 1991. Spatial structure and chaos in insect population dynamics. Nature 353:255-8.

Functional Responses

As host density increases, the number of hosts parasitized per parasitoid should increase. Holling (1959) called this the predator's functional response (following Solomon, 1949), and suggested that it might take three forms:

Type I, prey consumption rises linearly to a plateau

Type II, consumption rises asymptotically to saturation

Type III, consumption is a sigmoid function of prey density

We can simulate a linear functional response (Type I, with insatiable parasitoids) by assuming that our host survival function $f(N_t, P_t) = \exp(-a'TP_t)$, where P_t is the parasitoid density at time t, a' is the parasitoids' instantaneous search rate, and T is the fixed, constant search time available. Then

$$N_{t+1} = \lambda N_t \exp\left(-a'TP_t\right)$$
$$P_{t+1} = cN_t\left[1-\exp\left(-a'TP_t\right)\right]$$

where again N_t and P_t are the host and parasitoid population densities at time t, λ is the intrinsic growth factor of the hosts, and c is the numerical response indicating the number of parasitoids (often 1) produced per host consumed. Note that $a'T$ is equivalent to Nicholson's area of discovery, a, if the searching time, T, is one full generation; so this linear-functional-response formulation is identical to the basic Nicholson-Bailey model.

Often some handling time, T_h, is required for a parasotoid to oviposit on each host, and search time is consequently reduced. As host density rises, handling consumes an increasing proportion of the parasitoids' time budget, and the functional response is a saturating, Type II function. If a' and T_h are both constant and parasitoid search is random, the prey survival function

$$f\left(N_t, P_t\right) = \exp\left(\frac{-a'TP_t}{1+a'T_hN_t}\right)$$

illustrates this sort of response, giving the difference equations

$$N_{t+1} = \lambda N_t \exp\left(\frac{-a'TP_t}{1+a'T_hN_t}\right)$$
$$P_{t+1} = cN_t\left[1-\exp\left(\frac{-a'TP_t}{1+a'T_hN_t}\right)\right]$$

The dynamics of interactions with a Type II functional response are always less stable than the simple Nicholson-Bailey analog, because the hosts escape at high density. The magnitude of this destabilizing effect is determined by the ratio of T_h to total search time T, and is relatively unimportant if $T_h/T \ll 1$ (Hassell and May, 1973).

Sigmoid Type III functional responses result when one or more of the components of parasitoid searching activity (a', T, or both) are increasing functions of prey density. It is often

suggested that a type III functional response results when the parasitoids learn to be more efficient as prey density rises, but in fact responses should be sigmoid whenever payoffs at the lowest host densities are below some threshold required for constant searching activity. Hassell developed a Type III model in which *a*' varies with host density according to the expression

$$a' = \frac{bN_t}{1 + cN_t}$$

where *b* and *c* are constants (again, *c* is the numerical response, often 1.0 for parasitoids). This yields the prey survival function

$$\mathrm{f}\left(N_t, P_t\right) = \exp\left(\frac{-bTN_tP_t}{1 + cN_t + bT_hN_t^2}\right)$$

and the resulting difference equations for a simulation are

$$N_{t+1} = \lambda N_t \exp\left(\frac{-bTN_tP_t}{1 + cN_t + bT_hN_t^2}\right)$$

$$P_{t+1} = cN_t\left[1 - \exp\left(\frac{-bTN_tP_t}{1 + cN_t + bT_hN_t^2}\right)\right]$$

Sigmoid functional responses are potentially stabilizing, because the parasitoids impose a density-dependent effect on hosts at low density. While this stabilizing influence is observable in a continuous, differential equation formulation like the theta-logistic model, Hassell and Comins (1978) showed that it is too subtle to overcome the instability inherent in difference equation models with a one-generation delay between changes in predator density and prey mortality.

References

Hassell, M. P. 1978. *The Dynamics of Arthropod Predator-Prey Systems*. Monographs in Population Biology, Princeton University Press. Princeton, NJ.

Hassell, M. P. and Comins, H.N. 1978. Sigmoid functional responses and population stability. Theoretical Population Biology 9:202-221.

Hassell, M. P. and R. M. May. 1973. Stability in insect host-parasitoid interactions. J. Anim. Ecol. 42:693-736.

Holling, C.S. 1959. The components of predation as revealed by a study of small mammal predation of the European pine sawfly. Canadian Entomologist 91: 293-320.

Solomon, M.E. 1949. The natural control of animal populations. Journal of Animal Ecology 18:1-35.

Non-Random Searching

The Nicholson-Bailey assumption that parasitoids forage randomly is obviously oversimplified. Real hosts are likely to be distributed in a patchwork of high and low densities, and parasitoids can be expected to respond by orienting toward high-density patches. Because this parasitoid aggregation has the effect of giving hosts a refuge at low densities, it is a potentially important stabilizing factor in the dynamic interaction (Murdoch and Oaten 1975, Hassell 1978).

This simulation reproduces a model by May (1978), who assumed that parasitoid attacks show a negative binomial pattern. A negative binomial distribution is specified by its mean, and a clumping parameter, *k*. Distributions with a small *k* value (< 1) are strongly clumped, while those with large *k* (> 8) approach Poisson randomness. By specifying the statistical distribution of parasitoid attacks, May was able to model the dynamic effects of aggregation without explicitly including details of orientation and foraging behavior. His recursion equations are

$$N_{t+1} = \lambda N_t \left(1 + \frac{aP_t}{k}\right)^{-k}$$

$$P_{t+1} = N_t \left[1 - \left(1 + \frac{aP_t}{k}\right)^{-k}\right]$$

where all parameters are as given for the basic Nicholson-Bailey version, save for *k*, the negative binomial dispersion parameter, which can be interpreted as a coefficient of variance of parasitoid density among patches. Note that this recursion approaches Nicholson-Bailey as *k* approaches infinity. The dynamics of this model show diverging oscillations if $k > 1$, but the effect of parasitoid aggregation produces damped oscillations or a monotonic approach to equilibrial parasitoid and host densities if $k < 1$.

Populus also includes a version of this model with density-dependent prey growth. In this case, the prey recursion is

$$N_{t+1} = \lambda N_t \left(\exp\left\{\frac{-rN_t}{K}\right\}\right)\left(1 + \frac{aP_t}{k}\right)^{-k}$$

where this upper case *K* is the environmental carrying capacity and again, $r = \ln \lambda$. Interested students should see Hassell (1978) or Bedington, Free, and Lawton (1975, 1976) for the complex stability analysis of this model; but in general, stability varies inversely with host growth rate and directly with density dependence and the ratio *r*/*K*.

References

Beddington, J. R., C. A. Free, and J. H. Lawton. 1975. Dynamic complexity in predator-prey models framed in difference equations. Nature 225:58-60.

Beddington, J. R., C. A. Free, and J. H. Lawton. 1976. Concepts of stability and resilience in predator-prey models. J. Anim. Ecol. 45:791-816.

Chesson, P. and W. W. Murdoch. 1986. Aggregation of risk: relationships among host-parasitoid models. Am. Nat. 127:696-715.

Hassell, M. P. 1978. *The Dynamics of Arthropod Predator-Prey Systems*. Monographs in Population Biology, Princeton University Press. Princeton, NJ.

May, R. M. 1978. Host-parasitoid systems in patchy environments: a phenomenological model. J. Anim. Ecol 47:833-44.

Murdoch, W. W. and A. Oaten. 1989. Aggregation by parasitoids and predators: effects on equilibrium and stability. Am. Nat. 134:288-310.

Murdoch, W. W. and A. Oaten. 1975. Predation and population stability. Adv. Ecol. Res. 9:2-131.

Predator Interference

Parasitoids that aggregate in patches of high host density are likely to encounter one another in the course of their foraging activities. Many species have been shown to display aggressive behavior toward other nearby females; these interactions waste searching time and increase the parasitoids' tendency for dispersal. The first of two parasitoid interference models included in *Populus* is attributable to Hassell and Varley (1969). It assumes that the negative relationship between searching efficiency, *a*, and parasitoid density is linear on log-log scales

$$a = QP_t^{-m}$$

where both *Q* and *m* are constants. The interference constant, *m*, is interpretable as the slope of this decline in search efficiency with parasitoid density. This leads to the recursions

$$N_{t+1} = \lambda N_t \exp\left(-QP_t^{1-m}\right)$$
$$P_{t+1} = N_t\left[1-\exp\left(-QP_t^{1-m}\right)\right]$$

The stability of this model increases as values of *m* vary from 0 to 1.0, and declines as the intrinsic growth rate of hosts increases (Hassell and May 1973).

Models with a linear relationship between searching efficiency and parasitoid density are obviously oversimplified; efficiency cannot rise indefinitely as parasitoids become increasingly rare. We have therefore included a curvilinear model by Beddington (1975) who assumes that parasitoids encounter one another randomly at a rate, *b*, which is analogous to the rate of their encounter with hosts (*a*') introduced in the functional response models. He further assumes that after each encounter between parasitoids there is a period of wasted time, T_w, during which no further searching takes place. Beddington's recursions are

$$N_{t+1} = \lambda N_t \exp\left(\frac{-a'TP_t}{1+bT_wP_{t-1}}\right)$$
$$P_{t+1} = cN_t\left[1-\exp\left(\frac{-a'TP_t}{1+bT_wP_{t-1}}\right)\right]$$

In effect, this model allows the interference coefficient, *m*, to vary between 0 and 1.0 and its stability properties are similar to those of the linear version. It collapses back to the basic Nicholson-Bailey model if $bT_w = 0$. Students who are interested in interference are directed to Hassell's book for discussions of its importance at equilibrial densities, and its relation to aggregation and nonrandom foraging.

References

Beddington, J. R. 1975. Mutual interference between parasites or predators and its effect on searching efficiency. J. Anim. Ecol 44:331-340.

Hassell, M. P. 1978. *The Dynamics of Arthropod Predator-Prey Systems*. Monographs in Population Biology, Princeton University Press. Princeton, NJ.

Hassell, M. P. and R. M. May. 1973. Stability in insect host-parasitoid interactions. J. Anim. Ecol. 42:693-736.

Hassell, M. P. and G. C. Varley. 1969. New inductive population model for insect parasites and its bearing on biological control. Nature 223:1133-36.

Threshold Predator Reproduction

Simulations appropriate to a predator-prey interaction should differ in several respects from the parasitoid-host models in this set. Since predators usually consume many prey individuals that are smaller than the consumers themselves, the numerical response, c, will often be less than 1.0; in addition, since a certain amount of energy and resources are likely for the predators to mature and maintain themselves without reproducing, the functional relationship between prey availability and predator reproduction is unlikely to be a simple proportionality. Hassell's book describes a model by Beddington, Free, and Lawton (1976) that relates a predator's lifetime fecundity to the number of prey consumed as

$$F = c\left(\frac{N_a}{P_t} - \beta\right)$$

where c is the efficiency of prey conversion into predators (the numerical response) and β is the minimum threshold prey consumption required before predators begin to reproduce. Assuming that prey population growth is density-dependent, this assumption leads to the recursion equations

$$N_{t+1} = N_t \exp\left\{r\left(1 - \frac{N_t}{K}\right) - aP_t\right\}$$

$$P_{t+1} = c\left[\left\{N_t\left[1 - \exp\left(-aP_t\right)\right]\right\} - \beta P_t\right]$$

If $\beta = 0$, this model collapses to the density-dependent version of Nicholson-Bailey, but with $c\,\beta > 0$, the equilibrial densities of predators and prey are no longer globally stable. Instead, they have a local basin of attraction that shrinks as the $c\beta$ product increases. One practical implication of this behavior is that the success of such a predator in biological control releases would be sensitive to the initial densities of predator and prey.

References

Beddington, J. R., C. A. Free, and J. H. Lawton. 1976. Concepts of stability and resilience in predator-prey models. J. Anim. Ecol. 45:791-816.

Hassell, M. P. 1978. *The Dynamics of Arthropod Predator-Prey Systems*. Monographs in Population Biology, Princeton University Press. Princeton, NJ.

Hosts and Parasitoids with Insecticide

Because parasitoids are often released for biological control purposes in the context of an integrated program that includes pesticide applications, it is important to model the effect of insecticides on the dynamics of host-parasitoid interaction. This set of models was developed by Hassell (1984) using recursions of the same general form as others in this series from his 1978 book, with a host survival function that incorporates negative binomial clumping of the searching parasitoids and a type II functional response. Because the model is discrete, it is possible that insecticide may have different effects depending on the timing of the application relative to host and parasitoid life cycles. For this reason, four sub-models are presented as follows:

Model 1. In this case, insecticides act before parasitism and kill only hosts. The recursions are:

$$N_{t+1} = FN_t\left[\mathrm{f}\left(N_t I, P_t\right)\right]$$
$$P_{t+1} = N_t\left[1\text{- f}\left(N_t I, P_t\right)\right]$$

where

$$\mathrm{f}\left(N_t I, P_t\right) = \left[\frac{1+aP_t}{k\left(1+\theta N_t I\right)}\right]^{-k}$$

Model 2. Here, insecticides act after parasitism and kill only hosts.

$$N_{t+1} = FN_t \mathrm{f}\left(N_t, P_t\right) I$$
$$P_{t+1} = N_t\left[1\text{- f}\left(N_t, P_t\right)\right]$$

where

$$\mathrm{f}\left(N_t, P_t\right) = \left[\frac{1+aP_t}{k\left(1+aT_h N_t\right)}\right]^{-k}$$

Model 3. Next, insecticides act after parasitism and kill both hosts and parasitoids at the same rate.

$$N_{t+1} = FN_t \mathrm{f}\left(N_t, P_t\right) I$$
$$P_{t+1} = N_t I\left[1\text{- f}\left(N_t, P_t\right)\right]$$

where

$$\mathrm{f}\left(N_t, P_t\right) = \left[\frac{1+aP_t}{k\left(1+aT_h N_t\right)}\right]^{-k}$$

Model 4. Finally, if insecticides act before parasitism and also kill adult parasitoids at the same rate.

$$N_{t+1} = FN_t \mathrm{f}\left(N_t I, P_t I'\right)$$
$$P_{t+1} = N_t I\left[1\text{- f}\left(N_t I, P_t I'\right)\right]$$

where

$$\mathrm{f}\left(N_t I, P_t I'\right) = \left[\frac{1 + aP_t I'}{k\left(1 + aN_t I\right)}\right]^{-k}$$

The simulations show that insecticide applications are likely to lower the equilibrial host density resulting from host-parasitoid interactions alone unless adult parasitoids are affected (Model 4), but that in this latter case, equilibrial host densities rise. The degree of host depression that results from the insecticide application increases with the clumping of the parasitoid and the growth rate of the host. Model 2 consistently produces the lowest host equilibria, and Model 4 the highest.

Reference

Hassell, M. P. 1984. Insecticides in Host-Parasitoid Interactions. Theoretical Population Biology 26:378-86.

Polyphagous Predators

The preceding models in this set have all dealt with single pairs of predator and prey species. Natural interactions are rarely so isolated, and this simulation allows exploration of a more complex system with one predator and two competing prey species. It uses a discrete analog of the Lotka-Volterra competition model to describe the interaction between competing prey as

$$X_{t+1} = \lambda X_t \exp\left\{-g\left(X_t + \alpha Y_t\right)\right\}$$
$$Y_{t+1} = \lambda Y_t \exp\left\{-g'\left(Y_t + \beta X_t\right)\right\}$$

where X and Y denote the two competing prey densities, g and g' are constants, and α and β are competition coefficients like those of the Lotka-Volterra model. This competition model retains the linear Lotka-Volterra isoclines, but its dynamics are complicated by the lags inherent in the discrete formulation (May 1974).

Adding a predator to this system gives the recursions

$$X_{t+1} = \lambda X_t \exp\left\{-g\left(X_t + \alpha Y_t\right) - a_X P_t^{1-m}\right\}$$
$$Y_{t+1} = \lambda Y_t \exp\left\{-g'\left(Y_t + \beta X_t\right) - a_Y P_t^{1-m}\right\}$$
$$P_{t+1} = X_t\left[1 - \exp\left(-a_X P_t^{1-m}\right)\right] + Y_t\left[1 - \exp\left(-a_Y P_t^{1-m}\right)\right]$$

where, X and Y are the two competing prey, P is the predator, a is the area of discovery of the searching predator, and m is an interference constant, interpretable as the slope of the decline in search efficiency with increasing predator density. When $m = 0$, this simulation is analogous to the basic Nicholson-Bailey model, and increasing interference lends additional stability. With complete niche overlap ($\alpha\beta \geq 1$) competitive coexistence is impossible, but with $\alpha\beta < 1$, a predator can stabilize an otherwise unstable competitive interaction if it prefers the superior competitor (i.e., if $\frac{aX}{aY} \neq 1$).

If this random predator is replaced by one that switches, changing its preference between prey types to focus on the more common one (Murdoch 1969), it can be a stronger stabilizing influence. Hassell models two competing prey and a switching predator with the following system:

$$X_{t+1} = \lambda X_t \exp\left\{-g\left(X_t + \alpha Y_t\right) - \left(1+E\right) a_X P_t^{1-m}\right\}$$
$$Y_{t+1} = \lambda Y_t \exp\left\{-g'\left(Y_t + \beta X_t\right) - \left(1-E\right) a_Y P_t^{1-m}\right\}$$
$$P_{t+1} = X_t\left[1 - \exp\left(-\left\{1+E\right\} a_X P_t^{1-m}\right)\right] + Y_t\left[1 - \exp\left(-\left\{1-E\right\} a_Y P_t^{1-m}\right)\right]$$

where

$$E = s\left(\frac{X_t - Y_t}{X_t + Y_t}\right)$$

and *s* varies from 0 to 1 to express the degree of switching. When density-dependent competition between prey species is strong ($\alpha\beta$ near 1.0) this switching predator exerts a powerful stabilizing influence.

References

Hassell, M. P. 1978. *The Dynamics of Arthropod Predator-Prey Systems*. Monographs in Population Biology, Princeton University Press. Princeton, NJ.

May, R. M. 1974. Biological populations with non-overlapping generations: stable points, stable cycles, and chaos. Science 186:645-647.

Murdoch, W. W. 1969. Switching in general predators: experiments on predator specificity and stability of prey populations. Ecological Monographs 39:335-354.

Competing Predators

Hassell (1978) predicates his discussion of multi-parasitoid systems on a sequential model with one predator (P) acting first, and then a second (Q) acting on the surviving prey. A system with simultaneous attack by both parasitoids would be equivalent if one is the superior competitor, winning in all cases of multiple parasitism. This scenario is illustrated by equations of the general form

$$N_{t+1} = \lambda N_t \; \mathrm{f}_1(P_t) \; \mathrm{f}_2(Q_t)$$

$$P_{t+1} = N_t \left[1 - \mathrm{f}_1\left(P_t\right) \right]$$

$$Q_{t+1} = N_t \; \mathrm{f}_1\left(P_t\right) \left[1 - \mathrm{f}_2\left(Q_t\right) \right]$$

where $\mathrm{f}_1(P_t)$ and $\mathrm{f}_2(Q_t)$ are prey survival probabilities after the searching of predators P and Q, and N gives the number of prey. Since the most interesting outcomes of this model are cases that permit the stable coexistence of all three parties, Hassell includes parasitoid aggregation similar to that in the non-random searching model (above), giving the recursions

$$N_{t+1} = \lambda N_t \left\{ 1 + \left(\frac{a_1 P_t}{k_1} \right)^{-k_1} \right\} \left\{ 1 + \left(\frac{a_2 Q_t}{k_2} \right)^{-k_2} \right\}$$

$$P_{t+1} = N_t \left[1 - \left\{ 1 + \left(\frac{a_1 P_t}{k_1} \right)^{-k_1} \right\} \right]$$

$$Q_{t+1} = N_t \left\{ 1 + \left(\frac{a_1 P_t}{k_1} \right)^{-k_1} \right\} \left[1 - \left\{ 1 + \left(\frac{a_2 Q_t}{k_2} \right)^{-k_2} \right\} \right]$$

Here k_1 and k_2 are the negative binomial dispersion coefficients describing the clumping of P and Q in patches of high host density (May 1978, May and Hassell 1981). When $k_1 = k_2 = \infty$ this formulation reduces to a three-species Nicholson-Bailey model.

The stability analysis of this model given by May and Hassell (1981) shows that three-species equilibria are most likely when both parasitoid-host links are stabilizing; i.e., when $k < 1$ for both parasitoids. Stable coexistence is also more likely if the inferior competitor (Q) has the higher searching efficiency.

References

Hassell, M. P. 1978. *The Dynamics of Arthropod Predator-Prey Systems*. Monographs in Population Biology, Princeton University Press. Princeton, NJ.

May, R. M. 1978. Host-parasitoid systems in patchy environments: a phenomenological model. J. Anim. Ecol 47:833-44.

May, R. M. and M. P. Hassell. 1981. The dynamics of multiparasitoid-host interactions. Am. Nat. 117:234-261.

Host, Parasitoid and Hyperparasitoid

The final model we have taken from Hassell's 1978 book is a three-trophic-level simulation illustrating host (*N*) and parasitoid (*P*) interacting with a hyperparasitoid (*Q*). The hyperparasitoid is assumed to reproduce only in hosts that have been previously attacked by the parasitoid. Hassell's model invokes aggregation for its stability, as in the previous models of nonrandom searching and competing predator, using the recursions

$$N_{t+1} = \lambda N_t \left\{ 1 + \left(\frac{a_1 P_t}{k_1} \right)^{-k_1} \right\}$$

$$P_{t+1} = N_t \left[1 - \left\{ 1 + \left(\frac{a_1 P_t}{k_1} \right)^{-k_1} \right\} \right] \left\{ 1 + \left(\frac{a_2 Q_t}{k_2} \right)^{-k_2} \right\}$$

$$Q_{t+1} = N_t \left[1 - \left\{ 1 + \left(\frac{a_1 P_t}{k_1} \right)^{-k_1} \right\} \right] \left[1 - \left\{ 1 + \left(\frac{a_2 Q_t}{k_2} \right)^{-k_2} \right\} \right]$$

All terms retain the meanings introduced earlier in this set. In particular, a_1 and a_2 are the searching efficiencies of the parasitoid and hyperparasitoid, respectively, and k_1 and k_2 are their dispersion coefficients.

Thorough stability analysis by May and Hassell (1981) shows local stability of the three-party interaction as long as the parasitoid and hyperparasitoid both aggregate in patches where the density of their respective prey is high. In particular, such interactions are more likely to be stable when the searching efficiency of the hyperparasitoid is higher than that of the parasitoid $\left(\frac{a_2}{a_1} > 1 \right)$.

References

Hassell, M. P. 1978. *The Dynamics of Arthropod Predator-Prey Systems*. Monographs in Population Biology, Princeton University Press. Princeton, NJ.

May, R. M. and M. P. Hassell. 1981. The dynamics of multiparasitoid-host interactions. Am. Nat. 117:234-261.

Continuous Predator-Prey Models

Let's assume (1) that except for the presence of predators, prey live in an ideal (density-independent) environment, (2) that the predator's environment is similarly ideal and its population growth is limited only by the availability of prey, (3) that both predators and prey reproduce continuously with ageless populations of identical individuals, and (4) that the predation rate is proportional to the rate of encounter between predators and prey, which is a random function of population density. These simplifying assumptions underlie a very basic model of predator-prey dynamics, embodied in the Lotka-Volterra predator-prey equations.

If N is the number of prey and P is the number of predators, then in the absence of predators, prey grow exponentially,

$$\frac{\mathrm{d}N}{\mathrm{d}t} = r_1 N$$

where r_1 is the prey intrinsic growth rate. Without prey, the predator population will starve,

$$\frac{\mathrm{d}P}{\mathrm{d}t} = -d_2 P$$

where $-d_2$ is a measure of the predators' starvation rate.

The chance of encounter between predator and prey is CNP, where C is a constant related to prey escape ability and the number of prey a predator takes per unit time. CN is often called the "functional response" of the predator; by giving C a constant value, we are assuming that the number of prey taken by each predator varies linearly with prey abundance.

Bringing the two species together and introducing the encounter rate into both equations, we have

$$\frac{\mathrm{d}N}{\mathrm{d}t} = r_1 N - CNP$$

$$\frac{\mathrm{d}P}{\mathrm{d}t} = -d_2 P + gCNP$$

where g is a constant defining the conversion efficiency of prey into predators. The product gCN is the predator's "numerical response." It measures the *per capita* production of the predator progeny as a function of prey density.

The behavior of this model at equilibrium can be analyzed by setting

$$\frac{\mathrm{d}N}{\mathrm{d}t} = \frac{\mathrm{d}P}{\mathrm{d}t} = 0$$

Then

$$P = \frac{r_1}{C} \quad \text{and} \quad N = \frac{d_2}{gC}$$

These expressions imply that there is a constant number of predators (r_1/C) above which prey densities will decrease and below which they will increase. Likewise, there is a constant number of prey (d_2/gC) above which predator densities will increase and below which they will decrease.

Populus includes a second predator-prey model (the "theta-logistic") which makes fewer simplifying assumptions, introducing nonlinear functional responses and density-dependent prey population growth. The rate of change in the prey population size with time is described by the following equation:

$$\frac{\mathrm{d}N}{\mathrm{d}t} = r_1 N\left(1-\left(\frac{N}{K}\right)^{\theta}\right) - \mathrm{f}\left(N\right)P$$

In this equation, P is predator population size, f(N) is the predator's functional response, and the prey population-growth rate in the absence of the predator is given by the $rN(1 - (N/K)^{\theta})$. This is the familiar logistic model of population growth with an additional term, given by the Greek letter theta, which allows different types of density dependence. If theta is large, the probabilities of birth and death do not change much until the prey population approaches its carrying capacity. If theta is small, per capita birth or death rates (or both) decrease rapidly with increasing population size, even at small population densities. This model of density-dependent population growth was originally proposed by Gilpin and Ayala (1973).

The population dynamics of the predator are described by

$$\frac{\mathrm{d}P}{\mathrm{d}t} = gP\left[\mathrm{f}\left(N\right) - D\right]$$

The term f(N) is again the functional response. D represents the intake rate of prey required for a predator to just replace itself in the next generation. This form of the predator growth equation makes two implicit assumptions; (i) the predator population density does not affect an individual predator's chances of birth or death directly (only indirectly via effects on the prey population size), and (ii) the number of surviving offspring produced by a predator is directly proportional to the amount of prey it consumes.

The remaining component of the model is the functional response, denoted by f(N). The functional responses of many predators have been determined in laboratory experiments in which different numbers of prey are placed in an arena with a predator for a specified amount of time. The Canadian ecologist, C. S. Holling (1965) categorized the functional responses into 4 possible types. Three of these have been frequently observed (Hassell 1978) and are discussed in most ecology textbooks. The type 1 response rises linearly with prey density; the type 2 response rises at a continually decreasing rate, and the type 3 response is sigmoid ('S' - shaped).

The type 1 functional response by definition is given by a constant C multiplied by prey population density N. There are many different mathematical formulas for representing type 2 and type 3 responses, but the following two are most common:

$$f(N) = \frac{CN}{1+hCN}$$ for the type 2 response, and

$$f(N) = \frac{CN^2}{1+hCN^2}$$ for the type 3 functional response.

The parameters *C* and *h* can have a number of different possible biological interpretations. As the number of prey becomes very large, both of the above functional responses approach an asymptotic value of 1/*h*. One possible interpretation of *h* is that it represents the amount of time required to handle a single prey item; at very high prey populations, a predator spends almost all of its time handling (and very little time searching), so the rate at which it catches prey is just 1/*h*. Under this interpretation, prey are never captured while another prey item is being handled, and are captured at a rate *CN* (type 2) or CN^2 (type 3) while the predator is searching for prey.

References

Alstad, D. N. 2001. *Basic Populus Models of Ecology*. Prentice Hall, Upper Saddle River, NJ. Chapter 5.

Gilpin, M. E. and Ayala, F. J. 1973. Global models of growth and competition. Proc. Nat. Acad. Sci. 70:3590-3593.

Hassell, M. P. 1978. *The Dynamics of Arthropod Predator-Prey Systems*. Princeton University Press. Princeton, N. J.

Holling, C. S. 1965. The functional response of predators to prey density and its role in mimicry and population regulation. Mem. Ent. Soc. Can. 45:3-60.

Lotka, A. J. 1925. *Elements of Physical* Biology. Williams & Wilkins, Baltimore. Reissued as *Elements of Mathematical Biology*. Dover Publications Inc. New York. 1956.

Rosenzweig, M. L. and MacArthur, R. H. 1963. Graphical representation and stability conditions of predator-prey interactions. American Naturalist 97:209-223.

Volterra, V. 1926. Fluctuations in the abundance of a species considered mathematically. Nature 118:558-60.

Genetic Drift: A Monte Carlo Model

This simulation uses a random number generator to sample genes from a small parental population and pass them on to offspring. Population size is assumed to remain constant from generation to generation, and allelic frequency changes result only from the random sampling process. Drift can be simulated for 1 to 10 diallelic loci simultaneously. To run the model, you must specify a population size, *N*, and initial allelic frequencies for each locus.

Suppose that a population consists of one male and one female, and that both are heterozygous at a locus with two mutant alleles. There are four alleles in the total gene pool, 2 **A** alleles and 2 **a** alleles, so $p = q = 0.5$. The female will produce **A** and **a** eggs in equal frequency, and the male will produce half **A** and half **a** sperm. The probability of two independent events occurring together is the product of their individual probabilities, so if gametes are chosen at random and fused to form a filial population of two individuals, the probability that the first individual will be an **AA** is (0.5*0.5) = 0.25, and the probability that both progeny will be **AA**'s is (0.5*0.5)*(0.5*0.5) = 0.0625. Thus if $N = 2$, there is 1 chance in 16 that allelic frequency will change from $p = 0.5$ to $p = 1.0$ in a single generation simply through the random sampling of gametes.

In addition to the drift from $p = 0.5$ to $p = 1.0$, there are other possible outcomes; p could change to 0, 0.25, or 0.75, and the likelihood of these events is calculated similarly (you should be able to do it). A computer model which uses random numbers to mimic this stochastic sampling process is called a "Monte Carlo Simulation."

The process of genetic drift and its implications are discussed in most treatments of population genetics or evolutionary biology. For examples, see

References

Crow, J. F. 1986. *Basic Concepts in Population, Quantitative, and Evolutionary Genetics*. W. H. Freeman and Co. N. Y. pp. 42-50.

Hartl, D. L. 1988. *A Primer of Population Genetics*, 2nd Edition. Sinauer Associates, Inc. Sunderland, MA. pp 69-77.

Hardl, D. L. and A. G. Clark. 1997. *Principles of Population Genetics*. Sinauer Associates, Inc. Sunderland, MA. pp 267-294.

Futuyma, D. J. 1986. *Evolutionary Biology*. Sinauer Associates, Inc. Sunderland, MA. pp 129-131.

Roughgarden, J. 1979. *Theory of Population Genetics and Evolutionary Ecology: An Introduction*. MacMillan Publishing Co., Inc. New York. pp 57-80.

Smith, J. M. 1989. *Evolutionary Genetics*. Oxford University Press. pp. 24-27,

Genetic Drift: A Markov Model

A "Markov" model is one in which some system is projected forward by repeatedly multiplying some representation of its current state by a transition function. Suppose that a population has a constant size with one individual. Let's call the number of *A* alleles at a locus the "state" of the population, which can thus be 0, 1, or 2. If $p_t(0)$ is the probability that the population is in state 0 (with no *A* alleles), then

$$p_{t+1}(0) = 1\,p_t(0) + \left(\frac{1}{4}\right)p_t(1) + 0\,p_t(2) \tag{1}$$

$$p_{t+1}(1) = 0\,p_t(0) + \left(\frac{1}{2}\right)p_t(1) + 0\,p_t(2) \tag{2}$$

$$p_{t+1}(2) = 0\,p_t(0) + \left(\frac{1}{4}\right)p_t(1) + 1\,p_t(2) \tag{3}$$

and in general

$$\left[p_{t+1}(0),\ p_{t+1}(1),\ p_{t+1}(2)\right] = \left[p_t(0),\ p_t(1),\ p_t(2)\right]\begin{bmatrix} 1 & 0 & 0 \\ \frac{1}{4} & \frac{1}{2} & \frac{1}{4} \\ 0 & 0 & 1 \end{bmatrix} \tag{4}$$

Using vector-matrix notation (where **P** is the matrix of transition probabilities and $\mathbf{p_t}$ is the state vector at time *t*),

$$\mathbf{p_{t+1}} = \mathbf{p_t}\mathbf{P} \tag{5}$$

The individual terms of the transition matrix for a population of any size (*N* = the number of diploid individuals) are given by the *j*th term in the binomial expansion of $(p+q)^{2N}$ as

$$p_{ij} = \left(\frac{(2N)!}{(2N-j)!j!}\right)\left(\frac{i}{2N}\right)^{j}\left(1-\frac{i}{2N}\right)^{2N-j} \tag{6}$$

We can simulate the rate of losses or fixations that are likely among a large sample of populations of a given size using this Markov model.

Reference

Roughgarden, J. 1979. *Theory of Population Genetics and Evolutionary Ecology: An Introduction.* MacMillan Publishing Co., Inc. New York. pp 58-68.

Inbreeding

This module simulates inbreeding in a finite population, showing both expected values of the inbreeding coefficient, *F*, and realized values observed in a Monte Carlo drift simulation. No selection operates; changes in allele frequencies and *F* are due entirely to chance sampling effects.

Two alleles that are “autozygous” or "identical by descent" are copies of the same ancestral allele. The inbreeding coefficient *F* can be interpreted as the probability that an individual's alleles at a particular locus are identical by descent. It can also be interpreted as the probability that two alleles drawn randomly from different individuals in the population one generation earlier are identical by descent. *F* = zero means that there has been no inbreeding, while *F* = 1 means the population is completely inbred. In this case, all individuals in the population are genetically identical.

In the absence of new genetic variation contributed by mutation or immigration, *F* increases in finite populations over time. Simply by chance, some alleles will be lost and others will increase in frequency. The result is that individuals in later generations have greater and greater probabilities of carrying copies of the same ancestral allele.

The exact rate at which the inbreeding coefficient is expected to increase is given by:

$$F_t = 1 - \left(1 - \frac{1}{2N}\right)^t$$

where F_t is the inbreeding coefficient in generation *t*, and *N* is the population size. At the outset, when $t = 0$, it is assumed that there is random mating and $F = 0$. The equation (and intuition) tells us that the inbreeding coefficient is expected to increase more slowly in larger populations and more rapidly in smaller populations. The *Populus* simulation of inbreeding graphs this theoretical inbreeding coefficient, F_t, as a smooth, continuous curve.

Population of a given size will not necessarily have exactly the same inbreeding coefficient, even if they have been mating randomly for the same number of generations. The equation gives an expected *F*, but there is variation around that expectation. Just by chance a finite population can evolve to $F = 1$ more quickly than expected, or even move temporarily towards $F = 0$. The theoretical model tells us what to expect on average. The *Populus* inbreeding module also graphs the actual autozygosity of individuals, F_i and the entire population F_p that result from a Monte Carlo simulation. These two measures differ when individuals are autozygous (carry alleles that are identical by common descent), but do not carry the same allele. Under these conditions, it is possible for F_i to be larger than F_p. It is also possible to reach $F_i = 1.0$ before $F_p = 1.0$. In this case every individual has become autozygous, but some are autozygous for different alleles. Such a population may return to some $F_i < 1.0$, but $F_p = 1.0$ is always an absorbing state.

Unless there are other forces operating, drift leads inevitably to fixation of one allele, at which point $F_p = 1$. All finite populations are headed to the same end, but vary in the rate at which they approach that end.

References

Crow, J. F. 1986. *Basic Concepts in Population, Quantitative, and Evolutionary Genetics*. W. H. Freeman & Co.

Crow, J. F. and M. Kimura. 1970. *An Introduction to Population Genetics Theory*. Harper and Row. pp 61-170.

Falconer, D. S. 1989. *Quantitative Genetics* (3rd edn). Longman Scientific & Technical. pp 63-69, 85-103.

Hartl, D. L. and A. G. Clark. 1989. *Principles of Population Genetics* (2nd edn). Sinauer Associates. pp 235-280.

Roughgarden, J. 1979. *Theory of Population Genetics and Evolutionary Ecology: An Introduction*, MacMillan Publishing Co. pp 169-192.

Population Structure

Simple population genetic models usually assume that mating is completely random so that frequencies of the different genotypes in each new generation can be estimated from allelic frequencies among the uniting gametes. In natural populations with a patchy distribution, this assumption will be violated if the probability of within-patch matings is higher than that of between-patch matings. This "population structuring" has interesting genetic consequences that can be illustrated with a simple example:

Suppose that mice have a polymorphic enzyme system with two different alleles, and we have determined the genotype of every individual from the population living in a barn. In addition, suppose that mice seldom move between parts of the barn, so that the population is subdivided ("structured") into partially isolated subpopulations or "demes." Genetic drift will raise the frequency of "*a*" alleles in some demes and lower it in others. Suppose further that the "*a*" allele frequency in half of the demes drifts to $p = 1.0$, and in the other half to $p = 0$. Overall allelic frequency throughout the entire barn is $p = 0.5$, and the expected frequency of heterozygotes is $2p(1\text{-}p)$, or 1/2. However, demes where $p = 1.0$ will produce only "*aa*" genotypes, and demes where $p = 0$ will produce only "*bb*" genotypes, and there are no heterozygotes in the entire barn. This difference between the observed and expected heterozygote frequencies is evidence of population structure.

Inbreeding is a second process that reduces heterozygosity, and is conceptually related to population structuring. In the most extreme inbreeding system, hermaphroditic selfing, all of the progeny of homozygotes and half the progeny of heterozygotes will be homozygotes, so population heterozygosity will decline by 1/2 each generation. Less extreme inbreeding systems will produce a proportionally weaker decline in heterozygosity depending on the mating probability and relatedness of relatives.

Sewall Wright introduced several related "inbreeding coefficients" which allow us to measure and distinguish the genetic consequences of mating and dispersal patterns. To define them, we use three different estimates of heterozygosity:

H_i is the observed frequency of heterozygous individuals in a deme, or subpopulation, averaged among demes. It is also the probability that one particular gene locus in an individual will be heterozygous.

H_s is the expected frequency of heterozygous individuals in the deme or subpopulation. It is calculated as $2p(1\text{-}p)$, where p is the allelic frequency in that deme, and averaged among demes.

H_t is the expected frequency of heterozygotes in the entire population, calculated as $2p(1\text{-}p)$, where p is the population-wide allelic frequency.

Wright's three hierarchical inbreeding coefficients are then defined as follows:

F_{is} is the heterozygote deficiency caused by nonrandom mating within the demes or subpopulations, calculated as

$$F_{is} = \frac{H_s - H_i}{H_s}$$

F_{st} is the heterozygote deficiency caused by population subdivision and the divergent drift of allelic frequencies in the separate demes, calculated as

$$F_{st} = \frac{H_t - H_s}{H_t}$$

F_{it} measures the overall inbreeding coefficient resulting from both causes, and is calculated as

$$F_{st} = \frac{H_t - H_i}{H_t}$$

Our simulation assumes that a population is subdivided into a number of demes whose size (and drift rate) can be set by the user. Gametes are chosen randomly to form a new population each generation. Users can also set a migration rate, causing a fraction of the individuals in each deme to be replaced every generation by migrants that are representative of the population-wide allelic frequency. Two output graphs plot the allelic frequencies in all demes, and the three inbreeding coefficients, F_{is}, F_{st}, and F_{it}.

Different combinations of drift and gene flow will affect the equilibrial *F*-values. In this simulation *F*-statistics will also be affected initially by historical disequilibria. The demes can be initiated independently at different (or similar) frequencies to illustrate this founder effect.

Our program uses the expressions given above to calculate the *F*-statistics in a simple and instructive way. Students should be aware, however, that the algorithms used in real empirical research are more complex, incorporating either sample-size adjustments (Nei and Chesser 1983) or analyses of variance on the allelic frequencies (Weir and Cockerham 1984).

References

Hartl, D. L. and A. G. Clark. 1997. *Principles of Population Genetics*. Sinauer Associates, Sunderland MA. pp 111-162.

Nei, M, and R. K. Chesser, 1983. Estimation of fixation indices and gene diversities. ANN. HUM. GENET. 47:253-259.

Weir, B. and C. C. Cockerham. 1984. Estimating F-statistics for the analysis of population structure. EVOLUTION 38:1358-70.

Wright, S. 1968. *Evolution and the Genetics of Populations*. University of Chicago Press.

Drift and Selection

This module simulates the operation of natural selection in a finite population. Both genetic drift and natural selection affect allele frequencies; by adjusting population size and the relative fitnesses of the several genotypes, the user can study the interaction of these two evolutionary forces.

Drift tends to eliminate genetic variation. In any finite population, one allele will eventually increase to fixation, at a rate that depends on the population size.

Selection can either maintain or eliminate genetic variation. Selection in favor of the heterozygote genotype creates a stable polymorphism, but selection in favor of one of the two homozygotes eliminates variation in deterministic models.

When both selection and drift operate, there is an opposition of evolutionary forces if the heterozygote is most fit, with selection acting to maintain variation and drift acting to eliminate it. Which force predominates depends on the relative strengths of drift and selection. Drift is very strong if population size is small, and is weak if population size is large. Selection is strong if the relative fitnesses, "*w*" parameters, differ greatly, and is weak is the *w*'s are similar.

Kimura has provided a rule of thumb comparing the strengths of selection and drift, as follows: Define *s*, the selection coefficient such that homozygotes have fitnesses 1-*s* relative to the heterozygote fitness of 1. *N* is the population size. Selection predominates when $4Ns >> 1$, and drift predominates when $4Ns << 1$. By “predominate” we mean selection (or drift) usually wins the battle to maintain (or eliminate) variation. When $4Ns$ is close to 1, then we cannot predict the evolutionary outcome with any certainty.

Reference

Kimura, M. 1983. The Neutral Theory of Molecular Evolution. In: *Evolution of Genes and Proteins*, M. Nei and R. K. Koehn, eds. Sinauer Associates, Sunderland, MA pp. 208-233.

Woozleology

In his book *The Blind Watchmaker*, Richard Dawkins confronts the old saw analogizing evolution to the chance typewriter keystrokes of a monkey, who "sooner or later," will reproduce the works of Shakespeare. He sketches a computer program that uses cumulative selection to model "evolution" of the phrase "METHINKS IT IS LIKE A WOOZLE." Hamlet and Polonius thought the cloud that they were observing looked like a weasel, but my daughter Amy, who was 3 years old when I first coded this model, considered Milne the pinnacle of English literature. There are 26 letters in the alphabet and spaces function like an additional letter. Since the phrase has 28 characters and spaces, we expect the monkey to type it correctly by chance once in 27^{28} attempts. In fact, cumulative selection is a much more effective and rapid process. This metaphorical simulation works in the following way:

(a) An initial phrase consisting of 28 randomly chosen letters or spaces becomes the first-generation "parent." *Populus* steps through the 28 letter positions, drawing a random integer from the range 1 through 27 for each position. If the draw for a position is 1, the program assigns an *A*; if the draw is 26 it assigns a *Z*. Draws of 27 receive a blank space.

(b) This "parent" phrase (which is probably nonsense) is then allowed to "reproduce." If we set "broodsize" to 10, then *Populus* makes 10 descendent copies of the original phrase. For each letter or space in the parent phrase, the program tests a random real number from the range 0 to 1 against the user-specified "mutation rate." This determines whether that position in the copy receives the original parental letter, or a new, randomly chosen character. For example, if the mutation rate is set at 0.1 and *Populus* draws a random real number equal to or greater than 0.1, then the original parental letter from that position is copied faithfully. If the draw is less than 0.1, that position in the offspring copy phrase receives a "mutant" letter, determined by another integer draw from the range 1 through 27.

(c) Next, selection operates on the progeny. Each phrase is compared with the target phrase "METHINKS IT IS LIKE A WOOZLE," and the copy that matches the target at the largest number of positions becomes the next-generation parent. It is copied in turn to provide a new generation of progeny, and the process continues until cumulative mutation and selection produce the target phrase.

(d) The *Populus* program incorporates a recombination process that was not part of the Dawkins scenario. You can activate this feature by checking the diploid-sexual-process box in the input window and setting a non-zero crossover rate. Then *Populus* establishes two random parental phrases, $\mathbf{P}_1$ and $\mathbf{P}_2$. One of the parental phrases is arbitrarily chosen to serve as the model for offspring copies, as before; but this time *Populus* draws two random real numbers from 0 to 1 at each letter position. The program tests the first random draw against the "crossover rate." If the draw equals or exceeds the crossover rate, then the previously chosen parental phrase is the copy model for this letter position in the offspring phrase. If the draw is less than the specified crossover rate, transcription switches to the same letter position in the other parent, and continues from that second parent until another crossover occurs, further on. The second random draw at each letter position determines whether a faithful copy or a random mutation is placed in the offspring phrase. The best offspring phrases from first and last halves of the total brood become next-generation parents.

Depending on the parameter values specified, this program usually "evolves" the target phrase in a few dozen or a few hundred generations. This shows that the cumulative interaction of mutation and selection can easily produce results that would be highly improbable from a single-step random process. As a model of evolution by natural selection, the metaphor has obvious limitations, including its unrelenting focus on a fixed future target, and its limited modeling of the chance processes in Mendelian inheritance. Nevertheless, it provides elegant clarification of an issue that is misrepresented by creationists arguing from biological complexity in the tradition of Bishop Wilberforce.

Reference

Dawkins, Richard. 1986. *The Blind Watchmaker.* W. W. Norton & Co. New York. 332 pp.

Selection on a Diallelic Autosomal Locus

The process of evolution has two components, natural selection, and the inheritance mechanisms that make each individual genetically unique. This *Populus* simulation offers a deterministic model of selection with few complications of inheritance; it assumes that population size is infinite so that there are no effects of sampling chance, that the selection regime remains constant, and that the phenotype is determined directly by a single autosomal gene locus, without environmental effects.

There are several points in a life cycle where selection might operate. If we begin with newly fertilized zygotes, there may be individual differences (a) in survival to reproductive age, (b) mating ability, (c) the number of gametes produced, or (d) the probability that those gametes will fuse to form successful zygotes. Here we will assume that selection is manifested in viability and fecundity differences between genotypes, ignoring the complications of sexual selection, mating systems, meiotic drive, etc.

Suppose that two different alleles (*A* and *a*) of a gene that affects viability and fecundity are present in a population. We say that the population is *polymorphic* at this gene locus, and individuals can therefore have diploid genotypes of *AA*, *Aa*, or *aa*. If these genotypes survive and reproduce themselves at different rates, population composition will change over time as the frequency of the more fit allele increases.

If the frequency of *A* alleles is p and the frequency of *a* alleles is $(1-p) = q$, and if mating is random so that the alleles combine in proportion to their frequencies, then the expected frequencies of *AA*'s and *aa*'s are p^2 and q^2, respectively. Heterozygotes might be either *Aa* or *aA*, so their expected frequency is $2pq$. If each genotype has a different relative probability of survival and reproduction called its relative fitness (w_{AA}, w_{Aa} and w_{aa}), we can formulate an equation to project the increasing frequency of the most fit genotype as

$$p_{t+1} = (p_t)\frac{p_t w_{AA} + q w_{Aa}}{p_t^2 w_{AA} + 2 p_t q_t w_{Aa} + q_t^2 w_{aa}}$$

This is called a recursion equation because p_{t+1} can be repeatedly substituted for p_t to give a recursive prediction of allelic frequency as far into the future as we wish. It helps the intuition to note that this equation multiplies current allelic frequency (p_t) by a ratio of weighted averages. The numerator is a weighted average giving mean fitness among the *A*-carrying genotypes, and the denominator is the weighted average fitness among all three genotypes.

References

Crow, J. F. 1986. *Basic Concepts in Population, Quantitative, and Evolutionary Genetics.* W. H. Freeman and Co. pp. 70-82.

Crow, J. F. and M. Kimura. 1970. *An Introduction to Population Genetics Theory*. Harper and Row. pp 258-262, 270-272.

Falconer, D. S. 1996. *Quantitative Genetics* (4th edn). Longman Scientific & Technical. pp 25-45.

Hartl, D. L. and A. G. Clark. 1989. *Principles of Population Genetics* (2nd edn). Sinauer Associates. pp 147-164, 180-182, 199-201.

Roughgarden, J. 1979. *Theory of Population Genetics and Evolutionary Ecology: An Introduction*, MacMillan Publishing Co. pp 26-47.

Wilson, E. O. and W. H. Bossert. 1971. *A Primer of Population Biology*. Sinauer Associates. pp 47-61.

Selection on a Multi-Allelic Locus

Many polymorphic gene loci have more than two alleles segregating in natural populations. To develop a recursive model with multiple alleles at a single locus, we need a notation that allows us to keep track of their identities and frequencies; we will call the locus the A locus, and the alleles A_i, with frequencies p_i, where $i = 1, 2, .. n$, n is the number of alleles, and the allelic frequencies sum to 1.0. The genotypic frequencies are given by the square of the multinomial of allelic frequencies, so the frequency of het A_iA_j is $2p_ip_j$, and the frequency of homozygote A_iA_i is p_i^2.

We will refer to the viability of A_iA_j as w_{ij}, and the viabilities of all the genotypes can be written in a square viability matrix with w_{ij} in row i and column j.

	A_1	A_2	A_3
A_1	w_{11}	w_{12}	w_{13}
A_2	w_{21}	w_{22}	w_{23}
A_3	w_{31}	w_{32}	w_{33}

The weighted average of the elements in one row of this matrix gives the *marginal fitness*, w_i, of the allele that occurs in all the genotypes of that row. The weighting frequencies for calculating w_i are the p_j, the frequencies of the alleles that i is paired with in genotypic combinations. The marginal fitness is the average fitness of the allele in all of its genotypic combinations, weighted by their frequencies,

$$w_i = \sum_j w_{ij}\, p_j \tag{1}$$

The system of recursions that allows us to predict future allelic frequency for the several segregating alleles at this locus is then

$$p_{i,t+1} = \frac{p_{i,t}\, w_i}{\bar{w}} \tag{2}$$

where the population mean fitness, $\bar{w}$, is

$$\bar{w} = \sum_i w_i = \sum_i \sum_j w_{ij}\, p_i\, p_j \tag{3}$$

This recursion is exactly analogous to our two-allele recursion. It is the frequency-weighted average fitness of all i-carrying genotypes over the population average fitness including all alleles.

Equilibria for this set of recursions are found by setting the $p_{i,t+1} = p_{i,t}$ and solving for $\hat{p}$, which gives

$$w_1 = w_2 = w_3 = \ldots = \bar{w} \tag{4}$$

In words, all of the marginal fitnesses must be equal for the population to be in equilibrium. There are n trivial equilibria corresponding to fixation of each of the n alleles, and there may also

be interior polymorphic equilibria with several or all of the alleles maintained by selection. For a
three allele system, the general criterion for a stable, complete polymorphism (all of the alleles are maintained) is that the average fitness of the heterozygotess must be greater than the average fitness of the homozygotes.

The classic empirical example of a three-allele system is based on the three most common alleles at the human β-globin locus, $Hb\beta^A$, $Hb\beta^C$, and $Hb\beta^S$, which we will call *A*, *C*, and *S*. *S* homozygotes have sickle-cell anemia, which occurs when the hemoglobin forms long crystals under low oxygen tension. The table below is abstracted by Hartl and Clark (1989, p. 171) from Cavalli-Sforza and Bodmer (1971). It gives the observed genotypic counts and Hardy-Weinberg expectations for all six genotypes from a sample of 32,898 individuals from 72 West African populations, with estimates of their fitnesses calculated from the observed/expected ratio, and relative fitnesses, normalized such that $w_{AS} = 1$.

	Genotype					
	AA	*SS*	*CC*	*AS*	*AC*	*SC*
Observed	25374	67	108	5482	1737	130
Expected	25616	307	75	4967	1769	165
Obs/Exp	0.99	0.22	1.45	1.10	0.98	0.79
Rel Fitness	0.89	0.20	1.31	1	0.89	0.70

The first thing to be seen from this table is that if a population composed entirely of *AA* genotypes was invaded by a single *S* allele (which would occur in a heterozygote), *S* would increase in frequency, because a single *S* in a population of *A* alleles will have a marginal fitness of 1.0, which is greater than the population mean fitness of 0.89. With only these two alleles present, the population will evolve to the familiar 2-allele equilibrium,

$$\hat{p}_s = \frac{w_{SS} - w_{AS}}{w_{AA} - 2w_{AS} + w_{SS}} \tag{5}$$

For the relative fitnesses in the table, the equilibrial frequency of *S* is 0.1209 and mean fitness at equilibrium is 0.9033.

If a second mutation introduces the *C* allele into a population at equilibrium between *A* and *S*, its spread will be determined by its marginal fitness which is

$$w_C = p_A w_{AC} + p_S w_{SC} + p_C w_{CC} \tag{6}$$

When *C* is a rare mutant, the third term can be ignored, because $p_C \approx 0$. Therefore, since $p_S = 0.1209$, $p_A = 1 - p_S = 0.8791$. The marginal fitness of *C* when it is a rare mutant is thus

$$w_C = (0.8791)(0.89) + (0.1209)(0.70) = 0.8670 \tag{7}$$

which is less than the population mean fitness (at the equilibrium between *A* and *S*) of 0.9033. Thus *C* cannot invade when it is rare, even though a population that is fixed for *C* would have

global maximum mean fitness. If C were to be introduced in sufficient numbers to include a contribution from the third term in equation 6, then *C* would fix.

Because empirical electrophoretic work in the 1970's revealed many examples where multiple alleles segregated together in wild populations, there was widespread interest in the hypothesis that these polymorphisms could be maintained by selection. Subsequently, both analytical and numerical studies of this issue have demonstrated that the selective maintenance of multiple-allele polymorphisms is very unlikely.

References

Cavalli-Sforza, L.L. and W. F. Bodmer. 1971. *The Genetics of Human Populations*. W. H. Freeman and Co.

Crow, J. F. 1986. *Basic Concepts in Population, Quantitative, and Evolutionary Genetics*. W. H. Freeman and Co. pp. 85-108.

Hartl, D. L. and A. G. Clark. 1989. *Principles of Population Genetics*. Sinauer Associates, Inc. pp 168-176.

Selection on Two Loci

This module shows how selection operates when two loci influence fitness. There are more variables to keep track of than in the one-locus case. With alleles "*A*" and "*a*" at one locus, and "*B*" and "*b*" at the other locus, there are four types of gametes: *AB, Ab, aB, ab*. A new parameter "*D*" measures the statistical association between alleles at the two loci.

Under a special circumstance, selection at two loci behaves just like selection at one locus. The special condition is additivity of fitness effects, i.e., the fitness of *AABB* individuals is just the sum of fitness effects of *AA* plus effects *BB*. Under additivity, equilibria for each locus appear just as they would if the other locus were not there.

Another property of additive models is that *D* goes to zero, i.e., alleles at the two loci become randomly associated, even if they were initially non-randomly associated. This also occurs when there is no selection, as shown by the default parameters. The rate at which *D* goes to zero in these cases depends on *R*, the recombination fraction.

If fitness effects are non-additive ("epistasis"), then the situation can become very complicated. *D* will not necessarily go to zero. There can be many polymorphic equilibria, some stable and some unstable. The principle of maximized mean fitness no longer applies. The existence of certain equilibria is sensitive to *R*. Usually, strong non-additive selection and small *R* causes equilibria with non-zero *D*, i.e., selection builds up combinations of alleles that work well together, even though recombination tends to tear them apart.

References

Crow, J. F. 1986. *Basic Concepts in Population, Quantitative, and Evolutionary Genetics*. pp. 70-109.

D. L. Hartl and A. G. Clark (1997) *Principles of Population Genetics*. Sinauer, Sunderland, MA. pp. 211-255.

Hedrick, P. W. 2000. *Genetics of Populations*. Jones and Bartlett, Boston, MA.

Selection on a Sex-Linked Locus

This program shows how allelic frequencies change when the locus under selection is on a sex-determining chromosome. There are five possible genotypes: three in the homogametic sex (usually females) denoted *XX*, *Xx*, and *xx*, and two in the heterogametic sex (usually males), denoted *XY* and *xY*. There are two allelic frequencies to keep track of, *p* in females and *p* in males, where *p* is the frequency of the "*X*" allele.

Selection on a sex-linked locus differs from selection on an autosomal locus in several respects:

1) Oscillations of allelic frequency - In the one-sex autosomal model there are never oscillations in allelic frequency over time. However, in the sex-linked model there can be oscillations if allelic frequencies are initially different in males and females. The default parameter values illustrate oscillations. Notice that frequencies eventually become equal in the two sexes.

2) Genetic polymorphism - In the two-allele autosomal model there is only one mechanism that maintains genetic polymorphism: heterosis, or overdominance, where the heterozygote genotype has the highest fitness. For the sex-linked case there are two ways: either by this heterozygote advantage, or by differential selection in the two sexes (i.e., one allele is favored in one sex and the other allele is favored in the other sex). See if you can find examples of both types of polymorphism.

References

Crow, J. F. 1986. *Basic Concepts in Population, Quantitative, and Evolutionary Genetics*. pp. 70-109.

D. L. Hartl and A. G. Clark (1997) *Principles of Population Genetics*. Sinauer, Sunderland, MA. pp. 211-255.

Hedrick, P. W. 2000. *Genetics of Populations*. Jones and Bartlett, Boston, MA.

Selection and Mutation

Empirical studies of variability in natural populations often show rare, deleterious alleles that one might expect to be eliminated by natural selection. Huntington's chorea, cystic fibrosis, Tay-Sachs syndrome, and sickle-cell anemia are human diseases caused by rare deleterious alleles. While an overdominant advantage affects the frequency of sickle-cell (and possibly Tay-Sachs) in some selective environments, others have no positive effect whatever. Their frequency probably reflects a balance between the rates at which deleterious mutations appear and are eliminated by selection. As an example, consider the case of a deleterious recessive. At low frequencies (small q) its phenotype is seldom expressed because the heterozygous and homozygous genotypes in which it occurs are rare ($2pq$) and rare-squared (q^2), respectively. On the other hand, as the recessive becomes less common it appears through mutation from the alternative allelic type more frequently, because a larger fraction of the gene pool is mutable. As a result, we can expect an equilibrial frequency where the rates of selective removal and mutational origin balance.

Selection-mutation balances are easily simulated with an analog of our autosomal selection model. We will assume that selection operates against the "*a*" alleles, and that while p (the frequency of "*A*" alleles) changes under the influence of selection, mutation converts some "*A*" alleles to "*a*" at a rate μ per generation. Since the interesting equilibria occur when "*a*" alleles are rare and reverse mutations will be unimportant,

$$p' = p\frac{\left(pw_{AA} + qw_{Aa}\right)\left(1-\mu\right)}{\overline{w}}$$

where w_{AA} is the relative fitness of "*AA*" genotypes, etc.

Since gene expression is important in determining whether selection actually operates against an allele when it appears in heterozygotes, dominance has a strong effect on the mutation-selection balance. It is convenient to define one additional term, "*h*" such that $w_{AA} = 1$, $w_{Aa} = 1 - hs$, and $w_{aa} = 1 - s$ (where "s" is the selection coefficient against "*aa*"). When $h = 0$, "*a*" is completely recessive relative to "*A*," and when $h = 1$ it is completely dominant. $h = 1/2$ gives the additive case where heterozygote phenotypes are exactly intermediate between the two homozygotes.

One of the interesting consequences of the selection-mutation balance is a reduction in population mean fitness of $1 - (1-\mu) = \mu$, called the mutational load. Counter-intuitively, this load is independent of s, the selection coefficient against the different mutations, because severely detrimental mutations reach a lower equilibrial frequency than those that suffer a minor penalty and affect a larger fraction of the population.

References

Crow, J. F. and M. Kimura. 1970. *An Introduction to Population Genetics Theory*. Harper & Row. New York. pp. 258-262.

Hartl, D. L. and A. G. Clark. 1997. *Principles of Population Genetics*. Sinauer Associates, Sunderland, MA.

Maynard Smith, J. 1989. *Evolutionary Genetics*. Oxford University Press. pp. 55-60.

Interdemic Group Selection

1. Levin and Kilmer (1974) presented a simulation of group selection assuming that a population is subdivided into separate, randomly interbreeding demes, and that frequencies of altruistic and egoistic alleles at a single locus are affected by (a) selection on individuals within each deme, (b) genetic drift, (c) the exchange of migrants between demes, and (d) demic survival rates that vary with the local frequency of altruistic and egoistic individuals.

2. Simulation runs start with a single altruistic mutation, or a binomial sampling procedure establishes altruist frequencies in every deme near some arbitrary starting value. In the later case, 2*N* random numbers are drawn for each deme, and one altruistic allele is tallied for every draw which is smaller than the specified starting frequency.

3. Each generation incorporates four processes as follows:

   (a) First, natural selection operates on the individuals within each deme, using the simple, deterministic model of autosomal selection that we developed in lecture 6.

   (b) A binomial sample (as in 2 above) based on the altruist frequency resulting from individual selection is used to simulate genetic drift within each deme.

   (c) A portion of each deme is replaced by migrants from the population at large. *N* random numbers are drawn for each deme, and the number of draws that are smaller than the specified migration rate sets the number of individuals to be replaced. The appropriate alleles are eliminated from each deme by binomial sampling, and replaced from the population at large. Sampling from the population-wide gene pool occurs without replacement. Note therefore that this is an island model.

   (d) Finally, some demes are extinguished and replaced by colonists drawn from the population at large. Probabilities of survival, *PS* are calculated for each deme as

$$PS_i = a + bq_i^c \qquad (1)$$

   where q_i is the frequency of altruistic alleles in the *i*th deme and coefficients *a*, *b*, and *c* define the functional dependence of survival on the ratio of altruistic and selfish genes, as illustrated.

4. This model demonstrates that group selection is able to overcome countervailing selection at the individual level, but the range of

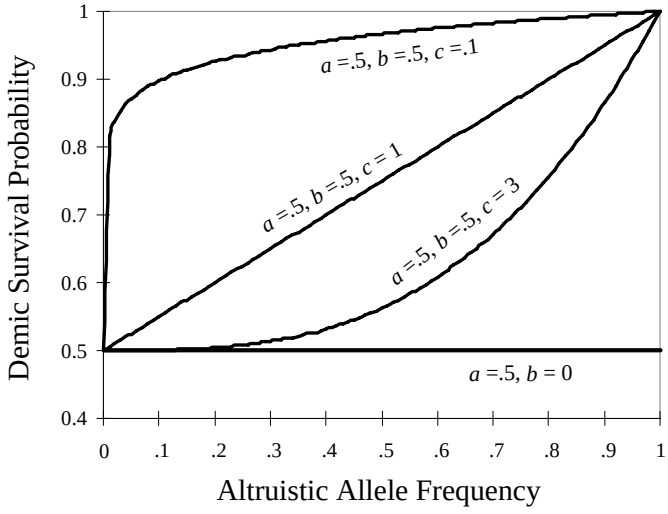

Figure 2. Four different demic survival functions for the Levin and Kilmer model. Curve shapes are specified by values of the *a*, *b*, and *c* fudge factors.

parameter values permitting this result is very restricted. In general,

a. Deme size must be very small, so that drift can cause interdemic variance in allelic frequencies. Also, in natural populations (but not in this simulation) small deme sizes will maintain vulnerability to demographic stochasticity and demic extinction will be high. Although it is not a result of this simulation (which lacks mutation), small deme size also reduces the probability that a "cheating" trait will evolve within the deme.

b. Gene flow between demes must be kept to a very low level, so that interdemic variance in allelic frequency is maintained.

5. Based on simulations like this one, it became the prevailing consensus in the mid 70's that group selection was seldom likely to provide substantial opposition for individual selection.

References

Levin, B. R. and W. L. Kilmer. 1973. Interdemic selection and the evolution of altruism: a computer simulation study. Evolution 28:527-545.

Lewontin, R. C. 1970. The units of selection. Ann. Rev. Ecol. Syst. 1:1-18.

Wade, M. J. 1977. An experimental study of group selection. Evolution 31:134-53.

Wade, M. J. 1982. Group selection: migration and the differentiation of small populations. Evolution 36:949-61.

Wade, M. J., and D. E. McCauley. 1980. Group selection: the phenotypic and genotypic differentiation of small populations. Evolution 34:799-812.

Williams, G. C. 1966. *Adaptation and Natural Selection*. Princeton University Press.

Intrademic Group Selection

1. Although a deme or randomly interbreeding subpopulation is the unit many evolutionists envision while thinking about group selection, D. S. Wilson has suggested alternative models focusing on the evolutionary consequence of various demic substructures. For example, while many life histories have a dispersing phase which makes demes very large, ecological interactions that affect fitness often take place in much more localized units, which Wilson calls "trait groups." After natural selection operates within these trait groups, demic frequency estimates require a weighted average among all trait groups in the deme.

2. An intrademic group selection model envisages the following scenario:

   a. A large, randomly interbreeding deme with altruistic and egoistic alleles segregating at any desired starting frequency is randomly subdivided into trait groups. Drift and founding effects will cause these groups to differ in altruist frequency.

   b. Natural selection operates within each trait group for one or more generations. Our algorithm is the same as that described for selection on a single autosomal locus, except that fitnesses of the genotypes are

$$W_{AA} = (1 + b\,q_i)(1 - 2s) \quad (1)$$

$$W_{AE} = (1 + b\,q_i)(1 - s) \quad (2)$$

$$W_{EE} = (1 + bq_i) \quad (3)$$

   where *A* and *E* represent the altruistic and egoistic alleles, *b* is the benefit realized by recipients of the altruism, *s* is the cost sustained by altruists, and q_i is the local frequency of altruistic alleles in the *i*th trait group. This process affects both the allelic frequencies and sizes of the trait groups.

   c. After selection within the trait groups, a new weighted average allele frequency is calculated for the deme as a whole, and new trait groups are drawn, using a binomial sampling procedure based on this updated frequency. The program draws 2*N* random numbers for each trait group and tallies one altruistic allele for each draw which is smaller than the overall demic frequency.

References

Williams, G. C. 1966. *Adaptation and Natural Selection*. Princeton University Press.

Wilson, D. S. 1975. A theory of group selection. Proc. Nat. Acad. Sci. USA 72:143-146.

Wilson, D. S. 1983. The groups selection controversy: history and current status. Ann. Rev. Ecol. Syst 14:159-87.

Kirkpatrick's Haploid Arbitrary Model of Sexual Selection

Elaborate sex-limited ornaments like the tails of peacocks and birds of paradise appear to increase their bearers' attractiveness to potential mates at a cost to their viability. These observations have posed an interesting challenge to evolutionists because, while it is plausible that some such traits might function in the competition between males for matings (Darwin 1871), an explanation for female preference is much more difficult; why should females evolve a predilection to choose traits that reduce male viability?

R. A. Fisher suggested that the evolution of female choice would initially require a reproductive advantage. For example, a female who chose mates possessing some attribute that conferred high viability might have highly viable progeny. If females with the strongest preferences choose males with the most pronounced traits, the genetic correlation between female choice and male attribute could produce a "runaway process" in which the male character evolves beyond the point where it shifts from viability asset to liability under the impetus of enhanced mating success.

This simulation reproduces a two-locus haploid model by Mark Kirkpatrick (1982). It assumes that there is a sex-limited diallelic locus in males (t), one allele (t_1) conferring a "normal" or "cryptic" phenotype with high viability, and one (t_2) conferring some arbitrary trait with reduced viability ($1 - s$, where $s > 0$). In females, there is a corresponding diallelic locus (p) such that some females (p_1) mate randomly or prefer normal males, while the others (p_2) prefer males with the reduced-viability trait. The intensity of female preferences is set by the parameter values a_1 and a_2; p_2 females prefer to mate with t_2 males by the factor a_2 and a_1 indicates the preference of p_1 females for t_1 males. There is no cost to the females of choosing mates. The recursion equations that Kirkpatrick developed from these assumptions are moderately complex and will not be given here; interested students are directed to the source.

Populus produces four different output screens for Kirkpatrick's model; 1) t_2 vs. p_2, the frequency of males with the secondary sexual characteristic vs the frequency of females that prefer the secondary males; 2) D vs. time, the linkage disequilibrium correlating the male trait and female choice alleles as selection proceeds; 3) male viability vs. time, illustrating declines in male viability if the secondary trait increases in frequency; 4) D vs. t_2 and p_2, in three dimensions.

These simulations produce lines of equilibria where the viability penalty experienced by males bearing the t_2 trait is exactly balanced by their enhanced attractiveness to females (given as a heavy blue line on the t_2 vs. p_2 graph). At low frequencies of the p_2 female choice allele, this mating advantage is often insufficient to maintain t_2 in the population, but at higher p_2 frequencies polymorphic equilibria or even fixation of the t_2 allele are possible. There is no direct selection on females; p frequencies change only as a correlated response to changes in male trait frequency, so linkage disequilibrium between the male and female loci is critical to the evolution of female choice. At polymorphic equilibria where p_1, p_2, t_1, and t_2 are all maintained in the population, this linkage disequilibrium (caused by non-random mating) is a permanent feature even with very high recombination rates. Finally, note that when the slope of the line of polymorphic equilibria is steep, small changes in the frequency of female choice alleles can effect large shifts in the composition of the male population.

References

Darwin, C. 1871. *The Descent of Man and Selection in Relation to Sex*. John Murray, London.

Fisher, R. A. 1958. *The Genetical Theory of Natural Selection*. 2nd ed., Dover, N.Y.

Kirkpatrick, M. 1982. Sexual selection and the evolution of female choice. *Evolution* 36:1-12.

Maynard Smith, J. 1991. Theories of sexual selection. *TREE* 6:146-51.

Handicap Models of Sexual Selection

1. The "handicap" or "viability indicator" hypothesis was introduced by Zahavi (1975). Zahavi's idea is that while conspicuous males suffer reduced viability, those that do survive to reproduce must be extraordinarily fit in other respects. If this vitality is inherited by both sons and daughters it may suffice to compensate the sons' handicap, and females should evolve a preference for conspicuous mates. John Maynard Smith (1976) outlined a handicap simulation which was developed and analyzed by Graham Bell (1978). Later, Malte Andersson (1986) added a wrinkle that increases realism and the efficacy of the handicap process. This *Populus* module reproduces both the Maynard Smith/Bell model, and Andersson's modification.

   a. Handicap models of sexual selection require at least three polymorphic gene loci; one to specify male ornamentation, one to specify viability, and one to specify female choice. Maynard Smith modeled a biparental, haploid system with free recombination. *This means that individuals carry only a single allelic copy of each gene, and there is an equal probability that this allele came from mother or father*. He also assumed a monogamous mating system to eliminate sexual selection mediated by a Fisherian mating advantage. This genetic system is quite unlike that of guppies, and the haploid simplification may be misleading (cf. Heisler and Curtsinger 1990). Free recombination certainly sets up a worst-case scenario for the handicap process. Sexual selection requires a correlation between the conspicuous trait and the high-viability allele, caused in this case by female choice; by reducing linkage disequilibrium, free recombination reduces the likelihood that conspicuous traits will spread by "hitch-hiking" with another favorably selected allele.

   b. Three diallelic loci in this simulation function as follows: The *A* locus codes a male-limited ornament; *A* males develop the ornament, while *a* genotype males are always cryptic. The *B* locus is expressed in both sexes; individuals with the *B* allele have a higher probability of survival to reproductive age than individuals with the *b* allele. The *C* locus codes female-limited choosiness; *C* females prefer to mate with males displaying the ornament, while *c* females mate randomly. We will refer to the frequencies of the *A*, *B*, and *C* alleles as *p*, *q*, and *r*, respectively, and to the *a*, *b*, and *c* frequencies as 1-*p*, 1-*q*, and 1-*r*.

trait	freq	state	
male ornament	*p*	*A* present	*a* absent
male/female fitness	*q*	*B* high	*b* low
female choice	r	*C* choosy	*c* random

   c. The Andersson version is identical, except that *A* males develop the ornament only if they are in good condition by virtue of carrying the *B* (high-viability) allele. This means that a female who chooses an ornamented male always gets a *B* mate. It maximizes the correlation between *A* and *B* alleles, and makes the Andersson sexual selection process work a little better than Maynard Smith/Bell.

2. An allelic-frequency recursion for this model would be frightfully complex, including marginal fitnesses for each of the six alleles across 32 genotypic combinations, and four

different linkage disequilibria among and between loci. To avoid all this, our simulation follows *genotypic* frequencies through each generation with the following steps:

a. To begin, we define an initial allelic frequency set, $IfS = \{p_0, q_0, r_0\}$, and calculate a vector of genotypic frequencies, {*ABC*, *ABc*, *AbC*, *Abc*, *aBC*, *aBc*, *abC*, *abc*}, for both males and females. We assume that the simulation begins in linkage equilibrium, thus frequencies will be $\{p_0q_0r_0, p_0q_0(1\text{-}r_0), p_0(1\text{-}q_0)r_0, p_0(1\text{-}q_0)(1\text{-}r_0), (1\text{-}p_0)q_0r_0, (1\text{-}p_0)q_0(1\text{-}r_0), (1\text{-}p_0)(1\text{-}q_0)r_0, (1\text{-}p_0)(1\text{-}q_0)(1\text{-}r_0)\}$. These two identical vectors of genotypic frequencies become the male and female zygotes.

b. Our genetic assumptions imply that there will be sexual and genotypic differences in viability to reproductive age. To accomplish this, we define a fitness set, $FS = \{\alpha,\beta,\varepsilon\}$. We set α as the baseline survival probability, β as the effect of the *A* locus, and ε as the effect of the *B* locus. Thus males with the *a* allele and all females will enjoy an increment, β, in viability over males that carry the conspicuous *A* allele. Likewise, individuals with the *B* allele will gain ε probability of surviving over those with the *b* allele. If there is no cost of female choice, the *C*-locus genotype has no effect on survival and either allele may be substituted, as indicated by question marks, below. The viabilities are:

Genotype	male viability	female viability
AB?	$\alpha + \varepsilon$	$\alpha + \beta + \varepsilon$
Ab?	$\alpha(+\beta)^*$	$\alpha + \beta$
aB?	$\alpha + \beta + \varepsilon$	$\alpha + \beta + \varepsilon$
ab?	$\alpha + \beta$	$\alpha + \beta$

*The survival of *Ab?* males is higher ($\alpha + \beta$) in the Andersson version than in Maynard Smith/Bell (α), because Andersson's *Ab?* males do not express the handicapping trait. Since the *FS* values are probabilities of surviving to reproductive age, their values are constrained such that $0 \leq \alpha, \beta, \varepsilon \leq 1$, and $0 \leq \alpha + \beta + \varepsilon \leq 1$.

c. After operating with this matrix of viabilities we re-normalize so that the adult male and female genotypic frequency vectors (which will no longer be identical) both sum to 1.0, and calculate male and female allelic frequencies at all three loci $\{p'_m, q'_m, r'_m\}$, $\{p'_f, q'_f, r'_f\}$. The prime notation will refer to frequencies in the reproductive adults, after viability selection.

d. 64 different mating combinations are possible between the eight male and female genotypes. The probability of each mating is determined by the relevant male and female genotypic frequencies, and by female preference. To quantify female preference factors for the Maynard Smith/Bell version, we will assume that *C* females mate with *A* males as long as they are available, and those that do not get an *A* male choose at random from those that remain. Females with the *c* allele also mate at random among the males that are left over after *C* females choose. Thus, for Maynard Smith/Bell only the *A* and *C* loci are

relevant to female choice, and there are four different preference classes with sixteen different combinations of male and female genotypes in each class:

	preference factor	
mating class	if $r_f' > p_m'$	if $r_f' \le p_m'$
??C female x A?? male	p_m'	r_f'
??C female x a?? male	$r_f' - p_m'$	0
??c female x A?? male	0	$p_m' - r_f'$
??c female x a?? male	$1 - r_f'$	$1 - p_m'$
	$\sum = 1$	$\sum = 1$

Because the handicapping traits in Andersson's version are only expressed by males in good condition, both the *A* and *B* loci are relevant to female choice, and there are six classes of mating preference with eight or sixteen genotypic combinations in each class:

	preference factor	
mating class	if $r_f' > p'$	if $r_f' \le p_m'$
??C female x AB? male (8)	$p_{B,m}'$	r_f'
??C female x Ab? male(8)	$\left(r_m' - p_{B,m}'\right)\frac{p_{b,m}'}{1-p_{B,m}'}$	0
??C female x a?? male (16)	$\left(r_m' - p_{B,m}'\right)\frac{1-p_{b,m}'-p_{b,m}'}{1-p_{B,m}'}$	0
??c female x AB? male (8)	0	$p_{B,m}' - r_f'$
??c femalex Ab? male (8)	$\left(1-r_f'\right)\frac{p_{b,m}'}{1-p_{B,m}'}$	$p_{b,m}'$
??c femalex a?? male (16)	$\left(1-r_f'\right)\frac{1-p_{B,m}'-p_{b,m}'}{1-p_{B,m}'}$	$1-p_{B,m}'-p_{b,m}'$
	$\sum = 1$	$\sum = 1$

e. Next, we estimate the expected frequency of each mating combination, based on female preference and the adult male and female genotypic frequencies. Illustrating with Maynard Smith/Bell, assume that the number of choosy (*??C*) females exceeds the availability of conspicuous (*A??*) males ($r'_f > p'_m$). The total frequency of matings in the *??C* female x *A??* male preference class will be p'_m. The sixteen genotypic combinations of matings within that class will each comprise a fraction of the class total proportional to their relative genotypic frequencies. If we call the frequencies of the four female genotypes in this group (*ABC*, *aBC*, *AbC*, and *abC*) x_1, x_2, x_3, and x_4, and the frequencies of the male genotypes (*ABC*, *AbC*, *ABc*, and *Abc*) y_1, y_2, y_3, and y_4, then the relative probability of *ABC* female x *ABC* male matings will be

$$\frac{x_1 y_1 p'_m}{\left(\sum_{i=1}^{4} x_i\right)\left(\sum_{i=1}^{4} y_i\right)}$$

where the denominator sums the product of male and female genotypic frequencies for each of the 16 combinations in the *??C* female x *A??* male preference class. We calculate relative probabilities for the other 15 matings in this class and for the other two classes similarly, changing the third term in the numerator to the appropriate female preference factor for each class (note that if $r'_f > p'_m$, all of the ornamented males will be mated by choosy females and *??c* female x *A??* male matings will not occur). Our procedure is identical for the Andersson version, except that there are six mating preference classes, with eight or sixteen mating combinations.

f. To complete the first generation, we tally the offspring genotypes that will result from each mating, weighted by the expected frequency of that mating. We assume that each mating produces the same number of offspring, and tally weighted contributions from each mating to the appropriate progeny genotypes. For example, the mating *ABC* female x *ABC* male will produce only one progeny genotype (*ABC*), but for the mating *abC* female x *ABC* male, the progeny will be *ABC*, *AbC*, *aBC*, and *abC* in equal proportions. Since both the mating preferences (step *d*, above) and the genotypic frequencies (step *c*, above) sum to 1.0, the resulting vector of progeny genotype frequencies does not need to be renormalized. Assuming that the sex ratios of our broods are balanced, we copy this output to form identical vectors of male and female genotypes to be used as zygotes for the next generation.

g. The *Populus* handicap simulation allows several modifications of the basic Bell and Andersson models. Bell's monogamous mating rules prevent sexual selection via a Fisherian mating advantage, but there is no reason why the handicap and Fisherian processes cannot function simultaneously. Bell suggested a set of polygamous mating rules for this purpose:

mating class	preference factor
??C female x *A??* male	r'_f
??C female x a?? male	0
??c female x A?? male	$p'_m\left(1-r'_f\right)$
??c female x a?? male	$\left(1-p'_m\right)\left(1-r'_f\right)$
	$\sum = 1$

These preferences imply that choosy females mate only with conspicuous males, while *??c* females mate randomly with any available male. Purely Fisherian sexual selection can be modeled with these preferences if there is no survival advantage conferred by the *B*-locus genotype (i.e., if $\varepsilon = 0$). When $\varepsilon > 0$, these mating preferences allow both sexual selection processes to function simultaneously.

h. Time and risk are involved in the choice of mates, and this cost should rise as choosy females increase in frequency relative to the conspicuous *AB?* males that are their preferred mates. Andersson suggested a simulation of this cost by eliminating a fraction $\frac{\mu r'_f}{p'_{B,m}}$ from the adult mating *??C* females. The resulting simulations show that imposing a small cost on choosy females may facilitate the spread of conspicuous alleles via sexual selection.

3. Handicap models illustrate a second-order selection process mediated by female choice. If the fitness advantage of the *B* allele (ε) is sufficiently large relative to the cost of the *A* allele (β), then surviving *A* males will have a higher *B* allele frequency than the male population at large (Bell showed the criterion to be $2\varepsilon\left(q_{A,m} - q_{a,m}\right) > \beta$. As a result, females that choose a conspicuous male improve their chance of getting a *B* mate. By this means both the *A* and *B* alleles become coupled in linkage disequilibrium with *C*. Although *B* is the only allele directly favored by viability selection, both *A* and *C* will hitch-hike to higher frequencies because their occurrence is correlated with the occurrence of *B*. This outcome is illustrated in a *Populus* run (Figure 3) on the next page.

a. It is logical to suppose that sexual selection becomes stronger as ε increases relative to β, and to some degree this is true; when *B* is strongly favored, *A* and *C* are hitchhiking on a vehicle that moves rapidly. However, the opportunity for linkage disequilibrium is greatest at intermediate frequencies; if selection carries *B* to fixation, every genotype will include a *B*, and the correlations required for an increase in the frequencies of *A* and *C* disappear. *Thus there is a fundamental conceptual problem with handicap models having to do with the maintenance of additive genetic variance. When the viability allele is strongly favored so that coupling yields a substantial boost for A and C, B passes very rapidly through the frequency range where the coupling correlation occurs. As a result, sexual selection by the handicap process is likely to be either transient or subtle*, and

Graham Bell concluded that the model has little evolutionary significance. Andersson is somewhat more sanguine because his process is a little more effective in generating linkage disequilibria. He also argues that there are likely to be many beneficial alleles at different loci increasing under selection; as each of these polymorphisms passes through intermediate frequencies, they may take turns advancing the *A* and *C* alleles. Whatever the general evolutionary significance of handicaps, the models have didactic value, teaching our intuition about multi-locus models, linkage, and correlated responses.

References

Andersson, M. 1982. Female choice selects for extreme tail length in a widowbird. Nature 299:818-820.

Andersson, M. 1986. Evolution of condition-dependent sex ornaments and mating preferences: sexual selection based on viability differences. Evolution 40:804-816.

Bell, G. 1978. The handicap principle in sexual selection. Evolution 32:872-885.

Heisler, I. L. and J. W. Curtsinger. 1990. Dynamics of sexual selection in diploid populations. Evolution 44:1164-1176.

Maynard Smith, J. 1985. Mini review: sexual selection, handicaps and true fitness. J. Theor. Biol. 57:239-242.

Maynard Smith, J. 1991. Theories of sexual selection. TREE 6:146-151

Moller, A.P. 1988. Female choice selects for male sexual tail ornaments in the monogamous swallow. Nature 332:640-642.

Moller, A.P. 1989. Viability costs of male tail ornaments in a swallow. Nature 339:132-135.

Zahavi, A. 1975. Mate selection - a selection for a handicap. J. Theor. Biol. 53:205-214.

Frequency-Dependent Selection: Diploid Model

"Frequency dependence" implies that the fitnesses of genotypes change as the genetic makeup of a population changes. This contrasts with classical models of population genetics, which assume that genotypic fitnesses are constant.

This model simulates a situation in which a large population of diploid organisms is subject to frequency dependent selection. Individuals are assumed to interact in pairs, in such a way that the fitness of each individual depends not only on its own genotype, but also on the genotype of its "social partner". The model applies to any situation in which organisms come together in pairs to compete for resources, or to assist each other in obtaining resources. For simplicity, pairs are assumed to form at random, like particles colliding randomly in a box.

The set up of the model is as follows. There are assumed to be three autosomal genotypes, *AA*, *Aa*, and *aa*. We must specify nine fitness parameters, one for each genotype interacting with each of the other genotypes:

		Interacting with:		
		AA	*Aa*	*aa*
	AA	w_1	w_2	w_3
Fitness of:	*Aa*	w_4	w_5	w_6
	Aa	w_7	w_8	w_9

We assume random mating or random union of gametes, so genotypes are initially present in Hardy-Weinberg frequencies, before selection operates.

What is the fitness of each genotype when they interact randomly in pairs? The fitness of *AA* will be w_1 if it interacts with another *AA*, w_2 if it interacts with an *Aa*, and w_3 if it interacts with *aa*. With randomly chosen "social partners", the probability of interacting with a particular genotype is simply its frequency in the population, so the total fitness of *AA* is

$$\text{Fitness}_{AA} = p^2(w_1) + 2pq(w_2) + q^2(w_3)$$

Similar calculations apply to the other genotypes. Once we have calculated relative fitnesses in this way, the equation for the new allele frequency is the same as for the classical constant fitness model:

$$p' = p\left(\frac{p(\text{Fitness}_{AA}) + q(\text{Fitness}_{Aa})}{\text{Population Mean Fitness}}\right)$$

This model differs from the classical constant-fitness model in some important ways. Most importantly, mean fitness may not be maximized under frequency dependence. It is possible to have stable genetic equilibria that are not maxima of the mean fitness surface; this means that the classical concept of an adaptive topography does not apply to frequency-dependent-selection models.

For a more recent and more general general discussion of frequency dependent selection see the Philosophical Transactions of the Royal Society, London, Series B, Vol 319, 1988, which presents a collection of papers on the subject.

Reference

Cockerham, C. C., P. M. Burrows, S. S. Young, and T. Prout. 1972. Frequency dependent selection in randomly mating populations. American Naturalist 106:493-515.

Frequency-Dependent Selection: ESS Model

One way to deal with the complexities of frequency dependent selection is to simplify the genetics, while retaining the frequency dependent nature of the fitnesses. The theory of Evolutionary Stable Strategies (ESS) does this by modeling frequency dependent evolution for a hypothetical asexual species.

This module simulates the evolution of discrete phenotypes in a large asexual population. In ESS terminology, the phenotypes are called "strategies", here denoted A, B, C, and D. Individuals interact in randomly formed pairs and affect each others fitness. A and B are "pure strategies", i.e., these two types of individuals always behave the same way in their interactions with other individuals. C and D are "mixed strategies"; they sometimes behave like A, and sometimes like B.

An evolutionarily stable strategy is defined as a strategy that cannot be invaded by any other strategy when almost everyone in the population adopts it. This module will allow you to specify two pure and two mixed strategies, and to determine which strategies can invade and which can be invaded.

The model functions as follows: There is a "payoff matrix" for the two pure strategies, specifying the increment to fitness obtained by *A* or *B* when interacting with *A* or *B*:

		Interacting with	
		A	*B*
Payoff to	*A*	E_1	E_2
	B	E_3	E_4

The fitness of strategies *A* or *B* is given by a constant, and terms that reflect payoffs in random encounters with other *A*'s and *B*'s:

$$\text{Fitness of } A = C + pE_1 + qE_2$$

$$\text{Fitness of } B = C + pE_3 + qE_4$$

where p and q are relative frequencies of *A* and *B* respectively, and C is the constant. In these simulations we assume that $C = 10$.

In addition to the pure strategies *A* and *B*, there are two mixed strategies, *C* and *D*. These mixed strategies sometimes behave like *A*, and sometimes like *B*.

The dynamics for any strategy are modeled after an asexual population. For instance:

$$\text{New Frequency of } A = \frac{(\text{Old Frequency of } A)(\text{Fitness of } A)}{\text{Mean Fitness of Population}}$$

This equation is used to determine whether a particular strategy can invade a population consisting primarily of another strategy.

An ESS is a strategy that cannot be invaded when common. In general, if the payoff matrix is

	A	*B*
Strategy *A*	E_1	E_2
Strategy *B*	E_3	E_4

there will be a mixed ESS if $E_1 < E_3$ and $E_4 < E_2$, the ESS being to adopt behavior *A* with probability

$$\frac{E_2 - E_4}{E_2 + E_3 - E_1 - E_4}$$

Try finding the ESS for the default payoff values on the input screen.

Reference

J. Maynard Smith, *Evolution and the Theory of Games*, Cambridge University Press, 1982.

Density-Dependent Selection with Genetic Variation

This model shows simultaneous evolution of gene frequency and population size. It is a hybrid model: it combines elements of the genetic model of selection on one locus, and the ecological model of logistic growth. There are assumed to be three genotypes that differ in intrinsic rate of increase (*r*) and carrying capacity (*K*). The *r*'s and *K*'s affect both the growth of the population and the change in gene frequencies.

A particular population can be represented by a point on an (*N*, *p*) plane. Over time, the point moves on the plane, showing how population size and gene frequency evolve.

This model was developed by Anderson (1971), Charlesworth (1971), and Roughgarden (1971). Its basic features are as follows:

1) The fitness of a genotype depends on its *r* and *K* values, and on population density. In particular,

$$w_{AA} = 1 + r_{AA} - \frac{r_{AA}}{K_{AA}} N$$

where *N* is total population density.

2) It is often assumed that there is a trade-off between *r* and *K* values. Some genotypes are highly fertile but not very good competitors at high density; these are the "*r*-strategists". Other genotypes might be less fertile but produce more robust progeny that are good competitors at high density; these are the "*K* strategists".

3) In a stable environment in which all mortality is due to density-dependent selection, the *K* values of the different genotypes determine the ultimate pattern of genetic equilibrium. If the heterozygote has the highest *K*, there will be a stable polymorphism; if it has the lowest *K* there will be an unstable polymorphic equilibrium. If one of the homozygotes has the highest *K* then fixation of that type will be a stable equilibrium.

4) As in the logistic model without genetic variation, the magnitude of the *r*'s determines whether there are oscillations in population size and/or gene frequency. Generally an *r* value in the range of 2 will produce some oscillations.

References

Anderson, W. W. (1971) Genetic equilibrium and population growth under density-regulated selection. American Naturalist 105: 489-498.

Charlesworth, B. (1971) Selection in density regulated populations. Ecology 52: 469-474.

Roughgarden, J. (1971) Density-dependent natural selection. Ecology 52: 453-468.

Population and Quantitative Genetics

This module illustrates connections between simple population and quantitative genetic models. For a given set of genotypic fitness values, the program will show how population mean fitness, heritability, and allelic frequencies change over time, and graph the adaptive topography.

The screens show four kinds of output, illustrating a one-locus deterministic selection model with random mating and discrete generations.

1. For any given set of relative fitnesses, there exists a curve called the adaptive topography that shows how the average fitness in the population changes as a function of allelic frequency. Sewall Wright proved that allelic frequencies always change in such a way that the mean fitness increases over time, i.e., populations climb "adaptive peaks" and do not go down into "adaptive valleys". To see this, try several different types of fitnesses. If the heterozygote is the most fit genotype, then the adaptive topography will have a peak at intermediate allelic frequencies; the population will "climb" this peak. If the heterozygote is the least fit, then there will be a valley at intermediate frequencies (verify that the population does not go down into the valley). If one of the homozygotes is the most fit, then the function will have no peak, and the population will move to fixation for the fittest genotype.

2. Heritability is defined as

$$\frac{\text{Additive Genetic Variance for Fitness}}{\text{Total Genetic Variance for Fitness}}$$

The additive variance is that part of the variance that is attributable to the effects of alleles. It does not include the variance that is due to interaction between alleles at a locus (that's dominance variance), to interaction between alleles at different loci (that's epistatic variance), or to environmental variation (that's environmental variance, V_e).

Notice that the heritability might rise or fall at first in any particular simulation, but eventually it goes to zero if you have specified enough generations to reach equilibrium. This is because the additive variance (which is the numerator of the heritability) inevitably goes to zero for simple deterministic models.

3. Mean fitness in a population changes as a function of time. It differs from the adaptive topography, which shows how mean fitness changes as a function of allelic frequency. Notice that for any fitnesses, the mean fitness will always increase over time.

4. Allelic frequency trajectories, i.e., allelic frequency as a function of time. Allelic frequencies can increase to one, decrease to zero, or reach a stable intermediate frequency, depending on the genotypic fitness values that you enter. If one of the homozygotes is the most fit genotype, then the frequency will go to zero or one. If the heterozygote is the most fit then there will be a stable intermediate equilibrium. If the heterozygote is the least fit then there will be historical effects; i.e., the ultimate state reached by the population will depend on the initial allelic frequency.

Heritability

Heritability expresses the degree to which phenotypic variation is determined by genetic variation. A heritability of 1.0 implies complete genetic determination, while a heritability of zero implies the opposite, that there is no genetic determination. This module computes the theoretical heritability of a quantitative trait in a hypothetical infinite population, and also simulates a Monte Carlo breeding experiment to estimate heritability in a finite population.

The total variance of phenotypic values in a population can be broken down into components: additive variance, dominance variance, epistatic variance, and environmental variance. The first three components added together constitute the total genetic variance.

Additive variance is the part of the variance that is due to the effects of individual alleles. Dominance variance arises from the inter-action of alleles at a single locus. Epistatic variance arises from the interaction of different loci.

Evolutionary biologists and plant and animal breeders are particularly interested in the additive variance, because it is the "usuable" genetic variance. That is, in a sexually reproducing species parents transmit alleles to their progeny, but not intact genotypes or multi-locus genotypes. For this reason, additive genetic variance is the most important quantity for predicting a population's response to selection. With additive variance a population can evolve; without it, there is usually no evolutionary change.

The usual measure of heritability, which is called the “narrow-sense heritability,” is defined as the proportion of the total variance that is additive, i.e.,

$$h_n^2 = \frac{V_a}{V_a + V_d + V_i + V_e}$$

where h^2 is heritability, the subscript n indicates narrow sense, and the subscripts a, d, i, and e refer to the additive, dominance, epistatic, and environmental variances, respectively.

In the Monte Carlo simulation, the heritability is estimated from the regression of offspring phenotypes on the average of the parental phenotypes. The heritability estimate is equal to the slope of the best-fit line.

Reference

Falconer, D. S. 1996. *Quantitative Genetics* (4th edn). Longman Scientific & Technical.

Directional Selection on a Quantitative Trait

This module simulates an artificial selection experiment. The user specifies genetic effects, population size, and the number of individuals selected to be parents of the next generation. The program shows the distribution of phenotypes in each generation, and how the mean phenotype changes in the population over generations.

Phenotypic selection regimes can be classified into three categories, depending on which phenotypes are favored. Stabilizing selection refers to selection in favor of the intermediate phenotypes. Disruptive selection means selection in favor of the extremes. Directional selection refers to selection in favor of one extreme, e.g., the biggest, tallest, etc. This module simulates a directional selection experiment in a finite population.

If there is usable genetic variation (i.e., additive genetic variance), then directional selection changes the mean phenotype in the population. The rate and magnitude of that change depend on a number of factors, including:

Allele frequency - alleles at intermediate frequencies contribute more usable genetic variance than alleles at extreme frequencies.

Population size - In very small populations, drift can cause the loss of usable genetic variation, inhibiting selection response. It can also cause unselected alleles to increase in frequency, simply by chance. In general, large populations respond more reliably to selection than small populations.

Number of individuals selected - Selecting the few most desirable individuals as parents of the next generation exerts a very strong selection pressure, but also increases the effect of drift. If you select too few individuals then the usable genetic variation might be lost; if you select too many, then the selection pressure is weak.

Genotypic values tell us what the phenotypes of the three genotypes would be in the absence of environmental effects. If the genotypic values are very similar, there will not be much progress by selection. If the genotypic values are very different then selection can usually change the population mean. Selection progress is also strongly affected by the heterozygote genotypic value; if the heterozygote is the "best" genotype then the population cannot be changed as much as the case where a homozygote is the best genotype.

Environmental variance - If the environmental variance is large, then an individual's phenotype is not a very reliable indicator of his genotype. Environmental effects are not transmitted to progeny, so large environmental variance inhibits selection response.

In a very large population, the expected response to one generation of directional selection is $R = h^2 S$, where R is the selection response (measured as the difference between the mean phenotypes of parents and offspring), h^2 is narrow sense heritability, and S is the selection differential (measured as the difference between the mean phenotype of all parents and the mean of the selected parents).

Reference

Falconer, D. S. 1996. *Quantitative Genetics* (4th edn). Longman Scientific & Technical. London.

Insect Resistance Managment

The Comins 2-Patch Model of Pesticide Resistance

Hugh Comins (1977) modeled the evolution of pesticide resistance in a habitat with both treated and untreated regions, linked by insect movement and gene exchange. In his model, larval pests in the treated region suffer mortality rates that vary with their genotype at a diallelic, autosomal resistance locus. If resistant alleles are initially rare, this treatment depresses pest density. After the survivors mature as adults, there is movement in both directions between the treated and untreated regions in proportion to insect abundance, so immigration into the treated area will exceed emigration. Adults in both regions then reproduce, and early larval survival is assumed to be density-dependent.

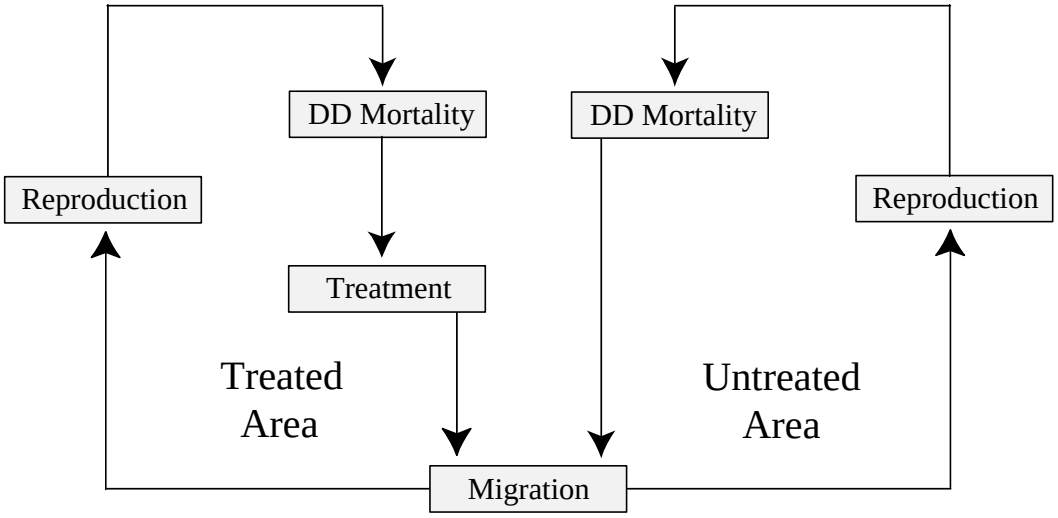

Figure 1. Schematic of the Comins pesticide-resistance-management model. The habitat is divided into treated and untreated patches. Increases in the frequency of resistant alleles under viability selection in the treated area are mitigated by the introgression of susceptible alleles from the untreated area.

Parameters of the Comins model are as follows:

G = Relative size of the treated and untreated units (untreated is G times as large as treated).

X = Population size and population density of insects in the treated unit.

Y = Population size of insects in the untreated unit, so that untreated density is Y/G.

r = the proportion of the insect population that moves from its natal location.

p = resistance allele frequency in the treated unit.

w = resistance allele frequency in the untreated unit.

L = the genotype-specific survival rate for resistant homozygotes exposed to the treatment.

K = genotype-specific survival rate for susceptible homozygotes exposed to the treatment.

h = the gene-expression parameter. The genotype-specific survival rate for heterozygotes is $hL + (1-h)K$, so when h = 0, resistance is fully recessive and when h = 1, resistance is fully dominant.

b = intensity of density-dependent mortality; if b = 1, mortality is sufficient to compensate in a single generation. Values of $b < 1$ gives an undercompensating, monotonic approach to equilibrium, and $b > 1$ gives overcompensating oscillations.

Numerical simulations of the Comins model invoke three steps in each generation. Beginning with reproduction, there is density-dependent egg and larval survival of the general form suggested by May, Conway, Hassell and Southwood (1974),

$$N_{t+1} = \lambda N_t^{1-b} \tag{1}$$

where b varies from 0 to 2, setting the intensity of density-dependent mortality. He assumes that the two regions have the same equilibrial insect density, but that the untreated region is G times larger in total area. His density-dependent reproduction equations for the treated (X) and untreated (Y) populations are

$$X' = X^{1-b} \tag{2}$$

$$Y' = G\left(\frac{Y}{G}\right)^{1-b} \tag{3}$$

Note that population growth rates in the treated and untreated regions are identical, and have been scaled out by expressing both densities in units of the equilibrial density.

In the second step of each simulated generation, pesticide-induced mortality alters allelic frequencies in the treated region. If R alleles are resistant and r alleles are susceptible, we can define the genotypic survival rates as

Genotype	Survival
RR (resistant homozygotes)	L
Rr (heterozygotes)	hL +(1-h)K
rr (susceptible homozygotes	K

Where h sets the expression of the resistant allele. If p and p' are frequencies of the resistant allele in the treated region before and after pesticide application (and if $q = 1 - p$), then the recursion equations for surviving insect density and resistant allele frequency in the treated region are

$$X'' = \left\{Lp'^2 + \left[Lh + K(1-h)\right]2p'q' + Kq'^2\right\}X' \tag{4}$$

$$p' = \frac{\left\{Lp^2 + \left[Lh + K(1-h)\right]pq\right\}X'}{X''} \tag{5}$$

When adult insects mature, their densities and allelic frequencies in both the treated and untreated regions are altered by migration. Comins models a migration process in which equal numbers of migrants move in both directions when the treated and untreated populations are at their density-dependent equilibria. Defining r as the migration rate, this implies that rX'' and $\frac{r}{G}Y'$ are the numbers of migrants that leave their origin. Insect densities after migration will be

$$X''' = (1-r)X'' + \frac{r}{G}Y' \tag{6}$$

$$Y'' = rX'' + \left(1 - \frac{r}{G}\right)Y' \tag{7}$$

If w and w' are the frequencies of resistant alleles in the untreated area before and after migration, the altered allelic frequencies in the treated and untreated areas will be

$$p'' = \frac{(1-r)p'X'' + \frac{r}{G}wY'}{X'''} \tag{8}$$

$$w' = \frac{rp'X'' + \left(1 - \frac{r}{G}\right)wY'}{Y''} \tag{9}$$

Finally, to begin the next generation, we set

$$X = X''' \qquad Y = Y'' \qquad p = p' \qquad w = w'$$

The fundamental question motivating this Comins model is whether the evolution of resistance under pesticide treatment can be counterbalanced or delayed by migration and the introgression of susceptible alleles from an adjacent untreated region. In brief, the answer is that it can. With additive gene expression and a 70% selection differential between homozygotes, the change from $r = 0$ to $r = 0.5$ delays resistance time (defined as the number of generations required to reach $p = 0.5$) from 5 to 56 generations. Note however, that the delay will always be transient. So long as the untreated region is finite and there is no fitness cost of resistance in the absence of selection, migrants will gradually increase resistant allele frequency in the untreated region. Then introgression of susceptible alleles will slow, and ultimately resistance will fix, throughout. The persistence of susceptibility is strongly affected by model parameters; for example, it is reduced in proportion to the selection differential and the dominance of the resistance allele. More subtly, resistance is slowed with under-compensating density dependence and intermediate migrations rates (Comins 1977).

The Alstad &Andow *Bt*-Resistance-Management Model

In 1995 when David Andow and I became interested in the problem of managing the evolution of European corn borer (ECB) resistance to transgenic *Bt* maize, I had already worked out a *Populus* simulation of the Comins patch model, and we decided to adapt it to incorporate several important features of ECB biology. First, corn borers are bivoltine, so we doubled the Comins cycle and inserted a period of density-independent over-winter mortality just prior to the spring migration. Second, ECB show a strong preference for phenologically advanced maize in the spring generation, such that there can be a 10-fold difference in oviposition in adjacent tall and short fields. We knew that this preference biased migration could have an important influence on the evolution of resistance, so we incorporated it into the recursion equations that effect the simulated migration. Note that as an ecological-genetic model, this simulation tracks both insect population density and the frequency of resistance alleles. As a result, it projects the influence of model parameter values on both the rate of evolution, and the density of insects (and hence the damage that they cause). It therefore allows us to evaluate both the evolutionary efficacy, and the probable grower acceptance of different management configurations.

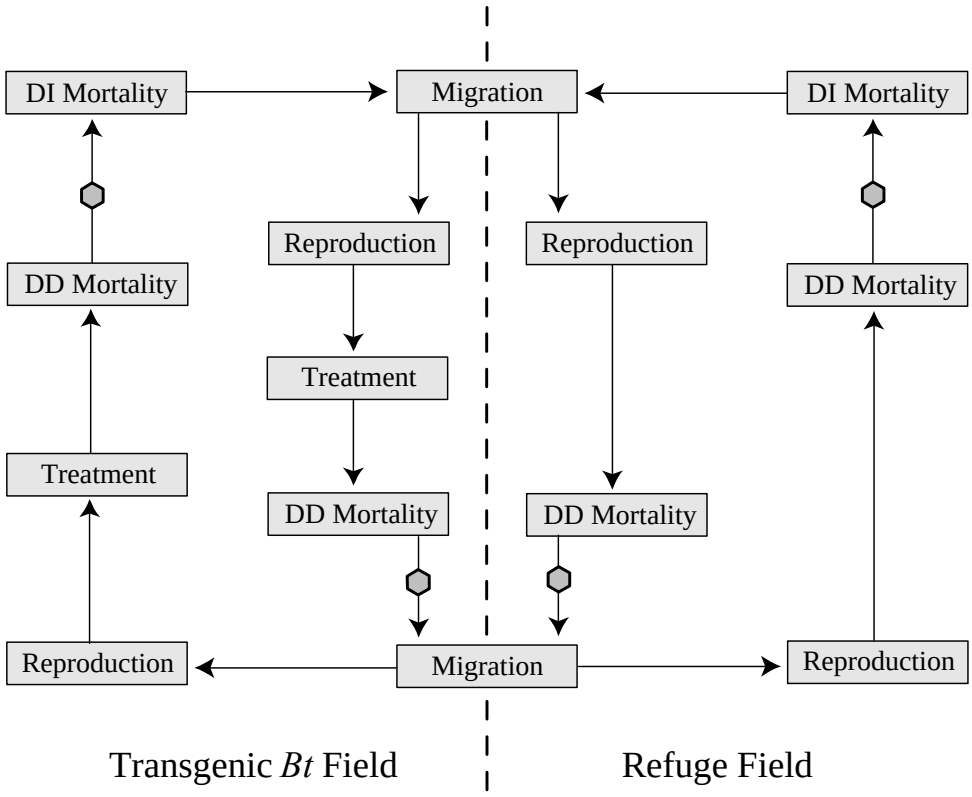

Figure 2. Schematic of the Alstad-Andow simulation of high-dose/refuge resistant management for European corn borers in transgenic *Bt* maize. Each arrow represents a simple recursion equation, described below. Generational densities in the graphical output are estimated at the hexagonal markers, following density-dependent larval mortality.

Parameters of the model:

G = Relative size of the toxic and nontoxic units (nontoxic is G times as large as toxic).

X = Population size and population density of ECB in the toxic unit.

Y = Population size of ECB in the nontoxic unit, so that nontoxic density is Y/G.

μ = the density-independent over-winter survival rate.

r = the proportion of the population that moves from its natal location. Separate values, r_1 and r_2 can be set for the first and second annual generations.

s = a preference factor; the toxic maize is s times more attractive than the nontoxic maize. Separate values, s_1 and s_2 can be set for the first and second annual generations.

p = resistance allele frequency in the toxic unit.

w = resistance allele frequency in the nontoxic unit.

F = the fecundity factor, interpretable as the average number of daughters produced per female.

L = the genotype-specific survival rate for resistant homozygotes exposed to the toxin.

K = the genotype-specific survival rate for susceptible homozygotes exposed to the toxin.

h = the gene-expression parameter. The genotype-specific survival rate for heterozygotes is $hL+(1-h)K$, so when h = 0, resistance is fully recessive and when h = 1, resistance is fully dominant.

a = reciprocal of the threshold density below which density-dependent larval mortality disappears.

b = intensity of density-dependent mortality; if b = 1, mortality is sufficient to compensate in a single generation. Values of $b < 1$ gives an under-compensating, monotonic approach to equilibrium, and $b > 1$ gives overcompensating oscillations.

Each simulation run commences with over-winter mortality acting on a population at equilibrium density, so that the numbers of spring survivors in toxic nontoxic units are μX and μY, respectively. Then, to represent a single growing season four successive steps are implemented for each of two generations. In the first step, migration of eclosing adults mixes a portion of the insects in toxic and nontoxic units, affecting the population densities and allelic frequencies.

$$X' = (1-r)X + \frac{srX}{s+G} + \frac{srY}{s+G}$$

$$Y' = (1-r)Y + \frac{GrY}{s+G} + \frac{GrX}{s+G}$$

$$p' = \frac{(1-r)pX + \frac{srpX}{s+G} + \frac{srwY}{s+G}}{X'}$$

$$w' = \frac{(1-r)wY + \frac{GrwY}{s+G} + \frac{GrpX}{s+G}}{Y'}$$

The second step for each insect generation involves reproduction, so that local population sizes grow by the insect fecundity factor.

$$X'' = FX'$$

$$Y'' = FY'$$

In the third step, selection resulting from the toxicity of the transgenic maize affects both insect density and allelic frequency in the toxic unit.

$$X''' = \left\{Lp'^2 + \left[Lh + K(1-h)\right]2p'q' + Kq'^2\right\}X''$$

$$p'' = \frac{\left\{Lp'^2 + \left[Lh + K(1-h)\right]p'q'\right\}X''}{X'''}$$

Finally, insects that survive the selection process experience density-dependent larval mortality before eclosing as winged adults of the succeeding generation.

$$X'''' = X''(1 + aX''')^{-b}$$

$$Y''' = Y''\left(1 + \frac{aY''}{G}\right)^{-b}$$

After two insect generations in a single growing season, an episode of density-independent over-winter mortality is imposed before the seasonal cycle begins again.

References

Alstad, D. N. and D. A. Andow. 1995. Managing the evolution of insect resistance to transgenic plants. Science 268:1894-6.

Alstad, D. N. and D. A. Andow. 1996. Implementing management of insect resistance to transgenic crops. AgBiotech News and Information 8:177-181.

Comins, H. N. 1977. The development of insecticide resistance in the presence of migration. J. theor. Biol. 64:177-97.

May, R. M., G. R. Conway, M. P. Hassell, & T. R. E. Southwood. 1974. Time delays, density-dependence and single-species oscillations. J. Anim. Ecol. 43:747-770.

A Stepping-Stone Cline Model of Selection and Migration

1. John Endler (1973) modeled a population arrayed in a linear string of semi-independent demes across some environmental gradient. Each deme experiences selection pressures which vary with its position on the gradient, and exchanges migrants once each generation with the two neighboring demes.

2. John published simulations of 50 such stepping-stone demes, assuming that the selection regime might vary from deme-to-deme in four different ways, as follows:

   a. In the "gradient mode," the fitness of *AA* genotypes decreases linearly while that of *aa* genotypes increases, from deme 1 to deme 50. Heterozygote fitness remains constant at a value halfway between the homozygote maxima and minima.

   b. In the "heterozygous advantage mode," homozygote fitnesses remain as they were in the gradient mode, but the heterozygotes have a spatially constant fitness which is always greater

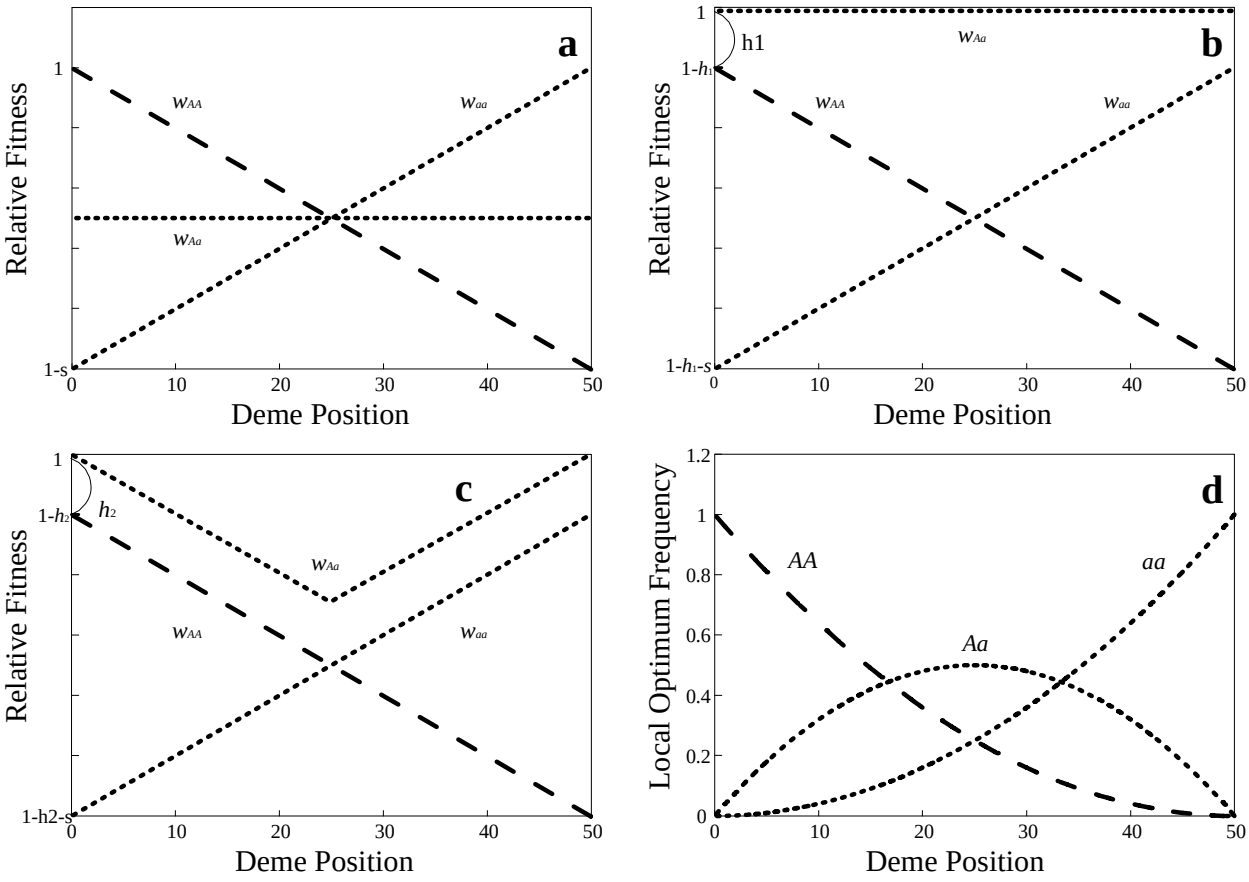

Figure 1. Four selection regimes used in the Endler cline simulation. Fifty demes are arranged as stepping stones accross an environmental gradient, and exchange genes once per generation with neighboring demes.

than either homozygote by a minimum amount, h_1.

c. In the "local heterozygous advantage mode," homozygote fitnesses are again as before, but heterozygote fitness also varies spatially, remaining a fixed amount, h_2, greater than the most fit homozygote.

d. In the "frequency-dependent mode," it is assumed that there is a locally optimal frequency of *A* alleles which decreases from deme 1 to deme 50. The local fitness of each genotype is decremented by an amount which varies with the deviation of that genotype's frequency from the local optimum.

3. In addition to these different patterns of selection, John allowed its overall intensity to be altered as well. Let *s* represent the maximum genotype-specific change in relative fitness across the environmental gradient; if $s = 1.0$, then the relative fitness of *AA* genotypes declines from 1 in deme 1 to (1-1/49) in deme 2, (1-2/49) in deme 3, and so forth. Gene flow migration is adjusted by varying the parameter *g*, the proportion of individuals in each deme coming from the adjacent demes in each generation. Half of the migrants come from the deme above, and half from the deme below on the environmental gradient. Demes 1 and 50 receive the full *g* proportion of migrants from their only neighboring deme.

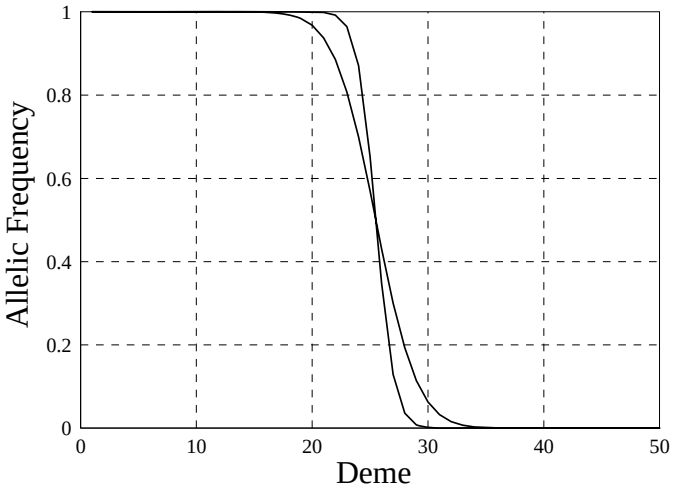

Figure 2. Equilibrial cline following two runs of the gradient selection scheme, with migration rates of $g = 0.1$ (steeper) and $g = 0.9$ (shallower).

4. The shape of the cline that develops in Endler's simulations depends on the nature of the spatially varying selection regime, but all of the clines are resistant to the attenuating effects of gene flow. For the *Populus* run at right, I used the gradient model of selection with an overall intensity range of $s = 0.9$. The graph shows two runs, both of which were allowed to come to equilibrium. For the steeper cline, the migration rate between demes was $g = 0.1$, while for the other it was $g = 0.9$

5. Those who refer to the original Endler paper should note a trivial error that demonstrates John's professorial aptitude. Figs 4 and 6, which purport to graph the equilibrial *p* values actually graph equilibrial *q*'s. *Populus* output presents the *p* values, hence our graphs have similar shapes, but reversed slopes. (When I showed John this paragraph, he laughed and said “Leave it in!”)

Reference

Endler, J. A. 1973. Gene flow and population differentiation. Science 179:243-50.

Multiple Niche Polymorphism

Local environments experienced by organisms vary from place to place, and it is reasonable to expect that this variation might affect the relative fitness of different genotypes. If the genotype with highest fitness varies from place to place, it is even possible that environmental variability may balance and sustain genetic variation.

Levene (1953) proposed that the environment is subdivided into a series of different niches. Zygotes produced by population-wide random mating enter each niche type in proportion to their frequencies, and the three genotypes survive with different relative fitnesses in the different habitats. Each niche type contributes a proportion of the next-generation zygotes which is fixed by the proportional area of each local environment, as illustrated on the left hand side of Figure 1 (next page). *The model is frequency-dependent, because each allele suffers reduced competition in the preferred patches when it is rare.*

There are a total of m different niche types, and c_i is the proportion of the zygotes that settle in each patch type i. If there is a diallelic locus with genotypes A_1A_1, A_1A_2, and A_2A_2 (this treatment is from Hedrick 1985, and I will preserve his notation), and their relative fitnesses in patch type i are $w_{11,i}$, 1, and $w_{22,i}$, respectively, then the allelic frequency recursion for the ith niche is

$$\Delta q_i = \frac{pq\left[p\left(1-w_{11,i}\right)-q\left(1-w_{22,i}\right)\right]}{\overline{w}_i} \tag{1}$$

where

$$\overline{w}_i = w_{11,i}p^2 + 2pq + w_{22,i}q^2 \tag{2}$$

The recursion over all m niche types is the weighted average of frequency change among the niches

$$\Delta q = \sum_{i=1}^{m} c_i \Delta q_i = pq\sum_{i=1}^{m} c_i\left[\frac{p\left(1-w_{11,i}\right)-q\left(1-w_{22,i}\right)}{\overline{w}_i}\right] \tag{3}$$

Now, if our question is to determine whether selection in a variable environment can maintain genetic variation at the A locus, we're asking if there is a stable polymorphic equilibrium. To facilitate analysis of the stability of this model, Hedrick (1985) rearranges equation 1 to define a function $h(q)$ such that

$$h(q) = \frac{\Delta q}{pq} = \sum c_i\left[\frac{p\left(1-w_{11,i}\right)-q\left(1-w_{22,i}\right)}{\overline{w}_i}\right] \tag{4}$$

This function is continuous and non-zero for the range $0 \le q \le 1$, so that if you can show that $h(0)$ is positive and $h(1)$ is negative, then there must be a stable interior equilibrium. For $q = 0$, equation 4 becomes

$$h(0) = \sum c_i\left(\frac{1-w_{11,i}}{w_{11,i}}\right) \tag{5}$$

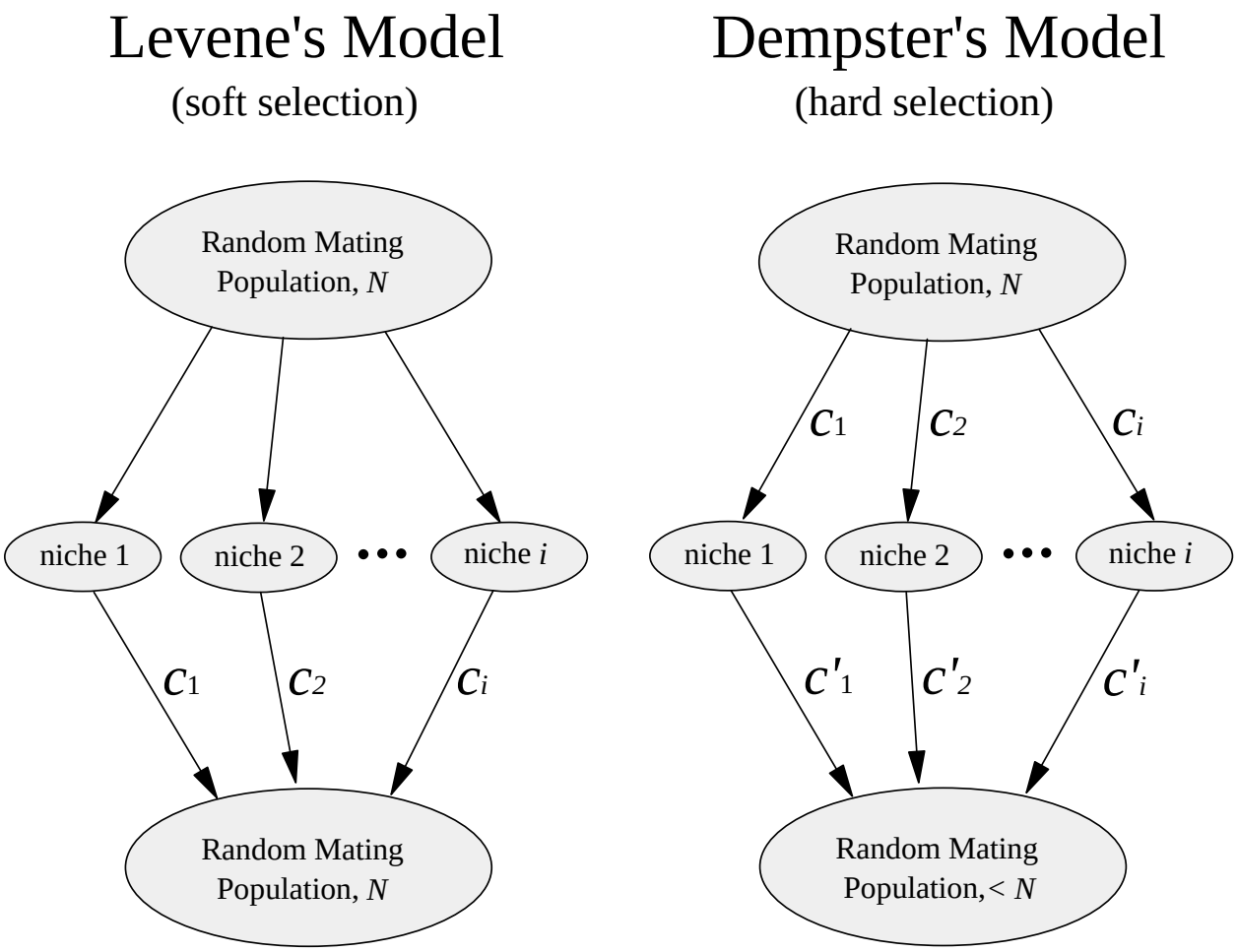

Figure 1. Schematic of the Levene and Dempster models of multiple-niche polymorphism. In the Levene version, a constant number of fertile adults emerge from each patch type. In Dempster's, a constant number of zygotes enter each patch type, and fewer emerge after viability selection. Redrawn after Hedrick, 1985.

This expression must be positive for A_2 to increase from low frequency, so the condition for a polymorphic equilibrium is

$$\sum c_i \left(\frac{1 - w_{11,i}}{w_{11,i}} \right) > 0 \tag{6}$$

$$\sum c_i \frac{1}{w_{11,i}} > 1 \tag{7}$$

$$\frac{1}{\sum c_i \frac{1}{w_{11,i}}} < 1 \tag{8}$$

We have rearranged the condition into the form recognizable as a harmonic mean of the relative

fitness of A_1A_1 over all niches. The same condition suffices to make $h(1)$ negative. So there will be a stable polymorphic equilibrium if the harmonic means of the homozygote fitnesses over all niches are less than 1. Note that this harmonic mean includes both the environmental proportions of the habitats (c_i) and the relative fitness values (w_{xx}).

Relative fitnesses and the relative proportions of the niche types determine whether this frequency-dependent model suffices to maintain a segregating polymorphism, and in fact the parameters must rather finely balanced.

Dempster (1955) pointed out that in the Levene model each niche contributes a constant proportion of the mating pool, independent of the composition of the niche. Dempster called this the *constant-fertile-adult-number* hypothesis; Wallace calls it *soft selection*.

Dempster proposed an alternative called the *constant-zygote-number* or *hard selection* hypothesis, illustrated on the right hand side of the figure on page 2. Here, a constant proportion of the zygotes (c_i) enter each niche before selection, and these proportions may subsequently be altered (c_i') by selection within the niche. The value of c_i' is

$$c_i' = \frac{c_i w_i}{\overline{w}_i} \tag{9}$$

where

$$\overline{w} = \sum c_i \overline{w}_i \tag{10}$$

Note that with this model the frequency dependence of Levene is absent.

The stability condition for the Dempster version is that the arithmetic mean of the heterozygote fitnesses in the several niche types must exceed that of the homozygotes. For the *Populus* simulation above right, all parameters were identical to those used in the stable Levene simulation on the left. Because the arithmetic mean is always greater than the harmonic mean, the Levene soft-selection regime is more likely to maintain polymorphism than Dempster's hard selection. This should seem intuitively reasonable, because the frequency dependent processes act to preserve a rare allele.

Both Dempster and Levene assume that populations are panmictic. Clearly many spatial habitats are sufficiently far apart that this is not true, and spatial selection models must be coupled with explicit treatments of migration.

References

Cannings, C. 1971. Natural selection at a multiallelic autosomal locus with multiple niches. J. Genetics 60:255-59.

Dempster, E. R. 1955. Maintenance of genetic heterogeneity. Cold Spring Harbor Symp. Quant Bio. 70:25-32.

Hedrick, P. W. 1985. *Genetics of Populations*. Jones and Bartlett Publishers, Inc. Boston.

Levene, H. 1953. Genetic equilibrium when more than one ecological niche is available. Amer.

Natur. 87:311-313.

Spatial Dilemmas

The appearance of cooperation among individuals who should be reproductive competitors is an interesting evolutionary challenge and a recurrent theme in behavioral ecology. One of the central metaphors of this literature is a game called the *prisoner's dilemma*, in which two individuals each have the choice of cooperating or defecting from a common enterprise. The reward (or *payoff*) realized by each strategy depends on the play of the opponent, and is typically represented in a *payoff matrix*. For a player adopting the strategy in the left hand column against an opponent adopting the strategy across the top row we represent the matrix as follows:

	Defect	Cooperate
Defect	*P*	*T*
Cooperate	*S*	*R*

The letters are mnemonic; *P* is the punishment for mutual defection, *T* is the temptation to defect, *S* is the "suckers payoff," and *R* is the reward for mutual cooperation. If cooperation entails a cost and defectors obtain some rewards without paying that cost, then

$$T > R > P > S$$

Under these assumptions, defecting is an unbeatable strategy; it yields a higher payoff than cooperating, no matter what the opponent does. Yet paradoxically, if both parties defect they receive smaller rewards than if both had cooperated, because $R > P$.

While the basic prisoner's dilemma implies that defection should win and selfishness should be the state of nature, there are two potential means by which cooperation might be salvaged. One approach, championed by Axelrod and Hamilton (1981), emphasizes repetition and learning. If an individual is predictably selfish based on past experience, then it would make sense to defect from future encounters with that individual. Axelrod (1984) sponsored a tournament between computer programs that played the prisoner's dilemma. The program that amassed the largest reward over multiple rounds of play employed a strategy called “tit for tat.” It cooperated on the first round, and on all subsequent rounds adopted the play made by the opponent in the previous round. Tit for tat is nice, in that it is never first to defect; it is provokable, in that it responds at once to a defection; and it is forgiving, in that it answers renewed cooperation from the opponent. Nowak and Sigmund (1993) have recently identified strategies capable of beating tit for tat if the players are error prone, but the example suffices to show that cooperation might plausibly evolve among animals that can recognize other individuals and remember their past performances.

A second means of facilitating cooperation relies not on repetition and reprisal, but on the players' spatial distribution. Nowak and May (1992) incorporate the prisoner's dilemma into a cellular automoton in which players are constrained to rectangular patches like the squares of a chessboard, interacting only with neighbors in the eight adjacent patches. To simplify, they allow only two strategies, always defect, and always cooperate. They also set $R = 1$, and $S = P = 0$, allowing only one parameter, *T*, to vary from run to run. In each round of play, patch owners

interact with all eight adjacent players and the sum of their payoffs from these encounters is tabulated. To begin the next round, each patch is given to that individual among the previous owner and adjacent neighbors who accumulated the largest total payoff in the previous round.

The contest for any particular square on this chessboard depends on the neighbors' scores, and hence on the behavior of the neighbors' neighbors. As a result, these simple rules produce complex and interesting dynamics. Under some conditions, groups of cooperators will grow, because they are beyond the reach of surrounding defectors. Likewise, successful defectors tend to surround themselves with defectors, reducing their long-term prospects. In general, the dynamics vary with the value of T, the temptation to defect. With $T > 1.8$, clusters of defectors tend to grow, and with $T < 2$, clusters of cooperators tend to grow. In the range $1.8 < T < 2.0$, there is a rich diversity of chaotic spatial patterns, with long-term coexistence of both defectors and cooperators; their relative abundances asymptotically approach a stable ratio. These conclusions are relatively insensitive to details of the game. When P is given a small postive value so that $T > R > P > S$ is strictly true, or when interactions are limited to the four neighbors on the sides of the prisoner's cell, or when interactions with oneself are included in the calculations, the sensitive range of T and the equilibrial frequencies of cooperators and defectors change slightly, but the basic dynamic patterns remain similar.

The spatial component gives this simple game massively parallel transfers of information from cell to cell. The result is an unpredictable array of patterns, including blinking clusters of cooperators or defectors that wink on and off, gliders that move across the chessboard intact, and a rich collection of objects, patterns and tentacles. Other simple games like hawk-dove give similarly complex and unpredictable dynamic patterns, and Sigmund (1992) speculates that some may be "as complex as universal computers." The chaotic behavior of these simple systems is intriguing, and emphasizes the potential importance of spatial structure for the evolution of cooperation, and probably for biological interactions in general.

References

Axelrod, R. 1984. *The Evolution of Cooperation*. Basic Books, New York. 1984.

Axelrod, R., and W. D. Hamilton. 1981. The evolution of cooperation. Science 211:1390-6.

Maynard Smith, J. 1982. *Evolution and the Theory of Games*. Cambridge University Press. 224 pp.

Nowak, M. A. and R. M. May. 1992. Evolutionary games and spatial chaos. Nature 30:826-9.

Nowak, M. and K. Sigmund. 1993. A strategy of win-stay, lose-shift that outperforms tit-for-tat in the prisoner's dilemma game. Nature 364:56-58.

Sigmund, K. 1992. On prisoners and cells. Nature 359:774.

The *Populus* Interaction Engine

The *Populus* Interaction Engine is a general-purpose tool designed to help you develop and analyze your own interesting new models of ecology and evolution. It allows you visualize the dynamics and equilibria of a model that you design from first principles, or to modify the equations underlying an existing *Populus* model (or one from the literature) and examine the effect of those changes. Models may be phrased as sets of continuous differential equations, or discrete, finite-difference equations. The Interaction Engine will parse your expressions, perform a numerical integration or step the difference equations, and plot the resulting dynamics. The input screen presents a number of plotting options, allows changes in simulation length, and other details.

The Interaction Engine produces three output types: an N vs t time trajectory, an N vs N phase-plane graph which can display phase trajectories or isoclines, and a console output that simply writes the output data to file. Equations for many interacting species can be plotted simultaneously on one N vs t graph when all of the populations are dependant (on the y-axis) and time is independant (on the x-axis). Only 2 or 3 dimensions can be plotted on a computer screen, so if you want an N vs N phase-plane graph, you must specify two or three equations to be plotted. The number of equations that can be incorporated in a model is limited only by your patience and the computational speed of your computer, but only two or three can be viewed simultaneously on a phase graph. The console output is useful if you want the numerical output for manipulation with a spreadsheet, statistical package, or presentation graphics tool.

Entering Equations

To specify equations that can be interpreted clearly by the Interaction Engine parser, you need to include operators that we often leave out when we write on paper. Here are some general suggestions and examples to guide your first efforts:

In general, you can enter equations just as you would enter them on a graphing calculator. They can contain parenthesis, operators, brackets, braces (eg (){}[]), functions (sin, cos, tan, ln, and !), variable parameters ($N1$, $N2$..), a time parameter (t), and common mathematical constants (e, π). The program does not differentiate between brackets, parenthesis, and braces; you can enter any, as long as they "balance" (eg. (1+2] is equivalent to (1+2)). If functions are typed without space between the function name and a numerical operand, the combination is interpreted as a constant parameter, so sin 10 returns the sine of ten, but sin10 identifies the variable "sin10," which is not wisely named. Values of e or π use the highest machine-specific precision unless you define a constant parameter with the names e or π and assign values truncated to lower precision. The program accepts strings and constants defined and assigned numerical values by the user.

Valid Operators, Functions,and Constants

The difference between functions and operators is in the number of values they require. A function will take one value, (sin 1.57) while an operator takes two (1*2), and constants require none at all. This definition allows some operators that wouldn't normally be considered as such. Here is a list of valid functions, operators, and constants with short descriptions of their implementation.

Functions:
sin x:
cos x:
tan x:
asin x: arcsine(x), with x in the range [-1.0,1.0]
acos x: arccosine(x), with x in the range [-1.0,1.0]
atan x: arctangent(x), with x in the range [-pi/2,pi/2]
ln x: natural log of x
!: factorial. This employs an approximation of the gamma function, producing values in the range [0,inf]. Even modest values of x, x! will overflow the Java double data type. Unlike other functions, the factorial symbol, '!', is placed after the term it evaluates.
abs x: if x is less than zero, it is multiplied by -1.
ipart x: returns the integer part of a number.
fpart x: returns the fraction part of a number.

Operators:
+,-,*,/: the standard arithmetic operators.
x%y: modulo, equivalent to y*fpart (x/y).
x^y: exponentiation, x to the power of y.
x sigfig y: formats x to y significant figures.
x min y: returns the smaller of two numbers x and y
x max y: returns the larger of two numbers x and y
x random y: a real-time random number generator. Each time the equation is evaluated, a different number will be produced somewhere in between x and y. This functionality is undefined for continuous equations. The numbers will be displayed in the java console for reference. If you have the Interaction Engine set to long run-times you may want to increase the buffer/window size to see all of the generated values (for Windows users this is done by accessing "Properties")

Constants:
π: the most precise representation of the mathematical constant π available.
e: the most precise representation of the mathematical constant 'e' (euler's number) available.
rand: produces a random value once between -1 and 1 before any equations are evaluated. i.e. this constant will be kept for all time t. the value used will be outputted to the java console for you to see what was used.
normal: produces a gaussian distributed random value once with a mean of 0.0 and a standard deviation of 1.0 before any equations are evaluated. The value will be placed on the java console so you to see it after the fact.

Error Messages
1) Brackets Unbalanced. This means that the number of open brackets is not equal to the number of closed.
2) Two Operators Next to Each Other. With 1+-1 the minus sign is not interpreted as a negation.
3) Invalid Token Inside of Open/Closed Bracket. Indicates an operator on the wrong side of a bracket, or a parenthetic closure immediately following an opening.

4) Invalid First Token, or Invalid Last Token. An operator that is not both preceded and succeeded by numbers gives this error.
5) Two Adjacent Numbers Without Operator. A space separates tokens, so if you put a space inside a number, then it is interpreted as 2 numbers and doesn't make sense.
6) Brackets in Incorrect Order.
7) Invalid Token Outside of Closed Bracket. Multiplication is not assumed after a closing bracket.
8) Operator on Inside of Function. You would see this if you typed sin * 8.
9) Invalid Decimal.
10) "Random" Not Defined for Continuous Equations. Use rand for continuous equations and "random" for discrete difference equations.
11) Invalid index for *N* character(s). The program looks for '*N*'s in your equations, and automatically calls them variable parameters. It then looks for the characters directly after the *N* to distinguish multiple *N* parameters; if those characters are not numbers, then you will get this error.
12) Parameter *N* Index Not Defined. You can't use a population of that doesn't exist. Any index lower than 1 or greater than the total number of equations will give this error.
14) Parameter *N*(number) not used. If you have selected not to calculate values for one of the equations, then you can't use it's population density in another equation.
15) Something Bad Happened. This is for the grab-bag classification for equations that make no sense based on errors that we have not anticipated.

Hints and Notes

The "java console" refers to the window that said "Populus Starting…" when the Populus program was started up. The title of this window is "PopRun" and should be in the taskbar.

The *Populus* Interaction Engine implemented for version 5.1 provides limited isocline analysis tool, currently functional when 2 equations are plotted, but not 3. We will provide a more extensive isocline tool in subsequent versions.

If you want a rand value generated with a different range than -1 to 1, then simply enter (*r**abs rand+low), *r* being the range desired and low being the lower end of the range.

The Default Example

The *Populus* Interaction Engine allows you to simulate the population dynamics of a community consisting of any number of species, with a separate equation for the dynamics of each species. In one- and two-species cases, it can be used to model population growth, competition, and predation, which are explored in more detail in other *Populus* modules. Using more species, you can examine the dynamics of communities in which several different pair-wise interactions occur. Some of the possibilities which you may want to examine are: (1) a linear food chain; (2) a group of species all of which compete with each other; (3) two predator species, each of which eat two prey. There are no restrictions on the kinds of ecological systems you can simulate with this general-purpose modeling engine.

Differential equation models of three or more interacting populations differ from those with two populations in two important respects: (1) it is possible for the population dynamics to be chaotic when there are three or more species; and (2) indirect effects occur whenever species *i* affects the

per capita growth rate of species *j*, and *j* affects the population growth rate of *k*. The default case represents the Gilpin (1979) one-predator-two-prey model, which exhibits chaotic behavior. Chaotic dynamics imply that the populations undergo continual change in which a particular set of population levels never occurs more than once, no matter how long the dynamics continue. In addition, the difference between the population densities in two different systems that are initially very similar in population densities, increases rapidly (exponentially) with time. For more information on chaos, see the book by Holden listed below. Chaos cannot occur in systems of two ordinary differential equations, although it can occur in difference equation models with one or two species. It is not yet known how frequently ecological models exhibit chaos. Chaos seems to be relatively rare in Lotka-Volterra-type models, in which the *per capita* growth rate of each species is a linear function of the population density of each other species. However, Michael Gilpin (see below) has demonstrated parameter values for a Lotka-Volterra one predator-two prey model that give chaotic dynamics.

Indirect effects have received more study than chaos. One of the simplest possible indirect effects occurs when there are three competing species. Species 1, for example, has a direct negative effect on each of the other two species by the definition of competition. However, it also has an indirect positive effect on each of the other two; it benefits species 2 by competing with (and reducing the population density of) competitor 3, and benefits species 3 by competing with species 2. Thus, it is possible for an increase in the population density of species 1 to increase the equilibrium density of species 3, if the indirect effect is larger than the direct one. There are a large number of possible indirect effects when there are four or more species.

References

Gilpin, M. E. 1979. Spiral chaos in a predator-prey model. American Naturalist 113:306-308.

Holden, A. V. 1986. *Chaos*. Princeton Univ. Press.

Yodzis, P. 1989. *An Introduction to Theoretical Ecology*. Harper and Row.